UNIVERSITÉ DE LA ROCHELLE
ÉCOLE DOCTORALE S2I
SCIENCES ET INGÉNIERIE POUR L'INFORMATION

THÈSE

pour obtenir le titre de

Docteur

de l'Université de La Rochelle
Spécialité : MATHÈMATIQUES ET APPLICATIONS

Présentée et soutenue par

Salman Amin MALIK

Sur le sujet:

Contributions aux équations aux dérivées fractionnaires et au traitement d'images

Thèse dirigée par Professeur Mokhtar KIRANE
Financée par HEC Pakistan
Préparée au Laboratoire de Mathématiques, Image et Applications–EA 3165

soutenue le 20 Septembre 2012

Jury :

F. Ben BELGACEM,	Professeur,	Université de Technologie de Compiègne. (Raporteur)
Z. BELHACHMI,	Professeur,	Université de Haute Alsace. (Examinateur)
C. CHOQUET,	Professeur,	Université de La Rochelle. (Examinateur)
M. KIRANE,	Professeur,	Université de La Rochelle. (Directeur de thèse)
A. ROUGIREL,	MCF(HDR),	Université de Poitiers. (Examinateur)
D. F. M. TORRES,	Professeur,	University of Aveiro, Portugal. (Raporteur)

Contributions to fractional differential equations and treatment of images

A THESIS SUBMITTED IN FULFILLMENT OF THE REQUIREMENTS
FOR THE DEGREE OF DOCTOR OF PHILOSOPHY IN
APPLIED MATHEMATICS

AT

UNIVERSITY OF LA ROCHELLE

GRADUATE SCHOOL S2I

SCIENCES ET INGÉNIERIE POUR L'INFORMATION

Presented by

Salman Amin MALIK

defended on 20th September 2012

Jury :

F. Ben BELGACEM,	Professor,	Université de Technologie de Compiègne. (Reporter)
Z. BELHACHMI,	Professor,	Université de Haute Alsace. (Examiner)
C. CHOQUET,	Professor,	Université de La Rochelle. (Examiner)
M. KIRANE,	Professeur,	Université de La Rochelle. (Advisor)
A. ROUGIREL,	MCF (HDR),	Université de Poitiers. (Examiner)
D. F. M. TORRES,	Professor,	University of Aveiro, Portugal. (Reporter)

To my parents

Hanifa Amin
&
Muhammad Amin MALIK

Acknowledgments

This thesis is an output of the research work that has been done during my graduate studies at La Rochelle as member of the Lab. MIA, University of La Rochelle. In this acknowledgement, I would like to convey my gratitude to all people who helped me in different ways during this period.

In the first place, I would like to express my deep gratitude to Prof. Mokhtar Kirane for his supervision, continuous guidance, for having trust in me and for tremendous encouragement he gave me throughout my graduate studies. His scientific intuition, ideas and passion for mathematics always inspire me and enrich my scientific growth as a student. I don't have any hesitation to say that he is the one who developed my research interest in the field of fractional differential equations. I am grateful to him in every possible way.

I would like to acknowledge E. Cuesta. It is a great pleasure to collaborate with him and I hope to keep up our collaboration in the future. I am thankful to Prof. W. E. Olmstead for his interest in my work.

I gratefully thank F. Ben Belgacem and D. F. M. Torres for accepting to be a member of the jury of my thesis and to report on it.

I am deeply indebted to Z. Belhachmi, C. Choquet, and A. Rougirel for being members of the jury. I would like to express my gratitude to the members of jury, it is a great pleasure and honor to present this thesis to the jury.

I would like to thank C. Sicard, S. Picq sécrétaires du Laboratoire MIA and S. Pinaud sécrétariat Department of Mathematics for helping me in administrative formalities during my studies.

The completion of this work was not possible without financial support from Higher Education Commission (HEC) of Pakistan. I am obliged to HEC for providing the financial support during my studies.

I am grateful to the Université de La Rochelle for supporting my international and national visits to different summer schools and conferences.

The completion of this work in time would be impossible for me without having a peace of mind which was due to the permanent support from my family. The prayers and support of my parents is always there for me and I can't return their love and affection throughout my life. I would like to express my appreciation and thanks to my wife Hina for the permanent support and for taking care of my daughters; without her support and understanding I would not be able to do anything in my life. My special gratitude is due to my brother, my sisters and their families for their loving support.

Salman Amin MALIK
La Rochelle, France.

Résume

Dans cette thèse, nous nous intéressons aux équations différentielles fractionnaires et leurs applications au traitement d'images. Une attention particulière à été apportée à une système non linéaire d'équations différentielles fractionnaires. En particulier, nous avons étudiée les propriétés qualitatives des solutions d'un système non linéaire d'équations différentielles fractionnaires qui explosent en temp fini. L'existence de solutions locales pour le système, le profil des solutions qui explosent en temp fini sont présentés.

Le problème inverse de la détermination du terme source inconnue et la distribution de température pour l'équation de la chaleur linéaire avec une dérivée fractionnaire en temp ont été etudiés. L'existence et l'unicité de la solution du problème inverse sont présenté.

D'autre part, nous proposons un modèle basé sur l'équation de la chaleur linéaire avec une dérivée fractionnaire en temps pour le débruitage d'images numériques (simplification, restauration ou amélioration). L'approche utilise une technique de pixel par pixel, ce qui détermine la nature du filtre (comme passe-bas ou en tant que filtre passe-haut). En contraste avec certain modèles basés sur les équations aux dérivées partielles pour le débruitage (simplification, restauration ou amélioration) de l'image, le modèle proposé est bien posé et le schéma numérique adopté est convergent. Une amélioration de notre modèle proposé est suggéré.

Abstract

The topics of this thesis are problems related to the fractional differential equations, i.e., differential equations involving derivatives of arbitrary order. The thesis can be divided into two major parts; the first part is concerned with the analytical treatment of some fractional differential equations or systems while the second part consists of an application of the fractional differential equation to image denoising (simplification, smoothing, restoration or enhancement).

The aim of the thesis is to study some problems related to fractional differential equations which are not considered to a large extent but deserve the attention of mathematicians, engineers and scientists due to their applications. Namely, the existence/nonexistence of global solutions (in time) for some nonlinear systems of differential equations involving fractional derivative in time, and inverse source problems for differential equations involving fractional derivative in time. For the former, a number of related questions arise, for example, the profile of the blowing-up solutions and principally bilateral bounds on the blow-up time.

In the first part of the thesis we study a nonlinear system of fractional differential equations with power nonlinearities; the solution of the system blows up in a finite time. We provide the profile of the blowing-up solutions of the system by finding upper and lower estimates of the solution. Moreover, bilateral bounds on the blow-up time are given.

We consider the inverse problem concerning a linear heat equation with a fractional derivative in time for the determination of the source term (supposed to be independent of the time variable) and temperature distribution from initial and final temperature data. The uniqueness and existence of the continuous solution of the inverse problem is proved. We also consider the inverse source problem for a two dimensional fractional diffusion equation. The results about the existence, uniqueness and continuous dependence of the solution of the inverse problem on the data are presented.

In the second part of the thesis, our aim is to apply the linear heat equation involving a fractional derivative in time for denoising (simplification, smoothing, restoration or enhancement) of digital images. The order of the fractional derivative has been used for getting an effect of anisotropic diffusion, which in result preserves the fine structures in the image during diffusion process. Furthermore, an improvement in the proposed model is suggested by using the structure tensor of the images.

The present thesis consists of seven chapters, the first chapter provides an introduction to the problems addressed and related state of the art work. The rest of the thesis contains the chapters corresponding to the articles published or prepared during the work of this thesis. The list of the publications is

1. M. Kirane and Salman A. Malik, The Profile of blowing-up solutions to a nonlinear system of fractional differential equations, Nonlinear Analysis:TMA 73 (2010) 3723-3736. (**Latest impact factor 1.279**)

2. M. Kirane and Salman A. Malik, Determination of an unknown source term and the temperature distribution for the linear heat equation involving fractional derivative in time, Appl. Math. Comp. 218, Issue 1, 163–170. (**Latest impact factor 1.534**)

3. M. Kirane and Salman A. Malik, An inverse source problem for a two dimensional time fractional diffusion equation with nonlocal boundary conditions. (**Submitted to Mathematical Methods in the Applied Sciences**)

4. E. Cuesta, M. Kirane, and Salman A. Malik, Image structure preserving denoising using generalized fractional time integrals, Signal Processing 92 (2012) 553-563. (**Latest impact factor 1.351**)

5. E. Cuesta, M. Kirane, and Salman A. Malik, On the Improvement of Volterra Equation Based Filtering for Image Denoising, In H. R. Arabnia et al, Proceedings of IPCV 2011, Las Vegas Nevada, USA, pp. 733-738.

The thesis can be divided into two parts: the first part Chapter 2, Chapter 3 and Chapter 4 corresponds to the articles 1, 2 and 3, respectively. The second part consisting of chapter 5 and 6 corresponds to the articles 4 and 5. We have arranged the articles in the thesis as accepted for the publications, with minor changes consisting of adding some remarks and comments. For the reader's convenience, the proofs of some results needed for the better understanding of the thesis are presented in the appendix.

Chapter 7 concludes the thesis by describing the results obtained (contribution) in this thesis and some perspectives arising from the thesis.

Workshops and Conferences as Speaker

- 02-04 April 2012, Inverse Problems, Control and Shape Optimization (PICOF'12), Poster Presentation **Title: On the inverse problem of linear heat equation involving fractional derivative in time**, Ecole Polytechnique, Palaisceau Cedex, France.

- 22 Nov. 2011-Compiègne **Title: Determination of an unknown source term and the temperature distribution for the linear heat equation involving fractional derivative in time**, Seminar de LMA, Université de Technologie de Compiègne, France.

- 29 Sep. 2011-La Rochelle, **Title: On the inverse problem of linear heat equation involving fractional derivative in time**, Seminar MIA University of La Rochelle, La Rochelle, France.

- 14 July 2011-Istanbul, **Title: Image structure preserving denoising: A framework within Fractional Calculus**, Koc University Graduate Summer School in Science and Engineering, Linear and Nonlinear Evolution Equations, Istanbul, Turkey.

- 17 Feb. 2011-Futuroscope, **Title: On the inverse problem of linear heat equation and application to image restoration**, Seminar LMA University of Poitiers, France.

- 15 Dec. 2010 - La Rochelle, **Title: The profile of blowing-up solutions to a nonlinear system of fractional differential equations**, Journée EDP University of La Rochelle, France.

- 15 Nov. 2010 - Amiens, **Title: The profile of blowing-up solutions to a nonlinear system of fractional differential equations**, Seminar A3 University of Picardie Jules Verne, France.

- 12-14 Oct. 2010-Marans, **Title: Qualitative Properties of solutions to a nonlinear system of fractional differential equations and fractional derivative based approach for image denoising**, école doctrole S2i, Marans, France.

- 7 Oct. 2010-La Rochelle, **Title: Propriétés qualitatives des solutions à un système non linéaire de l'équation différentielle fractionnaire et le débruitage des images par l'équation de Volterra**, Seminar MIA University of La Rochelle, France.

- 18-20 Feb. 2010, Poitiers, **Title: Image denoising using fractional time derivatives**, International Conference on PDE (in honor of 60th birthday of M. Chipot) University of Poitiers, France.

Workshops and Conferences as Participant

- 22-24 May 2012, **Seminar S2i**, La Rochelle, France.
- GDR 27 Sep. 2010, **One day meeting GDR Modéles mathématiques pour l'imagerie**, Paris, France.
- 17-21 May 2010, **Spring School on Nonlinear Partial Differential Equations**, Brussels, Belgium.
- 4-6 March 2010, **Seminar S2i**, Poitiers, France.
- 29 March-01 April 2010, **Mathematical methods for image processing**, University of Orleans, France.
- 25 Nov. 2009, **Half day on treatment of images and industrial applications**, University of Versaille St. Quentin en Yvelines, France.
- 15-19 June, 2009, **CNRS Summer school on image processing**, Figeac, France.

Contents

List of Figures

List of Tables

Chapter 1

Introduction

This chapter contains two major parts, namely "Introduction (Française)" and "Introduction (English)". In the first part we provide the introduction of the problems considered in this thesis in French and the second part consists of introduction in English.

Contents

1.1 Introduction (Française)

Dans cette thèse, nous nous intéressons à l'étude

1. D'un système non linéaire d'équations différentielles fractionnaires (FDS)

$$\begin{aligned} u'(t) + D^{\alpha}_{0_+}(u-u_0)(t) &= v(t)^q, \qquad t>0, \\ v'(t) + D^{\beta}_{0_+}(v-v_0)(t) &= u(t)^p, \qquad t>0, \end{aligned}$$

   où $u(0) = u_0 > 0, v(0) = v_0 > 0, p > 1, q > 1$ sont des constantes et $D^{\alpha}_{0_+}$, $D^{\beta}_{0_+}$, $0 < \alpha < 1$, $0 < \beta < 1$ sont les derivée fractionaire définies au sens de Riemann-Liouville.

   La solution du système non linéaire (FDS) peut exploser en temps fini. L'objectif de l'étude de ce système (FDS) est d'obtenir une estimation bilatérale pour la solution qui explose en temp fini et trouver une borne inférieure et une borne supérieure du temps d'explosion.

2. Dans le troisième et le quatrième chapitres, nous étudierons le problème inverse pour l'équation de diffusion linéaire en une dimension et en deux dimensions, respectivement. Nous sommes intéressés de trouver un terme source inconnue d'une équation de diffusion non locales. Les conditions aux limites considérées sont non locale et le problème spectral est non autoadjoint. Nous allons chercher des conditions pour lesquelles le problème inverse a une solution unique.

3. Dans la dernière partie de la thèse (Chapitres 5 et 6), nous étudierons le débruitage d'images numériques en utilisant l'équation de la chaleur linéaire avec une dérivée fractionnaire en temps.

   Pour la discrétisation du modèle proposé, nous avons utilisé un schéma numérique convergent. Le schéma numérique possède de nombreuses caractéristiques importantes relatives aux images numériques.

Pour mettre en lumière les points importants et éviter qu'ils ne soient pas cachés par la technique, nous donnons souvent dans cette introduction, des énoncés simplifiés des résultats. Des énoncés plus complets se trouvent dans les différents chapitres qui sont présentés ci-aprés.

1.2 Le profil de solutions qui explosent en temp fini d'un système non-linéaire d'équations différentielles fractionnaires

Dans la première partie, nous nous intéressons au système non linéaire d'équations différentielles fractionnaires (FDS)

$$\begin{array}{rcll} u'(t) + D^{\alpha}_{0+}(u - u_0)(t) & = & v(t)^q, & t > 0, \\ v'(t) + D^{\beta}_{0+}(v - v_0)(t) & = & u(t)^p, & t > 0, \end{array}$$

où $u(0) = u_0 > 0, v(0) = v_0 > 0, p > 1, q > 1$ sont des constantes données, D^{α}_{0+} et D^{β}_{0+}, $0 < \alpha < 1$, $0 < \beta < 1$ représentent les dérivées de Riemann-Liouville fractionnaires. Le système (FDS) a été étudié par Furati et Kirane [35]; ils ont montré l'existence de solutions du système (FDS) qui explosent en temps fini.

Theorem 1.2.1 ([35]). *Supposons que $0 < \alpha, \beta < 1$, $p > 1, q > 1$ et $u_0 > 0$, $v_0 > 0$, alors ils existent des solutions pour le système (FDS) qui explosent en temps fini.*

La démonstration se base sur une contradiction qu'on obtient si on suppose que $u_0 > 0, v_0 > 0$ en tenant compte de la formulation faible de la solution et avec un choix judicieux de la fonction test donnée par

$$\varphi(t) = \begin{cases} T^{-\lambda}(T-t)^{\lambda}, & t \in [0,T], \\ 0, & t > T. \end{cases} \tag{1.1}$$

La fonction $\varphi(t)$ vérifie

$$\int_0^T D^{\alpha}_{T-}\varphi(t)dt = C_{\alpha,\lambda}T^{1-\alpha}, \quad C_{\alpha,\lambda} = \frac{\Gamma(\lambda+1)}{\Gamma(\lambda-\alpha+2)}, \tag{1.2}$$

et pour $p > 1$, $\lambda > \alpha p - 1$ (voir l'annexe A.1.1)

$$\int_0^T \varphi^{1-p}(t) \left| D^{\alpha}_{T-}\varphi(t) \right|^p dt = C_{p,\alpha}T^{1-\alpha p}, \tag{1.3}$$

où

$$C_{p,\alpha} = \frac{1}{\lambda - p\alpha + 1}\left[\frac{\Gamma(\lambda+1)}{\Gamma(\lambda+1-\alpha)}\right]^p. \tag{1.4}$$

Pour le cas $0 < p, q \leq 1$ la solution du système (FDS) est globale.

Theorem 1.2.2 ([35]). *Supposons que $0 < \alpha, \beta < 1$, $0 < p, q \leq 1$, alors toutes les solutions du système (FDS) avec les conditions $u(0) = u_0 > 0$, $v(0) = v_0 > 0$ sont globale.*

Une fois qu'on a le résultat de l'existence de solutions de (FDS) qui explosent en temps fini, le question de leur profile se pose. Nous étudierons le profil des solutions du système (FDS).

Le profil des solutions de (FDS) qui explosent en temps fini s'obtient par l'obtention de certaines estimations par en-dessous et par au-dessus. Ces estimations sont en comparent les solutions de (FDS) qui explosent en temp fini avec les solutions des sous-systèmes obtenus en laissant tomber les dérivées fractionnaires du système (FDS)

$$\begin{aligned} u'(t) &= \lambda v(t)^q, \qquad t>0, \quad q>1, \\ v'(t) &= \lambda u(t)^p, \qquad t>0, \quad p>1, \end{aligned}$$

le système d'équations différentielles ordinaires (ODS) avec soit $\lambda = 1$ et en laissant tomber les dérivés usuelles de (FDS)

$$\begin{aligned} D_{0+}^{\alpha}(u-u_0)(t) &= \mu v(t)^q, \qquad t>0, \quad q>1, \\ D_{0+}^{\beta}(v-v_0)(t) &= \mu u(t)^p, \qquad t>0, \quad p>1, \end{aligned}$$

le système d'équations différentielles fractionnaires (PFDS), avec soit $\mu = 1$. Le système (ODS) est facile à résoudre; on obtient les expressions explicites des solutions qui explosent et une estimation du temps d'explosion (voir le Chapitre 2). Nous allons étudier le système (PFDS).

Nous allons présenter les Lemmes préliminaires et pour les démonstrations voir le chapitre 2.

Lemma 1.2.3. *Les composants de la solution (u, v) au système (FDS) vérifiént les équations intégrales*

$$u(t) = u_0 + \int_0^t e_{1-\alpha}(t-\tau)v(\tau)^q d\tau, \tag{1.5}$$

$$v(t) = v_0 + \int_0^t e_{1-\beta}(t-\tau)u(\tau)^p d\tau. \tag{1.6}$$

Lemma 1.2.4. *Pour le système (FDS), les fonctions $u'(t)$ et $v'(t)$ vérifient les équations intégrales*

$$u'(t) = v(t)^q + \int_0^t e'_{1-\alpha}(t-\tau)v(\tau)^q d\tau, \tag{1.7}$$

$$v'(t) = u(t)^p + \int_0^t e'_{1-\beta}(t-\tau)u(\tau)^p d\tau. \tag{1.8}$$

Lemma 1.2.5. *Le système (FDS) et les équations intégrales (1.5) - (1.6) sont équivalentes.*

Lemma 1.2.6. *Pour tout $u_0 > 0$, $v_0 > 0$, on a:*

$$u' > 0, \quad v' > 0.$$

Pour montrer l'existence locale de la solution du système (FDS) via ses équivalents équations intégrales (c.f (1.5) - (1.6)), nous avons besoin des ingrédients suivants:

- Tout d'abord, nous fixons pour $u, v \in C([0,T])$,

$$\Delta := \{t \in \mathbb{R}^+/0 \leq t \leq T, |u-u_0| < c, |v-v_0| < c\}.$$

Soit $K_1 := v_0^q, K_2 := u_0^p$.

Sur Δ les non-linéarités vérifient les conditions de Lipschitz

$$|v_1^q - v_2^q| \leq L_1|v_1 - v_2|, \qquad |u_1^p - u_2^p| \leq L_2|u_1 - u_2|, \tag{1.9}$$

où

$$L_1 := q(c+u_0)^{q-1}, \qquad L_2 := p(c+v_0)^{p-1}.$$

On pose $K := \max\{K_1, K_2\}$, $L := \max\{L_1, L_2\}$.

- Nous avons pour $0 \leq t \leq T$,

$$\int_0^t e_{1-\alpha}(t-\tau)d\tau \leq M_1 < \infty, \quad \int_0^t e_{1-\beta}(t-\tau)d\tau \leq M_2 < \infty,$$

où e_γ est définie par la fonction de Mittag-Leffler $e_\gamma := E_\gamma(-\lambda t^\gamma)$ pour $\lambda \in \mathbb{R}$.

De plus, on pose, pour tout $0 < \rho < 1$, $P := \min(\rho/L, c/K)$, et $h := \min(r, T)$, où $r := \min(r_1, r_2)$ et r_1, r_2 sont déterminées par

$$\int_0^t e_{1-\alpha}(t-\tau)d\tau \leq P, \quad 0 \leq t \leq r_1, \quad \text{and} \quad \int_0^t e_{1-\beta}(t-\tau)d\tau \leq P, \quad 0 \leq t \leq r_2.$$

Nous avons le théorème d'existence suivant.

Theorem 1.2.7. *Pour toute $u_0 > 0, v_0 > 0$ donné, les équations intégrales (1.5)-(1.6) admettent une solution unique, continue dans l'intervalle $0 \leq t \leq h$.*

Pour la preuve, nous utilisons la méthode itérative de picard (voir le Chapitre 2, le théorème 2.3.4).

Pour le système (PFDS), nous avons montré que les solutions explosent en temp fini.

Soit

$$s = \frac{p\alpha + \beta}{1 - pq}, \quad \tilde{s} = \frac{\alpha + q\beta}{1 - pq}, \quad C_v = K_2(K_1)^{\frac{p}{pq-1}}, \quad C_u = K_2^*(K_1^*)^{\frac{q}{pq-1}}, \tag{1.10}$$

où K_1, K_2, K_1^* et K_2^* sont données par les expression

$$K_1 = C_{p',\alpha}^{\frac{1}{p'}} C_{q',\beta}^{\frac{1}{pq'}}, \quad K_2 = C_{q',\beta}^{\frac{1}{q'}} C_{\beta,\lambda}^{-1},$$

$$K_1^* = C_{q',\beta}^{\frac{1}{q'}} C_{p',\alpha}^{\frac{1}{qp'}}, \quad K_2^* = C_{p',\alpha}^{\frac{1}{p'}} C_{\alpha,\lambda}^{-1},$$

et les constantes $\{C_{\alpha,\lambda}, C_{\beta,\lambda}\}$ et $\{C_{p',\alpha}, C_{q',\beta}\}$ sont donées par (1.2) et (1.4).

Theorem 1.2.8. *Soit $p > 1, q > 1$ et $u_0 > 0$, $v_0 > 0$, alors toute solution pour le système (PFDS) avec $\mu = 1$ explose en temp fini T_{max}. De plus, une limite supérieure sur le temps T_{max} est donné par $min\{T_u, T_v\}$ où*

$$T_v = \left[\frac{v_0}{C_v}\right]^{1/s} \quad T_u = \left[\frac{u_0}{C_u}\right]^{1/\tilde{s}},$$

avec $s, \tilde{s}, C_u$ et C_v sont données par (1.10).

Le système (PFDS) est équivalent au système d'équations intégrales non linéaires de Volterra suivant

$$\begin{cases} u(t) = u_0 + \frac{\mu}{\Gamma(\alpha)} \int\limits_0^t \frac{v(\tau)^q}{(t-\tau)^{1-\alpha}} d\tau, & t > 0, \\ v(t) = v_0 + \frac{\mu}{\Gamma(\beta)} \int\limits_0^t \frac{u(\tau)^p}{(t-\tau)^{1-\beta}} d\tau, & t > 0. \end{cases} \tag{1.11}$$

Suite à [90] le comportement asymptotique lorsque le temps approche le temps d'explosion pour le système (1.11) peut être obtenu. Nous avons

Theorem 1.2.9. *Les profils des comportement asymptotique de la solution $(u(t), v(t))$ du système (1.11) avec $\mu = 1$ sont donné par*

$$u(t) \sim C_{1,\alpha,\beta}(T_{max}^{\alpha,\beta} - t)^{-\delta}, \quad v(t) \sim C_{2,\alpha,\beta}(T_{max}^{\alpha,\beta} - t)^{-\xi}, \quad \text{quand} \quad t \to T_{max}^{\alpha,\beta}, \tag{1.12}$$

où $T_{max}^{\alpha,\beta}$ est le temps de l'explosion et

$$C_{1,\alpha,\beta} = \left(\frac{\Gamma(p\delta)}{\Gamma(p\delta - \beta)}\right)^{\frac{q}{pq-1}} \left(\frac{\Gamma(q\xi)}{\Gamma(q\xi - \alpha)}\right)^{\frac{1}{pq-1}},$$

$$C_{2,\alpha,\beta} = \left(\frac{\Gamma(q\xi)}{\Gamma(q\xi - \alpha)}\right)^{\frac{p}{pq-1}} \left(\frac{\Gamma(p\delta)}{\Gamma(p\delta - \beta)}\right)^{\frac{1}{pq-1}},$$

avec

$$\delta = \frac{\alpha + q\beta}{pq - 1}, \quad \xi = \frac{\beta + p\alpha}{pq - 1}. \tag{1.13}$$

Pour le système (PFDS), nous avons calculé la borne inférieure et la borne supérieure du temps d'explosion T_{max} via le système (1.11). Nous suivons l'analyse du papier [90] pour obtenir les résultats. Pour les démonstrations du Théorème 1.2.9 et Théorème 1.2.10 voir l'annexe A.1.

Theorem 1.2.10. *Pour le système d'équations intégrales de Volterra (1.11), $u(t) \to \infty$ et $v(t) \to \infty$ quand $t \to T_{max}$, où*

$$T_L \le T_{max} \le T_U.$$

Les limites T_L et T_U sont données par

$$T_L := \begin{cases} \theta \left[\frac{\alpha(r-1)^{r-1}}{\gamma r^r}\right]^{1/\alpha}, & si \;\; \alpha(r-1)^{r-1} \le \gamma r^r, \\ \theta \left[\frac{\beta(r-1)^{r-1}}{\gamma r^r} - \frac{\beta-\alpha}{\alpha}\right]^{1/\beta} & si \;\; \alpha(r-1)^{r-1} > \gamma r^r. \end{cases} \tag{1.14}$$

$$T_U := \begin{cases} \theta\left[\frac{\beta(r+1)}{\gamma(pq-1)}\right]^{1/\alpha}, & si\ \ \beta(r+1) \leq \gamma(pq-1), \\ \theta\left[\frac{\alpha(r+1)}{\gamma(pq-1)} - \frac{\beta-\alpha}{\beta}\right]^{1/\beta} & si\ \ \beta(r+1) > \gamma(pq-1), \end{cases} \tag{1.15}$$

où

$$\theta = \left[\frac{\Gamma(\beta)v_0^{q+1}}{\Gamma(\alpha)u_0^{p+1}}\right]^{1/(\beta-\alpha)}, \quad r := \max(p,q),$$

et

$$\gamma := \mu\left(\frac{[\Gamma(\beta)]^{\alpha}[v_0]^{\beta q+\alpha}}{\Gamma(\alpha)]^{\beta}[u_0]^{\alpha p+\beta}}\right)^{1/(\beta-\alpha)}.$$

En raison de la propriété de la complète monotonie de la fonction de Mittag-Leffler pour $0 < \alpha < 1$ (voir [38]) et en utilisant le Lemme 1.2.3 et le Lemme 1.2.4, la configuration suivante est obtenue

$$\begin{array}{cc} D_{0_+}^{\alpha}(u-u_0)(t) \leq v(t)^q, & D_{0_+}^{\beta}(v-v_0)(t) \leq u(t)^p, \\ u'(t) \leq v(t)^q, & v'(t) \leq u(t)^p. \end{array} \tag{1.16}$$

Les solutions de ces inégalités différentielles fournissent des estimations par au-dessus à la solution du système (FDS).

De plus, le système (FDS) avec $u' > 0, v' > 0$ et $u'' > 0, v'' > 0$ (c.f. Lemme 1.2.6) nous permettent d'écrire le système (ODSL)

$$u'(t) \geq \frac{v(t)^q\Gamma(2-\alpha)}{\Gamma(2-\alpha)+t^{1-\alpha}}, \qquad v'(t) \geq \frac{u(t)^p\Gamma(2-\beta)}{\Gamma(2-\beta)+t^{1-\beta}}.$$

L'analyse des inégalités ci-dessus conduit à un profil précis des solutions d'explosive du système (FDS).

1.3 Détermination d'un terme source et de la distribution de température pour l'équation de la chaleur avec une dérivée fractionnaire en temps

Dans cette partie, on cherche à trouver $u(x,t)$ (la distribution de température) et $f(x)$ (le terme de source) dans le domaine $Q_T = (0,1) \times (0,T)$ pour l'équation de diffusion fractionnaire suivante

$$D_{0_+}^{\alpha}(u(x,t) - \varrho u(x,0)) - u_{xx}(x,t) = f(x), \qquad (x,t) \in Q_T, \tag{1.17}$$

$$u(x,0) = \varphi(x) \quad u(x,T) = \psi(x), \qquad x \in [0,1], \tag{1.18}$$

$$u(1,t) = 0, \quad u_x(0,t) = u_x(1,t), \qquad t \in [0,T], \tag{1.19}$$

où $\varrho > 0$, $D^{\alpha}_{0_+}$ représente la dérivée fractionnaire d'ordre $0 < \alpha < 1$, définie au sens de Riemann-Liouville , $\varphi(x)$ et $\psi(x)$ sont les températures initiale et finale, respectivement.

Le choix du terme $D^{\alpha}_{0_+}(u - u_0)(t)$ dans l'équation (1.17) au lieu du terme usuel $D^{\alpha}_{0_+}u(t)$ a été fait pour éviter la singularité en zéro ainsi que pour imposer une condition initiale significative au problème.

Il y a très peu d'articles qui examinent le problème inverse des équations différentielles avec une dérivée fractionnaire en temps. Dans [17], les auteurs ont étudié le problème inverse de détermination de l'ordre de dérivée fractionnaire et le coefficient de diffusion pour une équation de diffusion (qu'ils considèrent comme la dérivée temporelle fractionnaire définie au sense de Caputo). Ils ont montré la détermination unique de l'ordre de la dérivée fractionnaire et le coefficient de diffusion (indépendant du temps); leur preuve est baseé sur le développement en fonctions propres de la solution faible au problème et la théorie de Gelfand-Levitan.

Dans [118], le problème inverse de la détermination d'un terme source (qui est indépendant de la variable temporelle) pour l'équation de la diffusion

$$\begin{aligned}
{}^{C}D^{\alpha}_{0_+}u(x,t) - u_{xx}(x,t) &= f(x), \qquad (x,t) \in Q_T,\\
u(x,0) &= \varphi(x), \qquad x \in [0,1],\\
-u_x(1,t) = 0, \quad u_x(0,t) &= 0, \qquad t \in [0,T],
\end{aligned}$$

où ${}^{C}D^{\alpha}_{0_+}$, pour $0 < \alpha < 1$ est la dérivée fractionnaire de Caputo a été considéré. La détermination unique du terme source a été montré à l'aide d'un prolongement analytique et avec le principe de Duhamel.

Pour la résolution des problèmes inverses, l'unicité de la solution est le point le plus important. Une fois que nous avons l'unicité du problème inverse, alors nous pouvons utilisé les schémas numériques qui sont stables et convergents pour obtenir une approximation (à une précision souhaitée) de la solution. Récemment, quelques articles traitent le problème inverse pour l'équation de diffusion fractionnaire par différents algorithmes numériques (voir [117], [79]).

Pour le problème (1.17)-(1.19) les conditions au bord sont non locales

$$u(1,t) = 0,\ u_x(0,t) = u_x(1,t),\ t \in [0,T].$$

Le problème spectrale associé au problème

$$-X'' = \lambda X, \quad X(1) = 0, \quad X'(0) = X'(1), \tag{1.20}$$

n'est pas auto-adjoint. Alors les fonctions propres ne forment pas une base orthonormée de $L^2(0,1)$.

Comment obtenir une base orthonormée de fonctions propres?

Par l'obtention d'un système biorthogonal de fonctions pour l'espace $L^2(0,1)$. Rappelons-nous que deux ensembles de fonctions S_1 et S_2 de $L^2(0,1)$ forment une système biorthogonal s'il existe un applications bijective entre eux telle que

$$\int_0^1 f_i g_j = \delta_{ij}, \tag{1.21}$$

où $f_i \in S_1$, $g_i \in S_2$ et δ_{ij} est le fonction delta de Kronecker.

Le système biorthogonal nous permet d'écrire la solution du problème inverse en fonction des fonctions propres et fonction propres associéesdu problème adjoint de (1.20) (parfois aussi appelé le problème conjugué).

Une suite $\{x_n\}_{n=1}^{\infty}$ dans un espace de Hilbert H est dite une suite de Riesz s'il existe des constantes $0 < c \leq C < \infty$ telles que

$$c \sum_{n=1}^{\infty} |a_n|^2 \leq \left\| \sum_{n=1}^{\infty} a_n x_n \right\|^2 \leq C \sum_{n=1}^{\infty} |a_n|^2,$$

pour toute suite de scalaires $\{a_n\}_{n=1}^{\infty}$ dans l'espace

$$\ell^2 := \left\{ (a_1, a_2, ..., a_n, ...)/a_n \in \mathbb{R} \ \text{ t.q } \sum_{n=1}^{\infty} |a_n|^2 < \infty \right\}.$$

Une base de Riesz pour un espace de Hilbert H est une suite de Riesz, qui est libre dans H et qui est génératrice de l'espace H.

La clé dans la détermination de la distribution de température et la source inconnue pour le système (1.17)-(1.19) est de le choix d'une base spéciale pour l'espace $L^2(0,1)$ comme suit

$$\{2(1-x), \quad \{4(1-x)\cos 2\pi nx\}_{n=1}^{\infty}, \quad \{4\sin 2\pi nx\}_{n=1}^{\infty}\}, \tag{1.22}$$

(voir l'annexe A.2 pour la construction de la base).

Dans [53], il est demontré que l'ensemble des fonctions (1.22) forment une base de Riesz pour l'espace $L^2(0,1)$.

Comme d'habitude, l'idée est de décomposer les fonctions inconnues $\{u(x,t), f(x)\}$ en termes de la base (1.64) comme suit

$$u(x,t) = 2u_0(t)(1-x) + \sum_{n=1}^{\infty} u_{1n}(t)4(1-x)\cos 2\pi nx + \sum_{n=1}^{\infty} u_{2n}(t)4\sin 2\pi nx, \tag{1.23}$$

$$f(x) = 2f_0(1-x) + \sum_{n=1}^{\infty} f_{1n}4(1-x)\cos 2\pi nx + \sum_{n=1}^{\infty} f_{2n}4\sin 2\pi nx, \tag{1.24}$$

où $u_0(t), u_{1n}(t), u_{2n}(t), f_0, f_{1n}$ et f_{2n} sont à déterminé.

L'ensemble de fonctions (1.22) n'est pas orthogonale et dans [86] un ensemble de fonctions donnée par

$$\{1, \quad \{\cos 2\pi nx\}_{n=1}^{\infty}, \quad \{x \sin 2\pi nx\}_{n=1}^{\infty}\}, \tag{1.25}$$

est obtenu qui avec (1.22) forment un système bi-orthogonal de fonctions.

Les inconnues sont déterminées en remplaçant les expressions de $\{u(x,t), f(x)\}$ dans l'équation (1.17) ce qui nous donne un système d'équations différentielles fractionnaires linéaires. Nous résolvons ces équations en utilisant les températures initiale et finale. L'unicité de la solution $\{u(x,t), f(x)\}$ est déterminée par la système biorthogonal.

1.4 Sur un problème inverse pour l'équation de diffusion en 2-dimensions avec des conditions aux limites non locales

Nous cherchons à déterminer la température $u(x,y,t)$, et un terme source (indépendant de la variable t) $f(x,y)$ pour l'équation de diffusion fractionnaire

$$D^{\alpha}_{0_+}(u(x,y,t)-u(x,y,0)) - \varrho\Delta u(x,t) = f(x,y), \qquad (x,y,t)\in Q_T, \quad (1.26)$$
$$u(x,y,0)=\varphi(x,y), \quad u(x,y,T)=\psi(x,y), \qquad (x,y)\in\Omega, \quad (1.27)$$
$$u(0,y,t)=u(1,y,t), \quad \frac{\partial u}{\partial x}(1,y,t)=0, \qquad (y,t)\in D, \quad (1.28)$$
$$u(x,0,t)=u(x,1,t)=0, \qquad (x,t)\in D, \quad (1.29)$$

où $D^{\alpha}_{0_+}$ représente la dérivée fractionnaire de Riemann-Liouville d'ordre $0<\alpha<1$, $\varrho>0$, $Q_T:=\Omega\times[0,T]$, $\Omega:=[0,1]\times[0,1]$, $D:=[0,1]\times[0,T]$, $\varphi(x,y)$ et $\psi(x,y)$ sont les températures initiale et finale, respectivement.

Le problème spectrale pour (1.26)-(1.29) est

$$-\frac{\partial^2 S}{\partial x^2}-\frac{\partial^2 S}{\partial y^2} = \lambda S, \qquad (x,y)\in\Omega, \quad (1.30)$$
$$S(0,y)=S(1,y),\ S(x,0) = S(x,1)=0,\ \frac{\partial S}{\partial x}(1,y)=0, \quad x,y\in[0,1]. \quad (1.31)$$

Le problème (1.30)-(1.31) est non-auto-adjoint. Les fonctions propres pour le problème spectrale n'est pas complète. Suivant [49], nous complétons les fonctions propres du problème (1.30)-(1.31) avec les fonctions propres associées (voir l'Annexe A.3) pour obtenir

$$\{Z_{0k}:=X_0(x)V_k(y), \quad Z_{(2m-1)k}:=X_m(x)V_k(y), \quad Z_{2mk}:=X_{2mk}(x)V_k(y)\}, \quad (1.32)$$

où

$$X_0(x) = 2, \quad V_k(y)=\sqrt{2}\sin(2\pi ky), \quad X_m(x)=4\cos(2\pi mx)$$
$$X_{2mk}(x) = 4(1-x)\sin(2\pi mx), \quad m,k\in\mathbb{N}.$$

L'ensemble des fonctions (1.32) est complèt et forme une base de Riesz pour l'espace $L^2(\Omega)$, mais il n'est pas orthogonal. Nous construisons une autre série complète de fonctions comprenant des fonctions propres et les fonctions propres associées du problème conjugué de (1.30)-(1.30)

$$\{W_{0k} := \tilde{X}_0(x)V_k(y), \quad W_{(2m-1)k} := \tilde{X}_m(x)V_k(y), \quad W_{2mk} := \tilde{X}_{2mk}(x)V_k(y)\}, \tag{1.33}$$

où

$$\tilde{X}_0(x) = x, \quad \tilde{X}_m(x) = x\cos(2\pi mx), \quad \tilde{X}_{2mk}(x) = \sin(2\pi mx),$$

pour $m, k \in \mathbb{N}$.

L'ensemble des fonctions (1.75)-(1.74) forme un système biorthogonal

$$\begin{array}{ccc} \{\underbrace{Z_{0k} := X_0(x)V_k(y)}, & \underbrace{Z_{(2m-1)k} := X_m(x)V_k(y)}, & \underbrace{Z_{2mk} := X_{2mk}(x)V_k(y)}\}, \\ \downarrow & \downarrow & \downarrow \\ \{W_{0k} := \tilde{X}_0(x)V_k(y), & W_{(2m-1)k} := \tilde{X}_m(x)V_k(y), & W_{2mk} := \tilde{X}_{2mk}(x)V_k(y)\}, \end{array}$$

pour $m, k \in \mathbb{N}$.

Notre premier résultat est le théorème suivant, qui étudie l'existence et l'unicité de la solution classique du problème direct (1.26)-(1.29).

Theorem 1.4.1. *Soit $\varphi(x,y)$ définie dans $\bar{\Omega}$ telle que $\varphi \in C^2(\Omega)$, $\varphi(0,y) = \varphi(1,y), \partial\varphi(1,y)/\partial x = 0$, et $\varphi(x,0) = \varphi(x,1) = 0$, alors il existe une solution unique classique du problème (1.26)-(1.29).*

Pour $\alpha = 1$ le problème direct a été étudie dans [50]; ici, nous retrouvons les résultats obtenus dans [50] pour $\alpha = 1$.

Notre approche pour la solvabilité du problème inverse est basée sur le développement de la solution $u(x,y,t)$ en utilisant le système ci-dessus biorthogonal.

On définit la solution du problème inverse:

Une paire de fonctions $\{u(x,y,t), f(x,y)\}$ est une solution du problème inverse qui satisfait $u(.,.,t) \in C^2(\Omega,\mathbb{R}), D^{\alpha}_{0_+}u(x,y,.) \in C([0,T],\mathbb{R})$, $f(x,y) \in C^2(\Omega,\mathbb{R})$ étant données les températures initiales et finales.

Nos principaux théorèmes sont

Theorem 1.4.2. *Soit $\varphi(x,y), \psi(x,y)$ définies dans $\bar{\Omega}$ telle que $\varphi, \psi \in C^2(\Omega)$, $\varphi(0,y) = \varphi(1,y), \partial\varphi(1,y)/\partial x = 0$, $\varphi(x,0) = \varphi(x,1) = 0$, $\psi(0,y) = \psi(1,y), \partial\psi(1,y)/\partial x = 0$, et $\psi(x,0) = \psi(x,1) = 0$. Alors il existe une solution unique du problème inverse (1.26)-(1.29).*

Theorem 1.4.3. *Pour toutes fonctions $\varphi, \psi \in L^2(\Omega)$ la solution du problème inverse (1.26)-(1.29) dépend continûment de la donnée initiale.*

1.5 Débruitage d'images par l'équation de la chaleur avec une dérivée fractionnaire en temps

Dans cette section, nous proposons une généralisation de l'équation intégrale linéaire fractionnaire

$$u(t) = u_0 + \partial^{-\alpha}Au(t), \quad 1 < \alpha < 2,$$

pour le débruitage d'images, où $\partial^{-\alpha}$ est l'intégrale fractionnaire au sens de Riemann-Liouville.

Le processus de débruitage d'images (simplification, lissage, restauration ou amélioration) peut être décrit comme dans la Figure 1.1. Nous avons une image bruitée ou dégradée $u(0)$ et à partir de cette image nous essayons de restaurer l'image idéale u (sans bruit). Dans la pratique, nous obtenons pas l'image idéale. Pour la validation des modèles de débruitage d'images nous considérons une image idéale et on ajoute un bruit à cette image pour obtenir une image bruitée ou dégradée. De cette manière, nous pouvons évaluer la performance du modèle pour le débruitage de l'images proposée.

La Figure 1.1 montre le process de débruitage d'une imageàa partir d'une image bruitée ou dégradée $u(0)$.

Comment obtenir le temps d'arrêt optimal?

Le temps optimale d'arrêt a été discuté par Dolecetta et Ferretti dans [30], et par Mrázek et Navara dans [87].

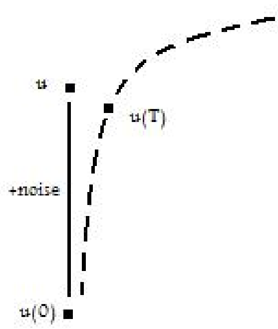

Figure 1.1: Le processus de débruitage d'image.

En 1960 Taizo Iijima [48] décrit une famille d'opérateurs qui satisfont aux quatre axiomes: linéarité, invariance par translation, invariance d'échelle et de la propriété semigroupe de simplification de l'image. Ces propriétés sont satisfaites par la solution des équations de la chaleur linéaire, lorsqu'il est appliqué à des images (voir l'annex A.4).

Pour l'équation de la chaleur linéaire

$$\begin{cases} \partial_t u(t,\mathbf{x}) &= \Delta u(t,\mathbf{x}), & (t,\mathbf{x}) \in [0,T]\times\Omega, \\ u(0,\mathbf{x}) &= u_0(\mathbf{x}), & \mathbf{x}\in\Omega, \\ \dfrac{\partial u}{\partial \eta}(t,\mathbf{x}) &= 0, & (t,\mathbf{x}) \in [0,T]\times\partial\Omega, \end{cases} \tag{1.34}$$

où $\Delta = \partial^2/\partial x^2 + \partial^2/\partial y^2$ est le Laplacien bidimensionnel, $u_0(\mathbf{x})$ est l'image initiale,

Ω est un domaine rectangulaire, la solution est donnée par

$$u(t,\mathbf{x}) = \int\limits_{\mathbb{R}^2} G_{\sqrt{2t}}(\mathbf{x}-\mathbf{y})u_0(\mathbf{x})d\mathbf{y} = (G_{\sqrt{2t}} * u_0)(\mathbf{x}), \tag{1.35}$$

où $G_\sigma(\mathbf{x})$ est le noyau Gaussien bidimensionnel:

$$G_\sigma(\mathbf{x}) = \frac{1}{2\pi\sigma^2}\ \ exp\left(-\frac{|\mathbf{x}|^2}{2\sigma^2}\right), \tag{1.36}$$

où $\mathbf{x} \in \mathbb{R}^2$, σ est un paramètre correspondant à l'écart-type. En raison de la diffusion isotrope de l'équation de la chaleur linéaire, le débruitage des images par des équations linéaires de la chaleur ne conservent pas les contours, les bords, la texture lors du processus de débruitage. Il y avait un besoin de processus de diffusion anisotrope qui ajuste un filtre passe-haut localement pendant le processus de diffusion.

Le but des modèles de débruitage d'images basées sur les équations aux dérivées partielles est de contrôler le processus de diffusion de l'équation de la chaleur linéaire. E. Cuesta et J. Finat [21] observe que l'intensité du processus de diffusion par l'équation de la chaleur linéaire peut être considérent une dérivé fractionnaire temporelle d'ordre $1 < \alpha < 2$; quand $\alpha \longrightarrow 2$ puis l'intensité du processus de diffusion est inférieure à celle de l'équation de la chaleur linéaire (1.34).

On propose pour contrôler le processus de diffusion de l'équation linéaire en choisissant l'ordre de la dérivée fractionnaire dans l'équation

$$\begin{cases} \partial_t^\alpha u(t,\mathbf{x}) &= \Delta u(t,\mathbf{x}), & (t,\mathbf{x}) \in [0,T]\times\Omega \\ u(0,\mathbf{x}) &= u_0(\mathbf{x}), & \mathbf{x}\in\Omega, \\ \partial_t u(0,\mathbf{x}) &= 0, & \mathbf{x}\in\Omega, \\ \dfrac{\partial u}{\partial \eta}(t,\mathbf{x}) &= 0, & (t,\mathbf{x}) \in [0,T]\times\partial\Omega, \end{cases} \tag{1.37}$$

où ∂_t^α représente la dérivée fractionnaire temporelle d'ordre $1 < \alpha < 2$ au sens de Riemann-Liouville. Par l'intégration fractionnaire la première équation du système (1.37) nous donne

$$u(t,\mathbf{x}) = u_0(\mathbf{x}) + \frac{1}{\Gamma(\alpha)}\int_0^t (t-s)^{\alpha-1}\Delta u(s,\mathbf{x})\,\mathrm{d}s,$$

avec une condition aux limites homogène de Neumann. Dans une forme compacte on a

$$u(t,\mathbf{x}) = u_0(\mathbf{x}) + \partial^{-\alpha}\Delta u(t,\mathbf{x}), \tag{1.38}$$

où $\partial^{-\alpha}$, pour $\alpha > 0$, représente l'intégrale d'ordre fractionnaire $\alpha \in \mathbb{R}^+$, au sens de Riemann - Liouville. L'équation fractionnaire intégrale interpole une équation linéaire parabolique et une équation linéaire hyperbolique (voir [33], [34]): la solution bénéficie des propriétés intermédiaires. L'équation de Volterra est bien posée pour tout $t > 0$. Elle permet de gérer la diffusion au moyen d'un *paramètre de* *viscosité* au lieu d'introduire une non-linéarité dans l'équation comme l'ont fait en Perona - Malik. Plusieurs expériences montrant les améliorations apportées par notre approche sont présentées au chapitre 5, section 5.6.

1.6 Sur l'amélioration du processus de débruitage d'images par l'équation de Volterra

Nous présentons une amélioration du modèle pour le débruitage d'images proposé dans [64] (voir Chapitre 5). Le facteur clé est la détermination de l'ordre de l'intégrale fractionnaire dans le modèle proposé dans [64] (voir Chapitre 5); par ce seul paramètre (α), nous pouvons contrôler le processus de diffusion. Obtenir le profil des α joue un rôle important pour le processus de débruitage. En fait, la nature du filtre proposé dans [64] (voir Chapitre 5) peut être changée en changeant le processus de détermination des α. Ici, nous proposons une méthode alternative pour la détermination de l'ordre de l'intégrale fractionnaire en utilisant le tenseur de structure de l'image.

Le tenseur de structure a été utilisé pour identifier plusieurs structures dans les images (voir e.g., [3, 10, 113] pour plus de détails) comme la texture, les coins, les jonctions T, etc; il est défini par

$$J_\rho(\nabla u_\sigma) := K_\rho \star (\nabla u_\sigma \otimes \nabla u_\sigma) \qquad \rho \geq 0, \tag{1.39}$$

où $u_\sigma = K_\sigma \star u(.,t)$,$\nabla u_\sigma \otimes \nabla u_\sigma := \nabla u_\sigma \nabla u_\sigma^t$, ρ est l'échelle de l'intégration, σ est appelée l'échelle locale ou le bruit.

Si λ_1, λ_2 sont les valeurs propres du tenseur de structure de (1.39) alors

- Les régions uniformes correspondent à $\lambda_1 = \lambda_2 = 0$
- Les chants droits correspondent à $\lambda_1 \gg \lambda_2 = 0$
- Les coins correspondent à $\lambda_1 \gg \lambda_2 \gg 0$.

Le choix de l'ordre de la dérivée dans le temps fractionnaire a été effectué pour chaque pixel en utilisant le *tenseur de structure* de l'image, ce qui nous permet de contrôler le processus de diffusion. Plusieurs expériences montrant une amélioration de notre approche à en termes de SNR, $PSNR$ sont présentés au chapitre 6, section 6.4.

Notre approche dans cette thèse pour le débruitage d'image reste isotrope, puisque la diffusion est régie par les scalaires α, tant au chapitre 5 qu'au chapitre 6. Il existe les approches générales vectorielle ([3, 113]) qui introduisent le tenseur de structure à la place de la fonction scalaire dans le modèle de débruitage, ce qui permet de contrôler la diffusion dans les images en tenant compte des deux directions orthogonals et peut conduire à des diffusions différentes sur chaque sens unique. Comme dit précédemment, la thèse portent sur l'approche scalaire, c'est à dire, pas de tenseur de diffusion est pris en compte dans l'équation du modèle.

Nous croyons que l'approche tensorielle dans le cadre du calcul fractionnaire donne de bons résultats.

1.7 Introduction (English)

In this thesis, we shall consider: a nonlinear system of fractional differential equations and study the local existence of its solutions, the occurrence of blowing-up solutions of the system. We also investigate the profile of blowing-up solutions concerning them. The inverse problem of a linear heat equation with a fractional derivative in time is considered. Let us mention that inverse problems for the differential equations involving fractional derivative is newly born field and there are very few articles concerning them (see Section 1.9). We have proposed a fractional derivative based model for the image denoising (simplification, smoothing, restoration or enhancement, section 1.12).

The importance of fractional calculus has been realized in the recent past because an explosion of research activities led to the fact that some phenomena from physics, finance, economics, fluid dynamics are well explained using fractional calculus.

Recently in [81], authors report some of the major documents published and events happened in the area of fractional calculus from 1974 till April 2010. According to which during this period 17 research monographs have been edited by different researchers; 67 books have been written by different authors; the topics are ranging from analytical theory of fractional calculus (for example [102], [62]) to applications, like viscoelasticity, nanotechnology (for example see [83], [7]). From 1974 to April 2010 there has been 35 international conferences fully devoted to the fractional calculus and its applications, and there are four journals publishing articles related to the fractional calculus and its applications.

The nonlinear analysis of differential equations involving fractional derivatives (specially fractional derivative in time) didn't get a reasonable attention. In particular, we can say that the theory of blow-up of solutions in finite time for the partial differential equations has been studied to a large extent from last few decades but the same problem, i.e., theory of blow-up of solutions in finite time for the fractional differential equations didn't get the attention of researchers. There are very few articles which consider the phenomena of blow-up and related questions see for examples [63], [108].

This chapter has six sections, in section 1.8 we describe some physical problems which has been modeled by fractional differential equations. In section 1.9 we consider a nonlinear system of fractional differential equations, sections 1.10 and 1.11 are concerned with the inverse problem of the linear heat equation in one and two dimensions, respectively. Sections 1.12 and 1.13 are about the application of a fractional differential equation to image processing.

1.8 Why study equations with fractional derivatives

This section is devoted to present some of the many physical applications which lead to equations involving fractional derivatives and integrals. These physical phenomena can be explained well using these equations.

Modifications in the laws of Physics

Several processes associated with complex physical systems have nonlocal dynamics which can be characterized by a long term memory in time. The fractional derivatives and integrals represent a non local behavior (due to the integral involved in the definition) associated with the past history related to the effects with memory. This is the main advantage of fractional calculus in explaining the processes associated with complex physical systems that have long term memory and/or long range spatial interactions.

Dynamics of fractal media: Generally the real media are characterized by complex and irregular geometry. Among several ways (Euclidean geometry, Stochastic models) for describing a complex structure of the media one is to use the fractal theory of sets of non integer dimensionality. But fractal media cannot be considered as continuous media as there are points and domains that are not filled of the medium particles. In [107] author proposed to replace the fractal medium with special continuous model i.e., replacement of fractal media with fractal mass dimension defined by some continuous medium described by fractional integrals. The fractional integrals are used to take in account the fractality of the media. This fractional continuous models allows to describe the dynamics of fractal media. The order of fractional integral is equal to the fractal mass dimension of the medium. For the proposed fractional continuous model several equations (Equation of continuity, equation of balance of momentum, equation of balance of energy, Euler's equations, Bernoulli integral equation, Navier-Stokes equations) concerning hydrodynamics of fractal media are considered.

The author [107] also consider the **dynamics of fractal rigid body** in the framework of fractional continuous media and compute the moments of inertia for fractal rigid body. The experiments shows that the fractional integrals can be used to describe the fractal rigid bodies. Furthermore, fractional Ginzburg-Landau equation, fractional generalizations of gradients system, Hamiltonian dynamical systems, fractional calculus of variation and fractional vector calculus used to described fractional quantum dynamics are discussed in [107]. For further reading of modeling and analysis of fractional order system we refer the reader to [92] and references therein.

A very valuable monograph about the modeling and applications of fractional integrals and derivatives to Polymer Physics, Rheology, Biophysics, thermodynamics, Chaotic systems has been edited by R. Hilfer [47].

Modifications in the laws of Mechanics

The basic mechanical models constructed from linear springs and dashpots, used one or both in form of series or parallel are

- The Hooke's model (a single spring)
- The Newton's model (a single dashpot)

- The Voigt's model (spring and dashpot in parallel)
- The Maxwell's model (spring and dashpot in series)
- The Zener's model (adding a spring in series to Voigt's model or in parallel to Maxwell's model)
- The anti-Zener's model (adding a dashpot in series to Voigt's model or in parallel to Maxwell's model).

By replacing the integer order derivative with the fractional derivative of order $\alpha \in (0, 1)$ (in the Riemann-Liouville or Caputo sense) a generalization of these laws of mechanics are considered in [83]. A study about the experimental verification of these theoretical laws is performed and it reveals that the order of fractional derivative i.e., α plays a significant role (along with other parameters) to better fit the experimental data (see [83] page 61).

Modification in the laws of Biomedical

In tissue electrode interface i.e., the interface used for recording some information of the tissues using some electronic devices such as in ECG (electrocardiogram), EMG (electromyography) or EEG (electroencephalograph) uses conventional lumped element circuit models of electrodes. In [51], the author discussed generalization of the order of differentiation (in the interface) through modification of the defining current-voltage relationships. The fractional order model provides improved description of bioelctrode behavior.

In [7] page 313 the authors introduce fractional derivative in the integer order model proposed in [40] for a delayed cellular neural network composed by only two cells. A chaotic behavior of the cells was observed in [40]. For the fractional order model (analog of the model proposed in [40]), the order of fractional derivative seems to explain the chaotic behavior observed in the experiments. Furthermore, the simulation results demonstrate that the values in which the system exhibits chaotic behavior decreases as the order of fractional derivative decreases, and these behaviors occur in a narrow region.

Let us present another model based on fractional derivative which is concerns Dengue epidemics. Dengue is the most rapidly spreading vector borne disease and has become a major public health concern in recent decades. In [94], the authors introduce the fractional derivative of order $0 < \alpha < 1$ in the ODE model of Dengue epidemics The numerical simulations of the model are more close to the real data of Dengue outbreak occurred in 2009 in Cape Verde in comparison to its integer order counterpart (for more details see [94]).

Modeling anomalous diffusion:

It is well known that reaction diffusion equation, transport equation, commonly used to explain the physical phenomena of diffusion process show in some situations a disagreement with experimental data (see Adams and Gelhar [1] page 3299).

The experimental data shows a long tail (non Gaussian) behavior of the water contamination as in Figure 1.2. This experimentally observed nonstandard behavior or anomaly is known as anomalous non Gaussian diffusion. Among several explanation for this anomalous diffusion (Continuous Time Random Walk CTRW, Stochastic process) one is by using fractional derivative in time or space, or both in the reaction diffusion equation, transport equation. There is a tremendous literature available see for example [46], [52] and references therein.

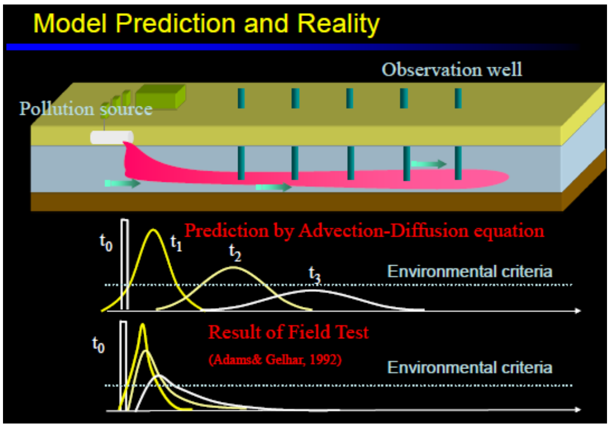

Figure 1.2: Long tailed behavior observed experimentally (Courtesy Dr. Yuko Hatano, Department of Risk Engineering, University of Tsukuba)

The fundamental solution of the operator $\partial_t - \Delta$ is Gaussian kernel which diffuses the solution very rapidly, only near $t = 0$ the long tail or slow diffusion is expected resulting no long tailed or so called up hill behavior of the solutions involving the operator $\partial_t - \Delta$.

The fundamental solution of the operator $\partial_t^\alpha - \Delta$, where ∂_t^α is the Caputo fractional derivative of order $0 < \alpha < 1$ is presented in [29]; it demonstrates that the fundamental solution shows the long tailed or up hill behavior. The parameter α i.e., order of fractional order derivative is important for explaining the anomaly of diffusion process.

Let us mention that an intermediate behavior to linear heat equation and linear wave equation for the solution of linear heat equation involving Caputo fractional derivative of order $1 < \alpha < 2$ has been proposed in [33, 34]. In chapter 5 and 6, experiments for image denoising validate that the diffusion in linear heat equation can be controlled by the order of fractional order derivative.

Modifications in the usual laws of Finance

It is well known that the continuous-time random walk (CTRW) is a good model for the dynamics in financial markets, as, in general, this dynamics is non-Markovian or non-local.

In [103] the authors present a so called 'the master equation' which governs the probability density profile of a CTRW and showed that it reduces to the fractional diffusion equation in the hydrodynamic limit under some assumptions. In fractional diffusion equation the order of fractional time derivative and space derivative considered are $0 < \alpha \leq 1$ and $0 < \beta \leq 2$, respectively. Later in [82] the authors provide an example which is consistence with the theory presented in [103], which validates that the concepts of CTRW and of fractional calculus are helpful in practical applications such as option pricing, as they provide an intuitive background for dealing with non-Markovian and non-local random processes.

Apart from the above few examples there are numerous physical phenomena from nanotechnology, control theory, viscoplasticity flow, biology, mechanical engineering, which has been modeled by using fractional integrals or derivatives for more details see the latest monographs [7, 71, 83, 101].

My achievements in fractional differential equations are presented hereafter.

1.9 The Profile of blowing-up solutions to a nonlinear system of fractional differential equations

We are concerned with the nonlinear nonlocal system (FDS)

$$\begin{aligned} u'(t) + D^{\alpha}_{0_+}(u-u_0)(t) &= v(t)^q, \qquad t>0,\\ v'(t) + D^{\beta}_{0_+}(v-v_0)(t) &= u(t)^p, \qquad t>0, \end{aligned}$$

where $u(0) = u_0 > 0, v(0) = v_0 > 0, p > 1, q > 1$ are given constants, $D^{\alpha}_{0_+}$ and $D^{\beta}_{0_+}$, $0 < \alpha < 1$, $0 < \beta < 1$ stand for the Riemann-Liouville fractional derivatives. The system (FDS) has been considered by Furati and Kirane [35]; they proved the existence of blowing-up solutions for the system (FDS) in finite time.

Theorem 1.9.1 ([35]). *Suppose that $0 < \alpha, \beta < 1$, $p > 1, q > 1$ and $u_0 > 0$, $v_0 > 0$, then solutions to the system (FDS) blow-up in a finite time.*

The method of proof is based on reaching a contradiction to the supposition $u_0 > 0, v_0 > 0$ by considering the weak formulation of the solution and with a judicious choice of the test function given by

$$\varphi(t) = \begin{cases} T^{-\lambda}(T-t)^{\lambda}, & t \in [0,T],\\ 0, & t > T. \end{cases} \tag{1.40}$$

The test function satisfies

$$\int_0^T D^{\alpha}_{T_-}\varphi(t)dt = C_{\alpha,\lambda}T^{1-\alpha}, \quad C_{\alpha,\lambda} = \frac{\Gamma(\lambda+1)}{\Gamma(\lambda-\alpha+2)}, \tag{1.41}$$

and for $p > 1$, $\lambda > \alpha p - 1$ (see Appendix A.1.1)

$$\int_0^T \varphi^{1-p}(t)\left|D^{\alpha}_{T-}\varphi(t)\right|^p dt = C_{p,\alpha}T^{1-\alpha p}, \tag{1.42}$$

where

$$C_{p,\alpha} = \frac{1}{\lambda - p\alpha + 1}\left[\frac{\Gamma(\lambda+1)}{\Gamma(\lambda+1-\alpha)}\right]^p. \tag{1.43}$$

For the sub-linear case, i.e., when $0 < p, q \leq 1$ the solution of the system (FDS) is global.

Theorem 1.9.2 ([35]). *Suppose that* $0 < \alpha, \beta < 1$, $0 < p, q \leq 1$, *then any solutions to the system (FDS) subject to* $u(0) = u_0 > 0$, $v(0) = v_0 > 0$ *is global.*

Once we have the result about the existence of blowing-up solutions of the system (FDS) then the question about the profile of the blowing- up solutions arise. We investigate the profile of blowing-up solutions of the system (FDS).

The profile of the blowing-up solutions of the system (FDS) is obtained by presenting some estimates from above and below. These estimates are determined by making a comparison of blowing-up solutions of the system (FDS) with the solutions of the sub-systems obtained by dropping the fractional derivative from the system (FDS)

$$\begin{aligned} u'(t) &= \lambda v(t)^q, \qquad t > 0, \quad p > 1, \\ v'(t) &= \lambda u(t)^p, \qquad t > 0, \quad q > 1, \end{aligned}$$

the system of ordinary differential equations (ODS) with either $\lambda = 1$, and by dropping the usual derivatives from (FDS)

$$\begin{aligned} D^\alpha_{0+}(u - u_0)(t) &= \mu v(t)^q, \qquad t > 0, \quad q > 1, \\ D^\beta_{0+}(v - v_0)(t) &= \mu u(t)^p, \qquad t > 0, \quad p > 1, \end{aligned}$$

the system of fractional differential equations (PFDS), with either $\mu = 1$. The system (ODS) is easy to solve and for the expressions for its blowing-up solutions and exact time of blow-up (see Chapter 2). We will investigate the system (PFDS).

Let us state the preliminary Lemmas and for the proofs the reader is directed to Chapter 2.

Lemma 1.9.3. *The components of the solution* (u, v) *to the system (FDS) satisfy the integral equations*

$$u(t) = u_0 + \int_0^t e_{1-\alpha}(t-\tau)v(\tau)^q d\tau, \tag{1.44}$$

$$v(t) = v_0 + \int_0^t e_{1-\beta}(t-\tau)u(\tau)^p d\tau. \tag{1.45}$$

Lemma 1.9.4. *For the system (FDS), the functions* $u'(t)$ *and* $v'(t)$ *satisfy the integral equations*

$$u'(t) = v(t)^q + \int_0^t e'_{1-\alpha}(t-\tau)v(\tau)^q d\tau, \tag{1.46}$$

$$v'(t) = u(t)^p + \int_0^t e'_{1-\beta}(t-\tau)u(\tau)^p d\tau. \tag{1.47}$$

Lemma 1.9.5. *The system (FDS) and the integral equations (1.44)-(1.45) are equivalent.*

Lemma 1.9.6. *For any $u_0 > 0$, $v_0 > 0$, it holds:*

$$u' > 0, \quad v' > 0.$$

For proving local existence of the solution to the system (FDS) via its equivalent integral equations (c.f (1.44)-(1.45)), we need the following ingredients:

- First, we set for $u, v \in C([0,T])$,

  $$\Delta := \{t \in \mathbb{R}^+ / 0 \le t \le T, |u - u_0| < c, |v - v_0| < c\}.$$

  Let $K_1 := v_0^q, K_2 := u_0^p$.
  On Δ the nonlinearities satisfy the Lipschitz conditions

  $$|v_1^q - v_2^q| \le L_1 |v_1 - v_2|, \qquad |u_1^p - u_2^p| \le L_2 |u_1 - u_2|, \tag{1.48}$$

  where

  $$L_1 := q(c + u_0)^{q-1}, \qquad L_2 := p(c + v_0)^{p-1}.$$

  We set $K := \max\{K_1, K_2\}$, $L := \max\{L_1, L_2\}$.

- We have for $0 \le t \le T$,

  $$\int_0^t e_{1-\alpha}(t-\tau)d\tau \le M_1 < \infty, \quad \int_0^t e_{1-\beta}(t-\tau)d\tau \le M_2 < \infty,$$

  where e_γ is defined via the Mittag-Leffler function $e_\gamma := E_\gamma(-\lambda t^\gamma)$ for $\lambda \in \mathbb{R}$.

Further, we set, for any $0 < \rho < 1$, $P := \min(\rho/L, c/K)$, and $h := \min(r, T)$, where $r := \min(r_1, r_2)$ and r_1, r_2 are determined by

$$\int_0^t e_{1-\alpha}(t-\tau)d\tau \le P, \quad 0 \le t \le r_1, \quad \text{and} \quad \int_0^t e_{1-\beta}(t-\tau)d\tau \le P, \quad 0 \le t \le r_2.$$

We have the following existence theorem.

Theorem 1.9.7. *For any $u_0 > 0, v_0 > 0$ given, the integral equations (1.44)-(1.45) have a unique continuous solution on the interval $0 \le t \le h$.*

For the proof we use the classical iterative method and then extend the solution to the interval $[h, 2h]$ so on and so forth till we reach T (see Chapter 2, Theorem 2.3.4).

For the system (PFDS), we provide the result about the blowing-up solutions in finite time.

Let us set:

$$s = \frac{p\alpha + \beta}{1 - pq}, \quad \tilde{s} = \frac{\alpha + q\beta}{1 - pq}, \quad C_v = K_2(K_1)^{\frac{p}{pq-1}}, \quad C_u = K_2^*(K_1^*)^{\frac{q}{pq-1}}, \tag{1.49}$$

where K_1, K_2, K_1^* and K_2^* are:

$$K_1 = C_{p',\alpha}^{\frac{1}{p'}} C_{q',\beta}^{\frac{1}{pq'}}, \quad K_2 = C_{q',\beta}^{\frac{1}{q'}} C_{\beta,\lambda}^{-1},$$

$$K_1^* = C_{q',\beta}^{\frac{1}{q'}} C_{p',\alpha}^{\frac{1}{qp'}}, \quad K_2^* = C_{p',\alpha}^{\frac{1}{p'}} C_{\alpha,\lambda}^{-1},$$

and the constants $\{C_{\alpha,\lambda}, C_{\beta,\lambda}\}$ and $\{C_{p',\alpha}, C_{q',\beta}\}$ are given by (1.41) and (1.43).

Theorem 1.9.8. *Let $p > 1, q > 1$ and $u_0 > 0$, $v_0 > 0$, then any solution to the system (PFDS) with $\mu = 1$ subject to the initial conditions $u(0) = u_0 > 0, v(0) = v_0 > 0$ blows up in a finite time T_{max}. Furthermore, an upper bound on the blow up time T_{max} is given by $min\{T_u, T_v\}$ where*

$$T_v = \left[\frac{v_0}{C_v}\right]^{1/s} \quad T_u = \left[\frac{u_0}{C_u}\right]^{1/\tilde{s}},$$

where $s, \tilde{s}, C_u$ and C_v are given in (1.49).

Notice that the system (PFDS) is equivalent to the following system of nonlinear Volterra integral equations

$$\begin{cases} u(t) = u_0 + \frac{\mu}{\Gamma(\alpha)} \int\limits_0^t \frac{v(\tau)^q}{(t-\tau)^{1-\alpha}} d\tau, & t > 0, \\ v(t) = v_0 + \frac{\mu}{\Gamma(\beta)} \int\limits_0^t \frac{u(\tau)^p}{(t-\tau)^{1-\beta}} d\tau, & t > 0. \end{cases} \tag{1.50}$$

Following [90], growth rates near the blow-up time for blowing up solutions to the system (1.50) con be obtained. They are stated in

Theorem 1.9.9. *The profiles of the components of the solution $(u(t), v(t))$ for the system (1.50) with $\mu = 1$ are given by*

$$u(t) \sim C_{1,\alpha,\beta}(T_{max}^{\alpha,\beta} - t)^{-\delta}, \quad v(t) \sim C_{2,\alpha,\beta}(T_{max}^{\alpha,\beta} - t)^{-\xi}, \quad \text{as} \quad t \to T_{max}^{\alpha,\beta}, \tag{1.51}$$

where $T_{max}^{\alpha,\beta}$ is the blow-up time and

$$C_{1,\alpha,\beta} = \left(\frac{\Gamma(p\delta)}{\Gamma(p\delta - \beta)}\right)^{\frac{q}{pq-1}} \left(\frac{\Gamma(q\xi)}{\Gamma(q\xi - \alpha)}\right)^{\frac{1}{pq-1}},$$

$$C_{2,\alpha,\beta} = \left(\frac{\Gamma(q\xi)}{\Gamma(q\xi-\alpha)}\right)^{\frac{p}{pq-1}} \left(\frac{\Gamma(p\delta)}{\Gamma(p\delta-\beta)}\right)^{\frac{1}{pq-1}},$$

with

$$\delta = \frac{\alpha + q\beta}{pq-1}, \quad \xi = \frac{\beta + p\alpha}{pq-1}. \tag{1.52}$$

For the system (PFDS), we have calculated the bounds for the blow-up time T_{max} via its equivalent integral equations (1.50). We follow the analysis of the valuable paper [90] for getting the bounds on the blow-up time. For the proofs of Theorem 1.9.9 and Theorem 1.9.10 see Appendix A.1.

Theorem 1.9.10. *For the system of Volterra integral equations (1.50), $u(t) \to \infty$ and $v(t) \to \infty$ as $t \to T_{max}$, where*

$$T_L \leq T_{max} \leq T_U.$$

The bounds T_L and T_U are given by

$$T_L := \begin{cases} \theta\left[\frac{\alpha(r-1)^{r-1}}{\gamma r^r}\right]^{1/(\alpha)}, & if \;\; \alpha(r-1)^{r-1} \leq \gamma r^r, \\ \theta\left[\frac{\beta(r-1)^{r-1}}{\gamma r^r} - \frac{\beta-\alpha}{\alpha}\right]^{1/(\beta)} & if \;\; \alpha(r-1)^{r-1} > \gamma r^r. \end{cases} \tag{1.53}$$

$$T_U := \begin{cases} \theta\left[\frac{\beta(r+1)}{\gamma(pq-1)}\right]^{1/(\beta)}, & if \;\; \beta(r+1) \leq \gamma(pq-1), \\ \theta\left[\frac{\alpha(r+1)}{\gamma(pq-1)} - \frac{\beta-\alpha}{\beta}\right]^{1/(\beta)} & if \;\; \beta(r+1) > \gamma(pq-1). \end{cases} \tag{1.54}$$

where

$$\theta = \left[\frac{\Gamma(\beta)v_0^{q+1}}{\Gamma(\alpha)u_0^{p+1}}\right]^{1/(\beta-\alpha)}, \quad r := \max(p,q),$$

and

$$\gamma := \mu\left(\frac{[\Gamma(\beta)]^{\alpha}[v_0]^{\beta q+\alpha}}{\Gamma(\alpha)]^{\beta}[u_0]^{\alpha p+\beta}}\right)^{\frac{1}{\beta-\alpha}}.$$

Due to the complete monotonicity property of the Mittag-Leffler function whenever $0 < \alpha < 1$ (see [38]) and using Lemma 1.9.3 and Lemma 1.9.4, the following configuration is obtained

$$\begin{array}{cc} D^{\alpha}_{0_+}(u-u_0)(t) \leq v(t)^q, & D^{\beta}_{0_+}(v-v_0)(t) \leq u(t)^p, \\ u'(t) \leq v(t)^q, & v'(t) \leq u(t)^p. \end{array} \tag{1.55}$$

Solutions of these differential inequalities provide the estimates from above to the solution of the system (FDS).

Furthermore, from the system (FDS) along with $u' > 0, v' > 0$ (c.f Lemma 1.9.6) and $u'' > 0, u'' > 0$ we have the system (ODSL)

$$u'(t) \geq \frac{v(t)^q \Gamma(2-\alpha)}{\Gamma(2-\alpha) + t^{1-\alpha}}, \qquad v'(t) \geq \frac{u(t)^p \Gamma(2-\beta)}{\Gamma(2-\beta) + t^{1-\beta}}.$$

The analysis of the above inequalities leads to the precise profile of the blowing up solutions of the system (FDS).

1.10 Determination of an unknown source term and the temperature distribution for the linear heat equation involving fractional derivative in time

We consider the inverse problem of finding $u(x,t)$ (the temperature distribution) and $f(x)$ (the source term) in the domain $Q_T = (0,1) \times (0,T)$ for the following fractional diffusion equation

$$\begin{aligned} D^{\alpha}_{0_+}(u(x,t) - \varrho u(x,0)) - u_{xx}(x,t) &= f(x), \qquad (x,t) \in Q_T, && (1.56)\\ u(x,0) = \varphi(x) \quad u(x,T) &= \psi(x), \qquad x \in [0,1], && (1.57)\\ u(1,t) = 0, \quad u_x(0,t) &= u_x(1,t), \quad t \in [0,T], && (1.58) \end{aligned}$$

where $\varrho > 0$, $D^{\alpha}_{0_+}$ stands for the Riemann-Liouville fractional derivative of order $0 < \alpha < 1$, $\varphi(x)$ and $\psi(x)$ are the initial and final temperatures, respectively.

Let us mention that for the solvability of inverse problems "uniqueness" of the inverse problem has more importance than existence and stability, because if we have the uniqueness of the inverse problem then we can obtained the existence and stability of the inverse problem by some efficient numerical schemes. If an inverse problem doesn't have a unique solution then we have no hope for solving it (see [54], pg. 21).

The choice of the term $D^{\alpha}_{0_+}(u - u_0)(t)$ in equation (1.56) rather than the usual term $D^{\alpha}_{0_+}u(t)$ has been made to avoid the singularity at zero as well as for imposing the meaningful initial condition to the problem.

There are very few articles which consider the inverse problem of differential equations involving fractional derivative in time. Let us mention that in [17], the authors consider the inverse problem of determination of order of fractional derivative and diffusion coefficient for one dimensional diffusion equation (they consider the fractional time derivative defined in the sense of Caputo). They proved the unique determination of order of fractional derivative and diffusion coefficient (independent of time); their proof based on the eigenfunction expansion of the weak solution to the problem and the involved Gelfand-Levitan theory.

In [118], the inverse problem of determination of source term (which is independent of time variable) for the so-called fractional diffusion equation

$$\begin{aligned} {}^{C}D^{\alpha}_{0_+}u(x,t) - u_{xx}(x,t) &= f(x), \qquad (x,t) \in Q_T, && (1.59)\\ u(x,0) &= \varphi(x), \qquad x \in [0,1], && (1.60)\\ -u_x(1,t) = 0, \quad u_x(0,t) &= 0, \qquad t \in [0,T], && (1.61) \end{aligned}$$

where ${}^{C}D^{\alpha}_{0_+}$, for $0 < \alpha < 1$ stands for the Caputo fractional derivative has been addressed. The unique determination of the source term is proved by using an analytic continuation along with Duhamel's principle.

As we have mentioned earlier for the solvability of inverse problems uniqueness of the solution is the most important point. Once we have the unique solvability of the inverse problem then efficient and stable numerical schemes could be adopted for getting an approximation (to a desired accuracy) of the solution. Recently, few articles addressed the inverse problem for the fractional diffusion equation by different numerical algorithms (see [117], [79]).

Let us mention that due to the nonlocal boundary conditions $u(1,t) = 0,\ u_x(0,t) = u_x(1,t),\ t \in [0,T]$, the underlying spectral problem

$$-X'' = \lambda X, \quad X(1) = 0, \quad X'(0) = X'(1), \tag{1.62}$$

violates the self adjointness property, so an orthonormal basis formed by the eigenfunctions in $L^2(0,1)$ is lacking.

How to overcome lack of orthonormal basis property of eigenfunctions?
The answer to that problem is to get the biorthogonal system of functions for the space $L^2(0,1)$. Let us recall that two set of functions S_1 and S_2 of $L^2(0,1)$ form a biorthogonal system of functions if a one-to-one correspondence can be established between them such that the integral of the product of two corresponding functions is equal to unity and the integral of the product of two non-corresponding functions is equal to zero i.e.,

$$\int_0^1 f_i g_j = \delta_{ij}, \tag{1.63}$$

where $f_i \in S_1$, $g_i \in S_2$ and δ_{ij} is the Kronecker delta. The biorthogonal system consisting of set of functions S_1 and S_2 is said to be complete, if the set of functions S_1 and S_2 are complete. By virtue of (1.63) the set of functions S_1 and S_2 forming biorthogonal system are linearly independent.

The biorthogonal system allow us to write the solution of the inverse problem into eigenfunctions and associated eigenfunctions i.e., the eigenfunctions of the adjoint problem of (1.62) (sometimes also called conjugate problem) and then try to get the unknowns.

Let us recall a sequence $\{x_n\}_{n=1}^{\infty}$ in a Hilbert space H is known as Riesz sequence if there exist constants $0 < c \leq C < \infty$ such that

$$c\sum_{n=1}^{\infty}|a_n|^2 \leq \left\|\sum_{n=1}^{\infty}a_n x_n\right\|^2 \leq C\sum_{n=1}^{\infty}|a_n|^2,$$

for all sequences of scalars $\{a_n\}_{n=1}^{\infty}$ in the ℓ^2 space,

$$\ell^2 := \left\{ (a_1, a_2, ..., a_n, ...)/a_n \in \mathbb{R} \ \text{ s.t } \ \sum_{n=1}^{\infty} |a_n|^2 < \infty \right\}.$$

A Riesz basis for a Hilbert space H is a Riesz sequence which is linearly independent and span the space H.

The key factor in determination of the temperature distribution and the unknown source term for the system (1.56)-(1.58) is the specially chosen basis for the space $L^2(0,1)$ which is

$$\{2(1-x), \quad \{4(1-x)\cos 2\pi nx\}_{n=1}^{\infty}, \quad \{4\sin 2\pi nx\}_{n=1}^{\infty}\}, \tag{1.64}$$

(see Appendix A.2 for the construction of the basis).

In [53], it is proved that the set of functions in (1.64) forms a Riesz basis for the space $L^2(0,1)$.

As usual the idea is to decompose the pair of unknown functions $\{u(x,t), f(x)\}$ in terms of the basis (1.64) as

$$u(x,t) = 2u_0(t)(1-x) + \sum_{n=1}^{\infty} u_{1n}(t)4(1-x)\cos 2\pi nx + \sum_{n=1}^{\infty} u_{2n}(t)4\sin 2\pi nx, \tag{1.65}$$

$$f(x) = 2f_0(1-x) + \sum_{n=1}^{\infty} f_{1n}4(1-x)\cos 2\pi nx + \sum_{n=1}^{\infty} f_{2n}4\sin 2\pi nx, \tag{1.66}$$

where $u_0(t), u_{1n}(t), u_{2n}(t), f_0, f_{1n}$ and f_{2n} are to be determined.

The set of functions (1.64) is not orthogonal and in [86] a set of functions given by

$$\{1, \quad \{\cos 2\pi nx\}_{n=1}^{\infty}, \quad \{x\sin 2\pi nx\}_{n=1}^{\infty}\}, \tag{1.67}$$

is constructed, which together with (1.64) form a biorthogonal system of functions.

The unknowns are determined by plugging the series expressions of $\{u(x,t), f(x)\}$ into the equation (1.56) which gives us a system of linear fractional differential equations and solving these equations using the initial and final temperature data. The uniqueness of the solution $\{u(x,t), f(x)\}$ is determined by using the basis (1.67). By using properties of Mittag-Leffler functions and biorthogonal basis (1.67)-(1.64) the term by term differentiation of the solution $\{u(x,t), f(x)\}$ has been justified which ensures the existence of the solution to the inverse problem.

1.11 An inverse source problem for a two dimensional time fractional diffusion equation with nonlocal boundary conditions

We are interested in determination of the temperature distribution $u(x,y,t)$, and a source term (independent of time variable) $f(x,y)$ for the following time fractional diffusion equation

$$D^{\alpha}_{0+}(u(x,y,t)-u(x,y,0))-\varrho\Delta u(x,t)=f(x,y), \qquad (x,y,t)\in Q_T, \quad (1.68)$$

$$u(x,y,0)=\varphi(x,y), \quad u(x,y,T)=\psi(x,y), \qquad (x,y)\in\Omega, \quad (1.69)$$

$$u(0,y,t)=u(1,y,t), \quad \frac{\partial u}{\partial x}(1,y,t)=0, \qquad (y,t)\in D, \quad (1.70)$$

$$u(x,0,t)=u(x,1,t)=0, \qquad (x,t)\in D, \quad (1.71)$$

where D^{α}_{0+} stands for the Riemann-Liouville fractional derivative of order $0<\alpha<1$, $\varrho>0$, $Q_T:=\Omega\times[0,T]$, $\Omega:=[0,1]\times[0,1]$, $D:=[0,1]\times[0,T]$, $\varphi(x,y)$ and $\psi(x,y)$ are the initial and final temperatures respectively.

Let us mention that the final temperature i.e., $u(x,y,t)=\psi(x,y)$ is the over determination condition required for the unique determination of the source term.

The underlying spatial spectral problem for (1.68)-(1.71) is

$$-\frac{\partial^2 S}{\partial x^2}-\frac{\partial^2 S}{\partial y^2} = \lambda S, \qquad (x,y)\in\Omega, \quad (1.72)$$

$$S(0,y)=S(1,y),\ S(x,0) = S(x,1)=0,\ \frac{\partial S}{\partial x}(1,y)=0,\ x,y\in[0,1]. \quad (1.73)$$

The boundary value problem (1.72)-(1.73) is non-self-adjoint. The eigenfunctions for the spatial spectral problem is not complete and following [49], we supplement the eigenfunctions of the boundary value problem (1.72)-(1.73) with associated eigenfunctions (see Appendix A.3) and obtain

$$\{Z_{0k}:=X_0(x)V_k(y), \quad Z_{(2m-1)k}:=X_m(x)V_k(y), \quad Z_{2mk}:=X_{2mk}(x)V_k(y)\}, \quad (1.74)$$

where

$$\begin{aligned} X_0(x) &= 2, \quad V_k(y)=\sqrt{2}\sin(2\pi ky), \quad X_m(x)=4\cos(2\pi mx)\\ X_{2mk}(x) &= 4(1-x)\sin(2\pi mx), \quad m,k\in\mathbb{N}. \end{aligned}$$

The set of functions (1.74) is complete and form a Riesz basis for the space $L^2(\Omega)$, but it is not orthogonal. We construct another complete set of functions consisting of eigenfunctions and associated eigenfunctions of the conjugate problem of (1.72)-(1.72)

$$\{W_{0k}:=\tilde{X}_0(x)V_k(y), \quad W_{(2m-1)k}:=\tilde{X}_m(x)V_k(y), \quad W_{2mk}:=\tilde{X}_{2mk}(x)V_k(y)\}, \quad (1.75)$$

where

$$\tilde{X}_0(x)=x, \quad \tilde{X}_m(x)=x\cos(2\pi mx), \quad \tilde{X}_{2mk}(x)=\sin(2\pi mx),$$

for $m,k\in\mathbb{N}$.

The set of functions (1.75)-(1.74) form a biortogonal system of function under the correspondence

$$\begin{array}{ccc} \{\underbrace{Z_{0k}:=X_0(x)V_k(y)}, & \underbrace{Z_{(2m-1)k}:=X_m(x)V_k(y)}, & \underbrace{Z_{2mk}:=X_{2mk}(x)V_k(y)}\}, \\ \downarrow & \downarrow & \downarrow \\ \{W_{0k}:=\tilde{X}_0(x)V_k(y), & W_{(2m-1)k}:=\tilde{X}_m(x)V_k(y), & W_{2mk}:=\tilde{X}_{2mk}(x)V_k(y)\}, \end{array}$$

for $m, k = 1, 2, ...$

First, we provide the result about existence and uniqueness of the classical solution of the direct problem in

Theorem 1.11.1. *Let $\varphi(x,y)$ be defined in $\bar{\Omega}$ such that $\varphi \in C^2(\Omega)$ and $\varphi(0,y) = \varphi(1,y), \partial\varphi(1,y)/\partial x = 0$, and $\varphi(x,0) = \varphi(x,1) = 0$, then there exist a unique classical solution of the problem (1.68)-(1.71).*

For $\alpha = 1$ the direct problem was considered in [50]; here, we recover the results obtained in [50] for $\alpha = 1$.

Our approach for the solvability of the inverse problem is based on the expansion of the solution $u(x,y,t)$ by using the above biorthogonal system.

Let us define the solution of the inverse problem:

A pair of functions $\{u(x,y,t), f(x,y)\}$ is a solution of the inverse problem satisfying $u(.,.,t) \in C^2(\Omega,\mathbb{R}), D^{\alpha}_{0+}u(x,y,.) \in C([0,T],\mathbb{R}),\ f(x,y) \in C^2(\Omega,\mathbb{R})$ given the initial and final temperatures.

Our main theorems are

Theorem 1.11.2. *Let $\varphi(x,y), \psi(x,y)$ be defined in $\bar{\Omega}$ such that $\varphi, \psi \in C^2(\Omega)$, $\varphi(0,y) = \varphi(1,y), \partial\varphi(1,y)/\partial x = 0$, $\varphi(x,0) = \varphi(x,1) = 0$ and $\psi(0,y) = \psi(1,y), \partial\psi(1,y)/\partial x = 0$, and $\psi(x,0) = \psi(x,1) = 0$. Then there exist a unique solution of the inverse problem (1.68)-(1.71).*

Theorem 1.11.3. *For any $\varphi, \psi \in L^2(\Omega)$ the solution of the inverse problem (1.68)-(1.71) depends continuously on the given data.*

1.12 Image structure preserving denoising using generalized fractional time integrals

In this section, we propose a generalization of the linear fractional integral equation

$$u(t) = u_0 + \partial^{-\alpha}Au(t), \quad 1 < \alpha < 2,$$

for image denoising (simplification, smoothing, restoration or enhancement), where $\partial^{-\alpha}$ is the fractional integral in the sense of Riemann-Liouville. For the better understanding of the reader, let us briefly describe the image denoising problem and some state of the art of partial differential equations based models for image denoising.

Among several problems of digital image processing one of the basic task is image denoising (simplification, smoothing, restoration or enhancement). The crucial step in image denoising is to distinguish between the interesting feature of an image to be enhanced or preserved and the noise in the image to be removed.

What do we mean by the interesting feature of an image or important information in image?

Its answer depends on the application, on client (user) in which features of the image one is interested in. In image denoising process, we have to remove the noise by keeping or preserving the important features of the image. These two tasks seem to be contradictory and infact they are.

The image denoising (simplification, smoothing, restoration or enhancement) process can be described as in Figure 1.3. We have a noisy or degraded image $u(0)$ and from that image we try to restore the ideal image u (without noise). In practice, we don't have the ideal image, for the validation of the image denoising models we consider an image to be an ideal and add some noise to that image for getting the noisy or degraded image. By this way we can evaluate the performance of the proposed image denoising model.

In practice or in real situation the image degradation could occur due to several reasons, for example, due to some inherent problem of the image capturing device such as bad focusing, dust on the lenses or due to the motion of target object or the capturing device. The Figure 1.3 shows image denoising process of a noisy or degraded image $u(0)$. We start from a noisy image and the denoising process removes the noise as the denoising evolves in time. The problem of stopping the denoising or restoration process demands the calculation of the optimal stoping time T for the denoising or restoration algorithm.

How to get the optimal stopping time?

The question is very interesting and important for the denoising models based on partial differential equations. However, we will not consider this question in this thesis and it will be the topic of future work. The optimal stoping time has been discussed by Dolecetta and Ferretti in [30], and by Mrázek and Navara in [87].

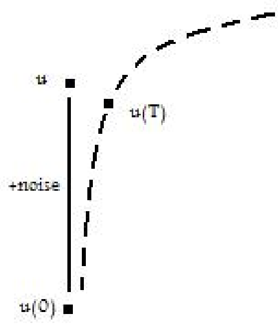

Figure 1.3: Optimal stoping time: u is the real scene, u(0) is the degraded or noisy image, $u(T)$ is the best possible restoration at the optimal time T.

In 1960 Taizo Iijima [48] described a family of operators which satisfy the four axioms: linearity, translation invariance, scale invariance and semigroup property for image simplification. These properties are satisfied by the solution of the linear heat equations, when applied to images (see Appendix A.4).

For the linear heat equation

$$\begin{cases} \partial_t u(t,\mathbf{x}) &= \Delta u(t,\mathbf{x}), & (t,\mathbf{x}) \in [0,T] \times \Omega, \\ u(0,\mathbf{x}) &= u_0(\mathbf{x}), & \mathbf{x} \in \Omega, \\ \dfrac{\partial u}{\partial \eta}(t,\mathbf{x}) &= 0, & (t,\mathbf{x}) \in [0,T] \times \partial\Omega, \end{cases} \tag{1.76}$$

where $\Delta = \frac{\partial^2}{\partial x^2} + \frac{\partial^2}{\partial y^2}$ is the two dimensional Laplacian, $u_0(\mathbf{x})$ is the initial image, Ω is a rectangular domain, the solutions is given by

$$u(t,\mathbf{x}) = \int\limits_{\mathbb{R}^2} G_{\sqrt{2t}}(\mathbf{x}-\mathbf{y}) u_0(\mathbf{x}) d\mathbf{y} = (G_{\sqrt{2t}} * u_0)(\mathbf{x}), \tag{1.77}$$

with $G_\sigma(\mathbf{x})$ is the two dimensional Gaussian kernel;

$$G_\sigma(\mathbf{x}) = \frac{1}{2\pi\sigma^2} \; exp\left(-\frac{|\mathbf{x}|^2}{2\sigma^2}\right), \tag{1.78}$$

where $\mathbf{x} \in \mathbb{R}^2$, σ is a parameter corresponding to standard deviation. Due to the isotropic diffusion of the linear heat equation, the image denoising by linear heat equations does not preserve the contours, edges, texture during denoising process. There was a need of anisotropic diffusion process that adjusts a high pass filter locally during the diffusion process.

In 1990, Pietro Perona and Jitendra Malik [91] proposed an anisotropic diffusion process and a high pass filter has been adjusted locally in that process. The anisotropic nonlinear diffusion equation proposed is

$$\partial_t u(t,\mathbf{x}) = \mathrm{div}\left(g(|\nabla u(t,\mathbf{x})|^2)\nabla u(t,\mathbf{x})\right), \tag{1.79}$$

subject to the initial and boundary conditions

$$u(0,\mathbf{x}) = u_0(\mathbf{x}), \qquad \mathbf{x} \in \Omega \tag{1.80}$$

$$\frac{\partial u}{\partial \eta}(t,\mathbf{x}) = 0, \qquad \partial\Omega, t > 0 \tag{1.81}$$

where $g(s) : [0,+\infty[\to [0,+\infty[$ is a decreasing function such that $g(0) = 1$ and $g(+\infty) = 0$. For $g = 1$, the heat equation is recovered. The term $g(|\bigtriangledown u|^2)$ is known as the *diffusion coefficient* (sometimes *edge stopping function*) and is designed to be very small near edge points, that is where gradient $\bigtriangledown u$ is large, $g(s)$ is relatively big at smooth regions in image (small values of $\bigtriangledown u$). Some examples of $g(s)$ are

$$g(s) = \frac{1}{1+\frac{s}{\lambda}} \qquad \text{or} \qquad g(s) = e^{-s/\lambda}, \tag{1.82}$$

where λ is known as contrast parameter (threshold on the value of $\bigtriangledown u$). The regions where $\bigtriangledown u > \lambda$ are considered as edges and the Perona-Malik model acts like backward heat equation. On the other hand, regions where $\bigtriangledown u < \lambda$ considered as uniform regions and Perona-Malik equation behaves like forward heat equation.

How to choose λ? This interesting question has been considered in [111]; the authors suggested two methods for automatically setting the value of λ at each iteration of the diffusion process. Also, in [39] a range of threshold (λ) value is suggested.

Due to inherent nature of forward-backward heat equation (when $\bigtriangledown u > \lambda, \bigtriangledown u \leq \lambda$) for the Perona-Malik model, it is very sensitive to small variations in the initial data. In 1997, the one dimensional analog of Perona-Malik model has been proved to be ill-posed (see [61]). A part from the ill-posedness nature of the Perona-Malik model, numerical experiments show promising results by Perona-Malik model with the drawback of having some staircase artifacts (see Chapter 5, section 5.6). Let us mention that the numerical scheme in the paper of Perona and Malik doesn't correspond to their equation as it has been observed by H. Amann [4].

Many modifications of the Perona-Malik model have been proposed to make it well-posed for example see [16], [4], [11].

Let us mention some recently proposed nonlocal partial differential equations based methods for image denoising. These methods are nonlocal due to the presence of fractional derivatives in space variable in terms of fractional Laplacian and fractional gradient. Two nonlocal models have been proposed for image denoising ([44]) which read

$$\left\{\begin{array}{rcll} \partial_t u(t,\mathbf{x}) & = & \frac{1}{1+\lambda^2[(-\Delta)^{1-\varepsilon}u]^2}\Delta u, & (t,\mathbf{x}) \in Q, \\ u(0,\mathbf{x}) & = & u_0(\mathbf{x}), & \mathbf{x} \in \Omega, \\ \frac{\partial u}{\partial \eta}(t,\mathbf{x}) & = & 0, & (t,\mathbf{x}) \in [0,T] \times \partial\Omega, \end{array}\right. \tag{1.83}$$

and

$$\left\{\begin{array}{rcll} \partial_t u(t,\mathbf{x}) & = & \operatorname{div}\left(\frac{1}{1+\lambda^2|(-\nabla)^{1-\varepsilon}u|^2}\nabla u\right), & (t,\mathbf{x}) \in Q, \\ u(0,\mathbf{x}) & = & u_0(\mathbf{x}), & \mathbf{x} \in \Omega, \\ u \quad \text{periodic} & & & t > 0, \end{array}\right. \tag{1.84}$$

where $\lambda > 0$ is a threshold parameter which determines the size of the gradients which will be preserved during diffusion process. The experiments show that the model (1.84) works better than the model (1.83) on the real images, so the second model is more suitable for the image denoising (see [44]). The experiments also revealed that for the model (1.84) the choice $\varepsilon = 0.1$ is the better for the denoising of real images. Let us remark that the problem of optimal choice of ε and λ is not addressed in [44].

The advantage of these models are:

- The models are mathematically well posed as it has been proved in [41], for the model (1.83) and for the model (1.84) in [42].
- Model (1.84) is a generalization of the Perona-Malik model; if we set $\varepsilon = 0$, we get the Perona-Malik model.
- Both models are characterized by nonlocal nonlinearities introduced in the models (fractional power of Laplacian and gradient). Due to these nonlinearities, the proposed models can be considered as nonlinear diffusion with slightly reduced intensities or new regularization models.

- Discretization of the models is well understood see [44].
- No artifacts as observed in the Perona-Malik model.

Recently, in [43], fourth order models involving fractional derivatives in space variables (as in the above models) are proposed for image denoising. The models are in fact generalizations of the Perona-Malik equation to the fourth order equation.

The aim of image denoising models based on partial differential equations is to control the diffusion process of linear heat equation. E. Cuesta and J. Finat [21] observed that the intensity of the diffusion process by linear heat equation can be controlled by taking fractional derivative in time of order $1 < \alpha < 2$; when $\alpha \longrightarrow 2$ then the intensity of the diffusion process is less than the one of linear heat equation (1.76).

We propose to control the diffusion process of linear heat equation by choosing the order of the fractional derivative in time for the equation

$$\left\{\begin{array}{rcll} \partial_t^\alpha u(t,\mathbf{x}) & = & \Delta u(t,\mathbf{x}), & (t,\mathbf{x}) \in [0,T]\times\Omega \\ u(0,\mathbf{x}) & = & u_0(\mathbf{x}), & \mathbf{x}\in\Omega, \\ \partial_t u(0,\mathbf{x}) & = & 0, & \mathbf{x}\in\Omega, \\ \dfrac{\partial u}{\partial \eta}(t,\mathbf{x}) & = & 0, & (t,\mathbf{x}) \in [0,T]\times\partial\Omega, \end{array}\right. \tag{1.85}$$

where ∂_t^α stands for the fractional time derivative of order $1 < \alpha < 2$ in the sense of Riemann–Liouville. Integrating both sides of the first equation of the system (1.85) leads to

$$u(t,\mathbf{x}) = u_0(\mathbf{x}) + \frac{1}{\Gamma(\alpha)}\int_0^t (t-s)^{\alpha-1}\Delta u(s,\mathbf{x})\,\mathrm{d}s,$$

with homogeneous Neumann boundary condition, or in a compact format

$$u(t,\mathbf{x}) = u_0(\mathbf{x}) + \partial^{-\alpha}\Delta u(t,\mathbf{x}), \tag{1.86}$$

where $\partial^{-\alpha}$, for $\alpha > 0$, stands for the fractional integral of order $\alpha \in \mathbb{R}^+$, in the sense of Riemann–Liouville. Since the fractional integral equation interpolates a linear parabolic equation and a linear hyperbolic equation (see [33], [34]), the solution enjoys intermediate properties. The Volterra equation is well–posed for all $t > 0$, and allows us to handle the diffusion by means of a *viscosity parameter* instead of introducing non–linearities in the equation as in the Perona–Malik and alike approaches. Several experiments showing the improvements achieved by our approach are presented in Chapter 5, section 5.6.

1.13 On the Improvement of Volterra Equation Based Filtering for Image Denoising

We present an improvement in the image denoising model proposed in [64] (see Chapter 5). The key factor is the determination of order of fractional integral in the model proposed in [64] (see Chapter 5); by this single parameter (order of fractional integral α), we can control the diffusion process. Getting the profile of the $\alpha's$ play a significant role during denoising process. In fact the nature of the filter proposed in [64](see Chapter 5) can be changed by changing the determination process of $\alpha's$, here we propose an alternative method for the determination of the order of the fractional integral by using the structure tensor of the image.

The structure tensor has been used for identifying several structures in images (see e.g., [3, 10, 113] for more details) such as texture like flow, corners, T junctions etc, it is defined as

$$J_\rho(\nabla u_\sigma) := K_\rho \star (\nabla u_\sigma \otimes \nabla u_\sigma) \qquad \rho \geq 0, \tag{1.87}$$

where $u_\sigma = K_\sigma \star u(.,t), \nabla u_\sigma \otimes \nabla u_\sigma := \nabla u_\sigma \nabla u_\sigma^t$, ρ is the integration scale, σ is called local or noise scale.

If λ_1, λ_2 are the eigenvalues of the structure tensor (1.87) then

- Uniform regions corresponds to $\lambda_1 = \lambda_2 = 0$
- Straight edges corresponds to $\lambda_1 \gg \lambda_2 = 0$
- Corners corresponds to $\lambda_1 \gg \lambda_2 \gg 0$.

The choice of the order of the fractional time derivative has been made for each pixel by using the *structure tensor* of image, which allows us to control the diffusion process. Several experiments showing improvement of our approach visually and in terms of SNR, $PSNR$ are presented in Chapter 6, section 6.4.

Let us mention that our approach in this thesis for image denoising remains isotropic, since the diffusion is governed by the scalars $\alpha's$, both in Chapter 5 and in Chapter 6. The models discussed in this thesis are also isotropic as the diffusion is controlled by the scalar function. For example for the Perona-Malik model the scalar function g has been considered. There exist general vector-valued approaches ([3, 113]) which introduce the structure tensor in place of the scalar function in the denoising model; this allows to control the diffusion in the images by considering the two orthogonal directions and can lead to different diffusions on each single direction. As said earlier, the thesis focus on the scalar approach, i.e., no tensor diffusion is considered in the model equation. We believe that the tensorial approach in the framework of fractional calculus fits very well.

The Profile of blowing-up solutions to a nonlinear system of fractional differential equations

Purpose of the paper:

The purpose of this paper [64] is two fold:

- First to present the bilateral estimates i.e., lower bound and upper bound of the blowing up solutions for the nonlocal semilinear system (FDS)

$$\begin{aligned} u'(t) + D^{\alpha}_{0+}(u - u_0)(t) &= v(t)^q, \qquad t > 0, \\ v'(t) + D^{\beta}_{0+}(v - v_0)(t) &= u(t)^p, \qquad t > 0, \end{aligned}$$

  where $u(0) = u_0 > 0, v(0) = v_0 > 0, p > 1, q > 1$ are given constants and D^{α}_{0+} and D^{β}_{0+}, $0 < \alpha < 1$, $0 < \beta < 1$ stand for the Riemann-Liouville fractional derivatives.

- Second to get a lower bound and an upper bound on the blow-up time for the system (PFDS).

$$\begin{aligned} D^{\alpha}_{0+}(u - u_0)(t) &= v(t)^q, \qquad t > 0, \\ D^{\beta}_{0+}(v - v_0)(t) &= u(t)^p, \qquad t > 0. \end{aligned}$$

The problem:

The problem in getting the bilateral estimates for the blowing up solutions of the system (FDS) are the superlinear nonlinearities in the system (FDS) as well as the fractional derivatives. Let us mention that the power nonlinearities and fractional derivatives are combined in the system (FDS).

Strategy:

Our strategy to get the profile of the blowing-up solutions of the system (FDS) is based on the comparison of the solution with the blowing-up solutions of the subsystems obtained from the system (FDS). A lower bound and an upper bound on the blow-up time are obtained via equivalent nonlinear Volterra integral equations.

Chapter 2

The Profile of blowing-up solutions to a nonlinear system of fractional differential equations

Abstract

We investigate the profile of the blowing up solutions to the nonlinear nonlocal system (FDS)

$$\begin{aligned} u'(t) + D^{\alpha}_{0+}(u-u_0)(t) &= v(t)^q, \qquad t>0,\\ v'(t) + D^{\beta}_{0+}(v-v_0)(t) &= u(t)^p, \qquad t>0, \end{aligned}$$

where $u(0)=u_0>0, v(0)=v_0>0, p>1, q>1$ are given constants and D^{α}_{0+} and D^{β}_{0+}, $0<\alpha<1$, $0<\beta<1$ stand for the Riemann-Liouville fractional derivatives. Our method of proof relies on comparisons of the solution to the system (FDS) with solutions of the subsystems obtained from the system (FDS) by dropping either the usual derivatives or the fractional derivatives.

Keywords: Nonlinear system, Fractional derivative, Integral equations, Blow up time, Laplace transform.

MSC [2010]: 26A33, 45J05, 34K37.

Contents

2.1 Introduction

In this paper, we are concerned with the profile of the blowing up solutions to the nonlinear system of fractional differential equations (FDS)

$$
\begin{aligned}
u'(t) + D^{\alpha}_{0_+}(u-u_0)(t) &= v(t)^q, \qquad t>0,\\
v'(t) + D^{\beta}_{0_+}(v-v_0)(t) &= u(t)^p, \qquad t>0,
\end{aligned}
$$

subject to the initial conditions

$$
u(0)=u_0, \qquad v(0)=v_0, \tag{2.1}
$$

where $p>1, q>1, u(0)=u_0>0, v(0)=v_0>0$ are constants, $D^{\alpha}_{0_+}$ and $D^{\beta}_{0_+}$ stand for the Riemann-Liouville fractional derivatives of orders $0<\alpha<1$ and $0<\beta<1$, respectively.

There are a couple of physical motivations for considering the system (FDS). Firstly, the type of nonlinearities in the system (FDS) appears in the systems describing processes of heat diffusion and combustion in two component continua with nonlinear heat conduction and volumetric release (they read $u_t=\Delta u+v^q$, $v_t=\Delta v+u^p$, the subscript t stands for the time derivative, while Δ stands for the Laplacian operator). Secondly, as suggested recently [71] one may take $\Delta D^{\alpha}_{0_+}(u-u_0)$ and $\Delta D^{\beta}_{0_+}(v-v_0)$ instead of $\Delta(u-u_0)$ and $\Delta(v-v_0)$. To simplify the analysis one may start by replacing $\Delta(u-u_0)$ and $\Delta(v-v_0)$ by $(u-u_0)$ and $(v-v_0)$, respectively.

It has been proved by Furati and Kirane in [35] that any solution of the system (FDS) with $p>1, q>1$, emerging from $(u_0,v_0), (u_0>0, v_0>0)$ blows up in a finite time. Moreover, they gave an upper bound for the blow up time. Their method of proof relies on the weak formulation of the system (FDS) with a judicious choice of the test function. Here, we present estimates from above and below of the blowing up solutions of the system (FDS) by comparing them with the solutions of the particular systems obtained from the system (FDS):

$$
\begin{aligned}
u'(t) &= \lambda v(t)^q, \qquad t>0, \quad p>1,\\
v'(t) &= \lambda u(t)^p, \qquad t>0, \quad q>1,
\end{aligned}
$$

the system of ordinary differential equations (ODS) with $\lambda=1$, and

$$
\begin{aligned}
D^{\alpha}_{0_+}(u-u_0)(t) &= \mu v(t)^q, \qquad t>0, \quad q>1\\
D^{\beta}_{0_+}(v-v_0)(t) &= \mu u(t)^p, \qquad t>0 \quad p>1,
\end{aligned}
$$

the system of fractional differential equations (PFDS), with $\mu=1$. As the solutions to the system (ODS) are easy to obtain, we will investigate in particular the system (PFDS). Precisely, we give sufficient conditions for the finite time blow up of solutions to the system (PFDS), under certain conditions. We also provide an upper bound for the blowing up time. The asymptotic behavior of the blowing up solutions to the system (FDS) near blow up time is given; this allows us to investigate the profile of the blowing up solutions of the system (FDS).

The mathematical analysis of initial and boundary value problems (linear or nonlinear) of fractional differential equations has become an area of interest for scientists because of their applications to various fields of science and engineering, the reader is referred to the articles [2, 36, 37, 67, 68, 88] and references therein. However, there are quite a few articles which consider the nonexistence of solutions of fractional differential equations and fractional systems (see [35], [63]). In this paper, we are going to investigate the profile of blowing up solutions to the system (FDS).

Our paper is organized as follows: some definitions and known results needed in the sequel are stated in the next section. Section 2.3 is devoted to our main results for the investigation of the profile of the blowing up solutions of the system (FDS). In the last section, we provide numerical approximations of the solutions, and the profiles are given for particular examples.

2.2 Preliminaries

In this section, the necessary definitions and notations from fractional calculus needed for the paper are recalled for the sake of the reader (See [62], [70], [102],[85], [38]).

The Riemann-Liouville fractional integral of order $0 < \alpha < 1$ is

$$J_{0_+}^{\alpha} f(t) := \frac{1}{\Gamma(\alpha)} \int_0^t \frac{f(\tau)}{(t-\tau)^{1-\alpha}} d\tau, \quad t > 0, \tag{2.2}$$

where $\Gamma(\alpha)$ is the Euler Gamma function and $f : \mathbb{R}^+ \to \mathbb{R}$ is a real valued integrable function. The integral (2.2) can be written as a convolution

$$J_{0_+}^{\alpha} f(t) = (\phi_\alpha \star f)(t), \tag{2.3}$$

where

$$\phi_\alpha := \begin{cases} \frac{t^{\alpha-1}}{\Gamma(\alpha)}, & t > 0, \\ 0 & t \leq 0. \end{cases} \tag{2.4}$$

The Laplace transform of the Riemann-Liouville integral of order $0 < \alpha < 1$ is

$$\mathcal{L}\{J_{0_+}^{\alpha} f(t) : s\} = \mathcal{L}\{f(t) : s\}/s^{\alpha}.$$

The Riemann-Liouville fractional derivative of order $0 < \alpha < 1$ is

$$D_{0_+}^{\alpha} f(t) := \frac{d}{dt} J_{0_+}^{1-\alpha} f(t) = \frac{1}{\Gamma(1-\alpha)} \frac{d}{dt} \int_0^t \frac{f(\tau)}{(t-\tau)^{\alpha}} d\tau. \tag{2.5}$$

In particular, when $\alpha = 0$, $D_{0_+}^{0} f(t) = f(t)$; note that the Riemann-Liouville fractional derivative of a constant is not equal to zero.

The Caputo fractional derivative of an absolutely continuous (or differentiable) function $f(t)$ of order $0<\alpha<1$ is defined by

$$ {}^C D^{\alpha}_{0_+} f(t) := J^{1-\alpha}_{0_+} f'(t) = \frac{1}{\Gamma(1-\alpha)} \int\limits_0^t \frac{f'(\tau)}{(t-\tau)^{\alpha}} d\tau. \tag{2.6} $$

The relation between the Riemann-Liouville and the Caputo fractional derivatives for an absolutely continuous function $f(t)$ is

$$ {}^C D^{\alpha}_{0_+} f(t) = D^{\alpha}_{0_+}\Big(f(t)-f(0)\Big), \quad 0<\alpha<1. \tag{2.7} $$

The formula for the integration by parts in $[0,T]$ is given by

$$ \int\limits_0^T f(t) D^{\alpha}_{0_+} g(t) dt = \int\limits_0^T D^{\alpha}_{T_-} f(t) g(t) dt, \tag{2.8} $$

see [62], where $D^{\alpha}_{T_-}$ is the right-sided fractional derivative defined by

$$ D^{\alpha}_{T_-} f(t) := -\frac{1}{\Gamma(1-\alpha)} \frac{d}{dt} \int\limits_t^T \frac{f(\tau)}{(\tau-t)^{\alpha}} d\tau, \ \ 0<\alpha<1. \tag{2.9} $$

The Laplace transforms of the Riemann-Liouville derivative $D^{\alpha}_{0_+} f(t)$ and the Caputo derivative ${}^C D^{\alpha}_{0_+} f(t)$ are

$$ \mathcal{L}\{D^{\alpha}_{0_+} f(t) : s\} = s^{\alpha} \mathcal{L}\{f(t) : s\} - J^{1-\alpha}_{0_+} f(0), \quad 0<\alpha<1, \tag{2.10} $$

$$ \mathcal{L}\{{}^C D^{\alpha}_{0_+} f(t) : s\} = s^{\alpha} \mathcal{L}\{f(t) : s\} - s^{\alpha-1} f(0), \quad 0<\alpha<1. \tag{2.11} $$

At this stage let us recall the test function considered in [35]:

$$ \varphi(t) = \begin{cases} T^{-\lambda}(T-t)^{\lambda}, & t\in[0,T], \\ 0 & t>T; \end{cases} \tag{2.12} $$

it satisfies (see Appendix A.1)

$$ \int\limits_0^T D^{\alpha}_{T-} \varphi(t) dt = C_{\alpha,\lambda} T^{1-\alpha}, \quad C_{\alpha,\lambda} = \frac{\Gamma(\lambda+1)}{\Gamma(\lambda-\alpha+2)}, \tag{2.13} $$

and for $p>1$, $\lambda>\alpha p-1$ (see Appendix A.1.1)

$$ \int\limits_0^T \varphi^{1-p}(t) \left| D^{\alpha}_{T-}\varphi(t)\right|^p dt = C_{p,\alpha} T^{1-\alpha p}, \tag{2.14} $$

where

$$ C_{p,\alpha} = \frac{1}{\lambda - p\alpha + 1} \left[\frac{\Gamma(\lambda+1)}{\Gamma(\lambda+1-\alpha)} \right]^p. \tag{2.15} $$

The main result in [35] is the

Theorem 2.2.1 ([35]). *Suppose $0 < \alpha, \beta < 1$, $p, q > 1$ and $u_0 > 0$, $v_0 > 0$, then solutions to the system (FDS) subject to (2.1) blow-up in a finite time.*

Let us recall that the blowing up solution of the system (ODS) with $\lambda = 1$

$$\begin{cases} u'(t) &= v(t)^q, \qquad t > 0, \quad p > 1, \\ v'(t) &= u(t)^p, \qquad t > 0, \quad q > 1, \end{cases} \tag{2.16}$$

subject to the initial conditions $(u(0) = u_0 > 0,\ v(0) = v_0 > 0)$ is

$$u_{od}(t) = C_1\Big(T_{max} - t\Big)^{-\frac{q+1}{pq-1}}, \qquad v_{od}(t) = C_2\Big(T_{max} - t\Big)^{-\frac{p+1}{pq-1}}, \tag{2.17}$$

where T_{max}, C_1 and C_2 are given by

$$\begin{aligned} T_{max} &= \left(\frac{C_2 u_0}{C_1 v_0}\right)^{\frac{pq-1}{p-q}}, \\ C_1 &= \left(\frac{(p+1)^q(q+1)}{(pq-1)^{q+1}}\right)^{\frac{1}{pq-1}}, \quad C_2 = \left(\frac{(p+1)(q+1)^p}{(pq-1)^{p+1}}\right)^{\frac{1}{pq-1}}. \end{aligned} \tag{2.18}$$

Alike, the blowing up solution of the system (ODS) with $\lambda = 1/2$

$$\begin{cases} u'(t) &= \frac{1}{2}v(t)^q, \qquad t > 0, \quad u(0) = u_0 > 0, \\ \\ v'(t) &= \frac{1}{2}u(t)^p, \qquad t > 0, \quad v(0) = v_0 > 0, \end{cases} \tag{2.19}$$

for $p, q > 1$, is given by

$$u^*_{od}(t) = C^*_1\Big(T^*_{max} - t\Big)^{-\frac{q+1}{pq-1}}, \qquad v^*_{od}(t) = C^*_2\Big(T^*_{max} - t\Big)^{-\frac{p+1}{pq-1}},$$

where T^*_{max}, C^*_1 and C^*_2 are given by

$$\begin{aligned} T^*_{max} &= \left(\frac{C^*_2 u_0}{C^*_1 v_0}\right)^{\frac{pq-1}{p-q}}, \\ C^*_1 &= 2^{\frac{q+1}{pq-1}}\left(\frac{(p+1)^q(q+1)}{(pq-1)^{q+1}}\right)^{\frac{1}{pq-1}}, \quad C^*_2 = 2^{\frac{p+1}{pq-1}}\left(\frac{(p+1)(q+1)^p}{(pq-1)^{p+1}}\right)^{\frac{1}{pq-1}}. \end{aligned}$$

Notice that the solution of the system (2.16) blows up earlier than the solution of the system (2.19) since $T^*_{max} = 2T_{max}$.

2.3 Main Results

Our first result provides the local existence of solutions to the system (FDS), for which we need some preliminary results which are given in the following Lemmas.

Let $e_\alpha(t) := E_\alpha(-t^\alpha)$ where $E_\alpha(t)$ is the Mittag-Leffler function of parameter α (see [62],[55]) .

Lemma 2.3.1. *The components of the solution (u, v) to the system (FDS) satisfy the integral equations*

$$u(t) = u_0 + \int_0^t e_{1-\alpha}(t-\tau)v(\tau)^q d\tau, \tag{2.20}$$

$$v(t) = v_0 + \int_0^t e_{1-\beta}(t-\tau)u(\tau)^p d\tau. \tag{2.21}$$

Proof. Taking the Laplace transform of both sides of the first equation of the system (FDS) and using (2.7) and (2.11), we obtain

$$\mathcal{L}\{u(t) : s\} = \frac{u_0}{s} + \frac{\mathcal{L}\{v(t)^q : s\}}{(s + s^\alpha)},$$

which, via the inverse Laplace transform, leads to:

$$u(t) = u_0 + \mathcal{L}^{-1}\left(\frac{\mathcal{L}\{v(t)^q : s\}}{(s + s^\alpha)}\right).$$

Notice that

$$\frac{\mathcal{L}\{v(t)^q : s\}}{(s + s^\alpha)} = \frac{s^{-\alpha}}{(s^{1-\alpha} + 1)}\mathcal{L}\{v(t)^q : s\} \quad \text{and} \quad \mathcal{L}\{e_\alpha(t) : s\} = \frac{s^{-\alpha}}{(s^{1-\alpha} + 1)},$$

we have

$$u(t) = u_0 + \mathcal{L}^{-1}\Big(\mathcal{L}\{e_\alpha(t) : s\}\mathcal{L}\{v(t)^q : s\}\Big).$$

By means of the inverse Laplace transform of convolution of functions, equation (2.20) is obtained. Following the same steps, we obtain equation (2.21). □

Lemma 2.3.2. *For the system (FDS), the functions $u'(t)$ and $v'(t)$ satisfy the integral equations*

$$u'(t) = v(t)^q + \int_0^t e'_{1-\alpha}(t-\tau)v(\tau)^q d\tau, \tag{2.22}$$

$$v'(t) = u(t)^p + \int_0^t e'_{1-\beta}(t-\tau)u(\tau)^p d\tau. \tag{2.23}$$

Proof. By virtue of the definition of the Caputo derivative, for $0 < \alpha < 1$, the equation corresponding to $u(t)$ in the system (FDS) takes the form

$$u'(t) + J_{0_+}^{1-\alpha}u'(t) = v(t)^q, \quad t > 0. \tag{2.24}$$

Taking the Laplace transform of both sides of equation (2.24), it follows

$$\mathcal{L}\{u'(t) : s\} = \frac{s^{1-\alpha}\mathcal{L}\{v(t)^q : s\}}{s^{1-\alpha} + 1}. \tag{2.25}$$

There are different ways of writing the solution from equation (3.13); for example we can write

$$\frac{s^{1-\alpha}\mathcal{L}\{v(t)^q : s\}}{s^{1-\alpha}+1} = s\left(\frac{s^{-\alpha}\mathcal{L}\{v(t)^q : s\}}{s^{1-\alpha}+1}\right),$$

and we obtain

$$u'(t) = \frac{d}{dt}\Big(e_{1-\alpha} \star v(t)^q\Big). \tag{2.26}$$

Another way of writing equation (3.13) is

$$\mathcal{L}\{u'(t)\} = \frac{s^{-\alpha}}{s^{1-\alpha}+1}\Big(s\mathcal{L}\{v(t)^q : s\} - |v(0)|^q\Big) + \frac{s^{1-\alpha}}{s^{-\alpha}+1}|v(0)|^q;$$

taking the inverse Laplace transform, we get

$$u'(t) = \int_0^t \frac{d}{dt}\Big(|v(t-\tau)|^q\Big)e_\alpha(\tau)d\tau + |v(0)|^q e_\alpha(t).$$

Noting that $e_{1-\alpha}(0) = E_{1-\alpha}(0) = 1$, equation (3.13) can be written as

$$\mathcal{L}\{u'(t) : s\} = \left(\frac{s^{1-\alpha}}{s^{1-\alpha}+1} - 1\right)|v(s)|^q + |v(s)|^q,$$

hence

$$u'(t) = \int_0^t |v(\tau)|^q e'_{1-\alpha}(t-\tau)d\tau + v(t)^q.$$

The equation (2.23) can be obtained similarly. □

The following lemma gives the equivalence between the system (FDS) and the integral equations (2.20)-(2.21).

Lemma 2.3.3. *The system (FDS) and the integral equations (2.20)-(2.21) are equivalent.*

Proof. From equation (2.22), we have

$$u'(t) = v(t)^q + e'_{1-\alpha}(t) \star v(t)^q, \tag{2.27}$$

since $0 < \alpha < 1$, and due to the formula (see [62] page 86)

$$D^\alpha_{0+}(u-u_0)(t) = t^{-\alpha}E_{1-\alpha,1-\alpha}(-t^{1-\alpha}) \star v(t)^q, \tag{2.28}$$

where $E_{\alpha,\beta}(t)$ is the Mittag–Leffler function of two parameters α and β.

As we have

$$e'_{1-\alpha}(t) = \sum_{n=1}^{\infty}\frac{(-1)^n t^{(n-1)-\alpha n}}{\Gamma((1-\alpha)n)},$$

by adding equations (2.27) and (2.28), we obtain

$$\begin{aligned} u'(t) + D^{\alpha}_{0_+}(u-u_0)(t) &= v(t)^q + \Bigg[\sum_{n=1}^{\infty} \frac{(-1)^n t^{(n-1)-\alpha n}}{\Gamma((1-\alpha)n)} \\ &+ t^{-\alpha} E_{1-\alpha,1-\alpha}(-t^{1-\alpha})\Bigg] \star v(t)^q. \end{aligned}$$

Now, the equation

$$u'(t) + D^{\alpha}_{0_+}(u-u_0)(t) = v(t)^q$$

is obtained by using the fact

$$t^{-\alpha} E_{1-\alpha,1-\alpha}(-t^{1-\alpha}) = \sum_{n=0}^{\infty} \frac{(-1)^n t^{n-\alpha(n+1)}}{\Gamma((1-\alpha)(n+1))}$$

which makes

$$\sum_{n=1}^{\infty} \frac{(-1)^n t^{(n-1)-\alpha n}}{\Gamma((1-\alpha)n)} + t^{-\alpha} E_{1-\alpha,1-\alpha}(-t^{1-\alpha}) = 0$$

by shifting the index of summation term by 1.

Following the same steps, the equation $v'(t) + D^{\beta}_{0_+}(v-v_0)(t) = u(t)^p$ can be obtained from the integral equation (2.21). $\square$

2.3.1 Existence of local solution to the system (FDS)

For the local existence of solutions to the system (FDS), we need the following:

- First we set for $u, v \in C([0,T])$, $\Delta := \{t \in \mathbb{R}^+/0 \le t \le T, |u-u_0| < c, |v-v_0| < c\}$. Let $K_1 := v_0^q, K_2 := u_0^p$. On Δ the nonlinearities satisfy the Lipschitz conditions

$$|v_1^q - v_2^q| \le L_1|v_1 - v_2|, \quad \text{and} \quad |u_1^p - u_2^p| \le L_2|u_1-u_2|, \tag{2.29}$$

  where $L_1 := q(c+u_0)^{q-1}, L_2 := p(c+v_0)^{p-1}$.

  We set $K := \max\{K_1, K_2\}$, $L := \max\{L_1, L_2\}$.

- We have for $0 \le t \le T$,

$$\int_0^t e_{1-\alpha}(t-\tau)d\tau \le M_1 < \infty, \quad \int_0^t e_{1-\beta}(t-\tau)d\tau \le M_2 < \infty.$$

- For any $\varepsilon > 0$, there exist $\delta_1 > 0$ and $\delta_2 > 0$ independent of t and b such that

$$\int_b^{b+\delta_1} e_{1-\alpha}(t-\tau)d\tau < \varepsilon, \quad 0 \le b \le t-\delta_1,$$

$$\int_b^{b+\delta_2} e_{1-\beta}(t-\tau)d\tau < \varepsilon, \quad 0 \le b \le t-\delta_2.$$

Further, we set for any $0<\rho<1$, $P:=\min(\rho/L, c/K)$, and then let $h:=\min(r,T)$, where $r:=\min(r_1,r_2)$ and r_1,r_2 are determined by

$$\int_0^t e_{1-\alpha}(t-\tau)d\tau \leq P, \quad 0\leq t\leq r_1, \quad \text{and} \quad \int_0^t e_{1-\beta}(t-\tau)d\tau \leq P, \quad 0\leq t\leq r_2.$$

Then we have the following existence theorem.

Theorem 2.3.4. *For any $u_0>0, v_0>0$ given, the integral equations (2.20)-(2.21) have a unique continuous solution on the interval $0\leq t\leq h$.*

Proof. We will use the iterative scheme for the existence of a solution in the interval $[0,h]$.

For this let us define

$$u_n(t)=u_0+\int_0^t e_{1-\alpha}(t-\tau)|v_{n-1}(\tau)|^q d\tau, \quad n=1,2,...,$$

$$v_n(t)=v_0+\int_0^t e_{1-\beta}(t-\tau)|u_{n-1}(\tau)|^p d\tau, \quad n=1,2,....$$

Then the constraints on P and h ensure that for each $n=1,2,...$, u_n and v_n are defined in $[0,h]$ and satisfy

$$|u_n(t)-u_0|\leq c \quad \text{and} \quad |v_n(t)-v_0|\leq c.$$

By the Lipschitz condition, for $0\leq t\leq h$, we have

$$\begin{aligned}
|u_{n+1}(t)-u_n(t)| &= \left|\int_0^t e_{1-\alpha}(t-\tau)\left(v_n^q-v_{n-1}^q\right)(\tau)d\tau\right| \\
&\leq L_1\int_0^t e_{1-\alpha}(t-\tau)|v_n(\tau)-v_{n-1}(\tau)|d\tau \\
&\leq L_1\sup_{0\leq t\leq h}|v_n(t)-v_{n-1}(t)|\int_0^t e_{1-\alpha}(t-\tau)d\tau \\
&\leq L_1P\sup_{0\leq t\leq h}|v_n(t)-v_{n-1}(t)|.
\end{aligned}$$

Hence we have

$$|u_{n+1}(t)-u_n(t)|\leq c(L_1P)^n\leq c\rho^n, \quad (n=0,1,...).$$

Alike, we obtain

$$|v_{n+1}(t)-v_n(t)|\leq c(L_2P)^n\leq c\rho^n, \quad (n=0,1,...).$$

The sequences $\{u_n(t)\},\{v_n(t)\}$ are uniformly convergent in $[0,h]$ as $0<\rho<1$, hence $(u_n(t),v_n(t))\to(u(t),v(t))$ is a continuous solution of the system of integral equations (2.20)-(2.21). □

Extension of the Solution: The solution of the system of integral equations (2.20)-(2.21) obtained in Thm 3.4 can be extended to the interval $[0,T]$.

Let $(\tilde{u},\tilde{v})$ be the solution of (2.20)-(2.21) on $[0,h]$ $(h<T)$ where $h=\min(r,T)$ then from Thm 3.4 the system of equations

$$u(t)=u_0+\int_0^h e_{1-\alpha}(t-\tau)|\tilde{v}(\tau)|^q d\tau+\int_h^{2h} e_{1-\alpha}(t-\tau)v(\tau)^q d\tau,$$

$$v(t)=v_0+\int_0^h e_{1-\beta}(t-\tau)|\tilde{u}(\tau)|^p d\tau+\int_h^{2h} e_{1-\beta}(t-\tau)u(\tau)^p d\tau,$$

has a solution $(\tilde{\tilde{u}},\tilde{\tilde{v}})$ on $[h,2h]$ $(2h\leq T)$ because

$$\int_0^h e_{1-\alpha}(t-\tau)|\tilde{v}(\tau)|^q d\tau \quad \text{and} \quad \int_0^h e_{1-\beta}(t-\tau)|\tilde{u}(\tau)|^p d\tau$$

are bounded and continuous.

The pair of functions

$$(u,v)(t)=\begin{cases}(\tilde{u},\tilde{v})(t), & t\in[0,h],\\ (\tilde{\tilde{u}},\tilde{\tilde{v}})(t), & t\in[h,2h],\end{cases} \tag{2.30}$$

is the solution of the system of integral equations on $[0,2h]$. We can continue in the same way finite times till we reach T.

The above analysis can be performed for the system

$$\begin{aligned} C_1u'(t)+C_2D^{\alpha}_{0_+}(u-u_0)(t) &= v(t)^q, \qquad t>0,\\ C_3v'(t)+C_4D^{\beta}_{0_+}(v-v_0)(t) &= u(t)^p, \qquad t>0,\end{aligned}$$

subject to the initial conditions

$$u(0)=u_0, \qquad v(0)=v_0,$$

where $C_i, i=1,...,4$ are nonnegative constants.

The system (PFDS) being a special case of the above system corresponding to $C_1=0=C_3, C_2=1=C_4$ admits local solutions.

Now, we consider the nonlinear system of fractional differential equations (PFDS) whose solution will serve to bound the solution of the system (FDS)

$$\begin{aligned} D^{\alpha}_{0_+}(u-u_0)(t) &= \mu v(t)^q, \qquad t>0,\\ D^{\beta}_{0_+}(v-v_0)(t) &= \mu u(t)^p, \qquad t>0,\end{aligned}$$

for $0<\alpha,\beta<1$, with $\mu=1$, subject to the initial conditions (2.1).

2.3.2 Necessary conditions for the existence of blowing-up solution for the system (PFDS)

For the system (PFDS), with $\mu = 1$, we will give the necessary conditions for solutions to blow up in a finite time; moreover an upper bound on the blow up time is provided.

Let us set:

$$s = \frac{p\alpha + \beta}{1 - pq}, \quad \tilde{s} = \frac{\alpha + q\beta}{1 - pq}, \quad C_v = K_2(K_1)^{\frac{p}{pq-1}}, \quad C_u = K_2^*(K_1^*)^{\frac{q}{pq-1}}, \tag{2.31}$$

where K_1, K_2, K_1^* and K_2^* are:

$$K_1 = C_{p',\alpha}^{\frac{1}{p'}} C_{q',\beta}^{\frac{1}{pq'}}, \quad K_2 = C_{q',\beta}^{\frac{1}{q'}} C_{\beta,\lambda}^{-1},$$

$$K_1^* = C_{q',\beta}^{\frac{1}{q'}} C_{p',\alpha}^{\frac{1}{qp'}}, \quad K_2^* = C_{p',\alpha}^{\frac{1}{p'}} C_{\alpha,\lambda}^{-1},$$

and the constants $\{C_{\alpha,\lambda}, C_{\beta,\lambda}\}$ and $\{C_{p',\alpha}, C_{q',\beta}\}$ are given by (2.13) and (2.15) respectively.

The result is given by

Theorem 2.3.5. *Let $p, q > 1$ and $u_0 > 0$, $v_0 > 0$, then any solution to the system (PFDS) with $\mu = 1$ subject to the initial conditions (2.1) blows up in a finite time T_{max}. Furthermore, an upper bound on the blow up time T_{max} is given by $min\{T_u, T_v\}$ where*

$$T_v = \left[\frac{v_0}{C_v}\right]^{1/s} \quad T_u = \left[\frac{u_0}{C_u}\right]^{1/\tilde{s}}.$$

Proof. The proof is by contradiction; suppose (u, v) is a global solution of the system (PFDS). Multiplying the equations of system (PFDS) by any function φ such that $D_{T_-}^{\alpha}\varphi$ exists and $\varphi(T) = 0$ and integrating over $[0, T]$; by virtue of (2.8), we obtain

$$\int_0^T u D_{T_-}^{\alpha}\varphi = u_0 \int_0^T D_{T_-}^{\alpha}\varphi + \int_0^T v^q \varphi, \tag{2.32}$$

$$\int_0^T v D_{T_-}^{\beta}\varphi = v_0 \int_0^T D_{T_-}^{\beta}\varphi + \int_0^T u^p \varphi. \tag{2.33}$$

We choose φ as in (2.12). Using Hölder's inequality, we obtain

$$\int_0^T u D_{T_-}^{\alpha}\varphi \leq \left[\int_0^T u^p \varphi\right]^{1/p} \left[\int_0^T \left|D_{T_-}^{\alpha}\varphi\right|^{p'} \varphi^{-p'/p}\right]^{1/p'}, \tag{2.34}$$

$$\int_0^T v D_{T_-}^{\beta}\varphi \leq \left[\int_0^T |v|^q \varphi\right]^{1/q} \left[\int_0^T \left|D_{T_-}^{\beta}\varphi\right|^{q'} \varphi^{-q'/q}\right]^{1/q'}, \tag{2.35}$$

where p, p', q, q' satisfy $p + p' = pp'$ and $q + q' = qq'$. If we set

$$\begin{aligned} \mathbf{I} &:= \int_0^T u^p \varphi, & \mathbf{J} &:= \int_0^T v^q \varphi, \\ \mathbf{A} &:= \int_0^T \left| D_{T_-}^{\alpha} \varphi \right|^{p'} \varphi^{-p'/p}, & \mathbf{B} &:= \int_0^T \left| D_{T_-}^{\beta} \varphi \right|^{q'} \varphi^{-q'/q}, \end{aligned} \tag{2.36}$$

then (2.32), (2.33), (2.34) and (2.35) lead to:

$$\mathbf{J} \leq \mathbf{I}^{1/p} \mathbf{A}^{1/p'} \quad \text{and} \quad \mathbf{I} \leq \mathbf{J}^{1/q} \mathbf{B}^{1/q'}.$$

As $u_0 > 0, v_0 > 0$ and $\int_0^T D_{T_-}^{\alpha} \varphi > 0$ when $\varphi(t)$ is selected as in (2.12), it is clear that

$$\mathbf{J}^{1-\frac{1}{pq}} \leq \mathbf{A}^{1/p'} \mathbf{B}^{1/pq'}, \tag{2.37}$$

$$\mathbf{I}^{1-\frac{1}{pq}} \leq \mathbf{A}^{1/qp'} \mathbf{B}^{1/q'}. \tag{2.38}$$

Using (2.14), with $\lambda \geq max\{\alpha p' - 1, \beta q' - 1\}$, we have

$$\mathbf{A} = C_{p',\alpha} T^{1-\alpha p'}, \qquad \mathbf{B} = C_{q',\beta} T^{1-\beta q'}.$$

Consequently, (2.37) takes the form

$$\mathbf{J}^{1-\frac{1}{pq}} \leq K_1 T^{s_1}, \tag{2.39}$$

where

$$s_1 = 1 - \alpha - \frac{\beta}{p} - \frac{1}{pq}.$$

Thus $\mathbf{J}$ is bounded under the constraint $s_1 \leq 0$ which is equivalent to

$$1 - \frac{1}{pq} \leq \alpha + \frac{\beta}{p}.$$

The equality (2.33) and the estimates (2.35) allow us to write

$$v_0 \int_0^T D_{T_-}^{\beta} \varphi \leq \mathbf{J}^{1/q} \mathbf{B}^{1/q'}, \tag{2.40}$$

which in virtue of (2.40) becomes

$$v_0 \leq K_2 \mathbf{J}^{1/q} T^{r_1}, \tag{2.41}$$

where $r_1 = -1/q$.

Letting $T \to \infty$, in (2.41) we obtain the contradiction $0 < v_0 \leq 0$. Similarly, an analysis could be done along $\mathbf{I}$; it leads to

$$1 - \frac{1}{pq} \leq \beta + \frac{\alpha}{q}.$$

To obtain an estimation on the blow up time, we estimate $\mathbf{J}$ in (2.41) by (2.39) to obtain

$$\begin{aligned} v_0 &\leq K_2(K_1)^{\frac{p}{pq-1}} T^{\frac{ps_1}{pq-1}+r_1} \\ &=: C_v T^s \end{aligned}$$

where $s < 0$.

Whereupon a bound on the blow-up time is given by

$$T_{max} \leq T_v = \left[\frac{v_0}{C_v}\right]^{1/s}.$$

A similar bound on T_{max} can be obtained in terms of u_0 if we use (2.32) and (2.38); it reads

$$T_{max} \leq T_u = \left[\frac{u_0}{C_u}\right]^{1/\tilde{s}}.$$

Finally, $T_{max} \leq \min\{T_u, T_v\}$. $\square$

Now, we present bilateral estimates of the blowing up solutions to the system (FDS) via the solutions of systems (PFDS) and (ODS).

The solution of the system (PFDS) is a solution to the nonlinear system of Volterra equations

$$\begin{cases} u(t) = u_0 + \frac{\mu}{\Gamma(\alpha)} \int\limits_0^t \frac{v(\tau)^q}{(t-\tau)^{1-\alpha}} d\tau, & t > 0, \\ v(t) = v_0 + \frac{\mu}{\Gamma(\beta)} \int\limits_0^t \frac{u(\tau)^p}{(t-\tau)^{1-\beta}} d\tau, & t > 0. \end{cases} \tag{2.42}$$

Following [90], growth rates near the blow-up time for blowing up solutions to the system (2.42) are available. They are stated in

Theorem 2.3.6. *The profiles of the components of the solution $(u(t), v(t))$ for the system (2.42) with $\mu = 1$ are given by*

$$u(t) \sim C_{1,\alpha,\beta}(T^{\alpha,\beta}_{max} - t)^{-\delta}, \quad v(t) \sim C_{2,\alpha,\beta}(T^{\alpha,\beta}_{max} - t)^{-\xi}, \quad \text{as} \quad t \to T^{\alpha,\beta}_{max}, \tag{2.43}$$

where $T^{\alpha,\beta}_{max}$ is the blow-up time and

$$C_{1,\alpha,\beta} = \left(\frac{\Gamma(p\delta)}{\Gamma(p\delta - \beta)}\right)^{\frac{q}{pq-1}} \left(\frac{\Gamma(q\xi)}{\Gamma(q\xi - \alpha)}\right)^{\frac{1}{pq-1}},$$

$$C_{2,\alpha,\beta} = \left(\frac{\Gamma(q\xi)}{\Gamma(q\xi - \alpha)}\right)^{\frac{p}{pq-1}} \left(\frac{\Gamma(p\delta)}{\Gamma(p\delta - \beta)}\right)^{\frac{1}{pq-1}},$$

with

$$\delta = \frac{\alpha + q\beta}{pq - 1}, \quad \xi = \frac{\beta + p\alpha}{pq - 1}. \tag{2.44}$$

Let us notice at this stage that the analysis in [90] gives no information on $T_{max}^{\alpha,\beta}$.

Theorem 2.3.7. *For the system of Volterra equations (2.42), $u(t) \to \infty$ and $v(t) \to \infty$ as $t \to T_{max}$, where*

$$T_L \le T_{max} \le T_U.$$

The bounds T_L and T_U are given by

$$T_L := \begin{cases} \left[\frac{\Gamma(\beta)v_0^{q+1}}{\Gamma(\alpha)u_0^{p+1}}\right]^{1/(\beta-\alpha)} \left[\frac{\alpha(r-1)^{r-1}}{\gamma r^r}\right]^{1/(\alpha)}, & if \;\; \alpha(r-1)^{r-1} \le \gamma r^r, \\ \left[\frac{\Gamma(\beta)v_0^{q+1}}{\Gamma(\alpha)u_0^{p+1}}\right]^{1/(\beta-\alpha)} \left[\frac{\beta(r-1)^{r-1}}{\gamma r^r} - \frac{\beta-\alpha}{\alpha}\right]^{1/(\beta)} & if \;\; \alpha(r-1)^{r-1} > \gamma r^r. \end{cases} \tag{2.45}$$

$$T_U := \begin{cases} \left[\frac{\Gamma(\beta)v_0^{q+1}}{\Gamma(\alpha)u_0^{p+1}}\right]^{1/(\beta-\alpha)} \left[\frac{\beta(r+1)}{\gamma(pq-1)}\right]^{1/(\beta)}, & if \;\; \beta(r+1) \le \gamma(pq-1), \\ \left[\frac{\Gamma(\beta)v_0^{q+1}}{\Gamma(\alpha)u_0^{p+1}}\right]^{1/(\beta-\alpha)} \left[\frac{\alpha(r+1)}{\gamma(pq-1)} - \frac{\beta-\alpha}{\beta}\right]^{1/(\alpha)} & if \;\; \beta(r+1) > \gamma(pq-1). \end{cases} \tag{2.46}$$

where $r := \max(p,q)$ and

$$\gamma := \mu\left(\frac{[\Gamma(\beta)]^{\alpha}[v_0]^{\beta q+\alpha}}{\Gamma(\alpha)]^{\beta}[u_0]^{\alpha p+\beta}}\right)^{\frac{1}{\beta-\alpha}}. \tag{2.47}$$

For the proof of the theorem see Appendix A.1.

2.3.3 Analysis of the results

It is a well known fact [38] that the Mittag-Leffler function $E_{1-\alpha}(-t^{1-\alpha}) =: e_{1-\alpha}(t)$ is completely monotone for $t > 0$, $0 < \alpha < 1$; so, in particular $e'_{1-\alpha}(t) \le 0$ for $t > 0$. Then equations (2.22) and (2.23) allow us to write

$$u'(t) \le v(t)^q, \qquad v'(t) \le u(t)^p, \qquad t > 0. \tag{2.48}$$

The differential inequalities (2.48) lead to the estimates from above of the solution (u,v) for $0 < t < T_{max} < +\infty$

$$u(t) \le C_1\Big(T_{max} - t\Big)^{-\frac{q+1}{pq-1}}, \qquad v(t) \le C_2\Big(T_{max} - t\Big)^{-\frac{p+1}{pq-1}},$$

where T_{max}, C_1 and C_2 are given in (2.18). To obtain estimates from below for u and v, we notice that the system (FDS) can be written as:

$$D_{0+}^{\alpha}(u-u_0)(t) = v(t)^q - u'(t), \quad D_{0+}^{\beta}(v-v_0)(t) = u(t)^p - v'(t), \quad t > 0. \tag{2.49}$$

Using inequalities (2.48) we obtain

$$D_{0+}^{\alpha}(u-u_0)(t) \ge 0, \quad D_{0+}^{\beta}(v-v_0)(t) \ge 0.$$

Lemma 2.3.8. *For any $u_0 > 0$, $v_0 > 0$, it holds:*

$$u' > 0, \quad v' > 0.$$

Proof. Let $u'_- = max(0, -u')$, $u'_+ = max(0, u')$, $v'_- = max(0, -v')$, $v'_+ = max(0, v')$, so, $u' = u'_+ - u'_-$ and $v' = v'_+ - v'_-$. We are intended to show that $u'_- = 0$ and $v'_- = 0$. From the system (FDS) and using $DD^\alpha_{0_+} = D^\alpha_{0_+}D$ (where D is the first order integer derivative) we have

$$\begin{aligned} u'' + D^\alpha_{0_+}u' &= qv^{q-1}v', &(2.50)\\ v'' + D^\beta_{0_+}v' &= pu^{p-1}u'. &(2.51)\end{aligned}$$

Multiplying both sides of the equation (2.50) with u'_- and using the definitions of u'_+ and u'_-, we get the equation

$$(u''_-)(u'_-) + (u'_-)D^\alpha_{0_+}(u'_-) = -qv^{q-1}v'(u'_-). \tag{2.52}$$

Taking the integral over $[0, T]$ and using the inequality $\int_0^T w(t)D^\alpha_{0_+}w \geq 0, w(0) = 0, 0 < \alpha < 1$ [106], the following inequality is obtained

$$\begin{aligned} \int_0^T (u''_-)(u'_-) &\leq -q\int_0^T v^{q-1}v'(u'_-),\\ &= -q\int_0^T v^{q-1}v'_+(u'_-) + q\int_0^T v^{q-1}v'_-(u'_-),\\ &\leq q\int_0^T v^{q-1}v'_-(u'_-),\end{aligned}$$

Using Hölder's inequality, we obtain

$$\begin{aligned} \frac{d}{dt}\left(\frac{1}{2}\int_0^T (u'_-)^2\right) &\leq qC(T)\varepsilon\int_0^T (v'_-)^2 + qC(T)C^*(\varepsilon)\int_0^T (u'_-)^2,\\ &\leq C_1\left(\int_0^T (v'_-)^2 + \int_0^T (u'_-)^2\right), &(2.53)\end{aligned}$$

where $C_1 = max\{qC(T)\varepsilon, qC(T)C^*(\varepsilon)\}$, since v is locally bounded. Likewise, we obtain

$$\frac{d}{dt}\left(\frac{1}{2}\int_0^T (v'_-)^2\right) \leq C_2\left(\int_0^T (v'_-)^2 + \int_0^T (u'_-)^2\right). \tag{2.54}$$

Adding (2.53) and (2.54), we obtain

$$\frac{d}{dt}\Big(\int_0^T (u'_-)^2 + (v'_-)^2\Big) \leq C\Big(\int_0^T (v'_-)^2 + \int_0^T (u'_-)^2\Big), \tag{2.55}$$

where $C = max(2C_1, 2C_2)$. Using Gronwall's inequality and the fact that $u'_-(0) = v'_-(0) = 0$, we conclude that $u'_- = 0$ and $v'_- = 0$; hence the result. □

At this stage, the following configuration is obtained

$$\begin{array}{ll} D^{\alpha}_{0+}(u-u_0)(t) \leq v(t)^q, & D^{\beta}_{0+}(v-v_0)(t) \leq u(t)^p, \\ u'(t) \leq v(t)^q, & v'(t) \leq u(t)^p. \end{array} \tag{2.56}$$

Furthermore, from the system (FDS) along with $u' > 0, v' > 0$ (c.f. Lemma 1.9.6) and $u'' > 0, u'' > 0$ we have the system (ODSL)

$$u'(t) \geq \frac{v(t)^q\Gamma(2-\alpha)}{\Gamma(2-\alpha)+t^{1-\alpha}}, \qquad v'(t) \geq \frac{u(t)^p\Gamma(2-\beta)}{\Gamma(2-\beta)+t^{1-\beta}}.$$

The analysis of the above inequalities gives us the precise profile of the blowing up solutions of the system (FDS).

2.4 Numerical implementation

For the numerical treatment of the system (FDS), we will approximate the solution (u, v) through equations (2.20) and (2.21). The approximation of solutions to the system (PFDS) is obtained via its equivalent form given by the system of Volterra equations in (2.42).

The numerical approximations of the solutions to both systems (FDS) and (PFDS) require the approximations of the convolution integrals; this has been studied to a reasonable extent in the literature. One of the techniques is the convolution quadrature method in which the quadrature weights are determined by the Laplace transform of the convolution kernel and a linear multistep method (see [77] and references therein).

In this work, the backward Euler convolution quadratures are used for approximating the convolution integral

$$\int_0^t K(t-\tau)g(\tau)d\tau. \tag{2.57}$$

Let $\varrho > 0$ be the time step of the discretization, then

$$\begin{aligned} \int_0^t K(t-\tau)g(\tau)d\tau &= \int_0^t \Big(\frac{1}{2\pi i}\int_\gamma e^{s(t-\tau)}\mathcal{L}\{K(\tau):s\}ds\Big)g(\tau)d\tau \\ &= \frac{1}{2\pi i}\int_\gamma y(s,t)\mathcal{L}\{K(\tau):s\}ds, \end{aligned}$$

where γ is a suitable path connecting $-i\infty$ to $+i\infty$ and

$$y(s,t) = \int_0^t e^{s(t-\tau)} g(\tau) d\tau$$

is the solution of the initial value problem

$$y' = sy + g, \qquad y(0) = 0, \quad 0 \leq t \leq T. \tag{2.58}$$

The backward Euler convolution quadrature is obtained as

$$\int_0^{t_n} K(t_n - s) u(s) \sim \frac{1}{2\pi i} \int_\gamma \mathcal{L}\{K(\tau) : s\} y_n(s) ds,$$

where $t_n = n\varrho$, and $y_n(s)$ stands for the approximation of $y(s, t_n)$ reached by the backward Euler method applied to (2.58). Therefore, if $\delta(\sigma)$ is the generating polynomial for the backward Euler method that is $\delta(\sigma) = 1 - \sigma$, then

$$\int_0^{t_n} K(t_n - \tau) g(\tau) d\tau \sim \sum_{j=0}^{n} q_{n-j}^{\alpha} g(t_j); \tag{2.59}$$

the convolution quadrature weights (CQW) q_j^α are given by the coefficients of

$$\sum_{j=0}^{+\infty} q_j^\alpha \sigma^j = \mathcal{L}\left\{K(t) : \frac{\delta(\sigma)}{\varrho}\right\}. \tag{2.60}$$

For more details on the convolution quadrature methods one is referred to [77] and references therein.

Let for $n \geq 0$ the approximation of $u(t_n)$ be u_n, then the discritization of the system (FDS) via equations (2.20), (2.21) by the backward Euler convolution quadrature method gives

$$u_n = (1 - q_0^\alpha q_0^\beta)^{-1} \left[u_0 + q_0^\alpha v_0 + \sum_{j=0}^{n-1} q_{n-j}^\alpha v_j + q_0^\alpha \left(\sum_{j=0}^{n-1} q_{n-j}^\beta u_j \right) \right], \tag{2.61}$$

$$v_n = (1 - q_0^\alpha q_0^\beta)^{-1} \left[v_0 + q_0^\beta u_0 + \sum_{j=0}^{n-1} q_{n-j}^\alpha u_j + q_0^\beta \left(\sum_{j=0}^{n-1} q_{n-j}^\alpha v_j \right) \right], \tag{2.62}$$

for $n = 1, 2, 3, \ldots$, where the quadrature coefficients q_j^α, q_j^β are determined from equation (2.60) with $K(t) = e_{1-\alpha}$ and $K(t) = e_{1-\beta}$, respectively. Similarly, a numerical scheme for the system (PFDS) can be obtained.

Setting

$$\psi_{v_{n-1}} = \left[u_0 + q_0^\alpha v_0 + \sum_{j=0}^{n-1} q_{n-j}^\alpha v_j + q_0^\alpha \left(\sum_{j=0}^{n-1} q_{n-j}^\beta u_j \right) \right],$$

Algorithm 1 Algorithm for the numerical approximation of solution to system (FDS).

Input : $p > 1, q > 1, 0 < \alpha, \beta < 1$, and u_0, v_0 satisfy (2.1).
Initializations : Fix step length h, compute t_i for all $i = 1, 2, ..., n$, $u^1 = u_0, v^1 = v_0$ and $u^1_{temp} = u_0^p, v^1_{temp} = v_0^q$.
CQW : Calculate convolution quadrature weights, $CQW\alpha$, $CQW\beta$ using Fast Fourier Transform (FFT) as in [14].
for $i = 2, ..., n$
Calculation of $\psi_{u_{n-1}}$ and $\psi_{v_{n-1}}$.

$u^i_{temp1} = u_0 + CQW\alpha(1) * v^1 + CQW\alpha(1) * (u^{i-1} * CQW\beta) + v^{i-1}_{temp} * CQW\alpha$

$v^i_{temp2} = v_0 + CQW\beta(1) * u^1 + CQW\beta(1) * (v^{i-1} * CQW\alpha) + u^{i-1}_{temp} * CQW\beta$

Calculate u^i, v^i from equations (2.61)-(2.62).
Control on blow − up : if (u^i=overflow or v^i=overflow), **break**
else $u^i_{temp} = (u^i)^p, v^i_{temp} = (v^i)^q$.
end if
end for
Output : Numerical approximation of solutions to system (FDS).

$$\psi_{u_{n-1}} = \left[v_0 + q_0^\beta u_0 + \sum_{j=0}^{n-1} q^\alpha_{n-j} v_j + q_0^\beta \left(\sum_{j=0}^{n-1} q^\alpha_{n-j} u_j \right) \right],$$

the algorithm for the above numerical scheme is

Example 1:
For the Figure 2.1 we set $p = 1.5, q = 2, \alpha = 0.75, \beta = 0.5$; the initial conditions are $u_0 = 3, v_0 = 2$. In Figure 2.1 (a) the solution curves $u(t)$ corresponding to the systems (FDS), (ODS) and (ODSL) are plotted. The dotted curve is the solution of the system (ODS) with $\lambda = 1$. As expected, the middle solid curve corresponds to the solution of the system (FDS). Finally, the dash followed by a dot curve is the solution of the system (ODSL).

Likewise, in Figure 2.1 (b) the solution curves $v(t)$ for the systems are plotted. It could be seen that the solution curves of the system (FDS) are between the solution curves of (ODS) and (ODSL).

Example 2:
In the second example, we take the parameters $p = 1.1, q = 1.4, \alpha = 0.5 = \beta$; the initial conditions $u_0 = 3 = v_0$. In Figure 2.2 (a) the solution curves $u(t)$ corresponding to the systems (FDS), (ODS) and (ODSL) are plotted. The dotted curve (which serve as lower bound for the solution curve of (FDS)) is the solution of the system (ODSL). The solid curve is the solution of the system (FDS) and the dash followed by dot curve is the solution of the system (PFDS) with $\mu = 1$.

In Figure 2.2 (b) the corresponding solution curves $v(t)$ for the systems are plotted. The profiles of the solution curves for the system (FDS) match the analysis of section 3.3.

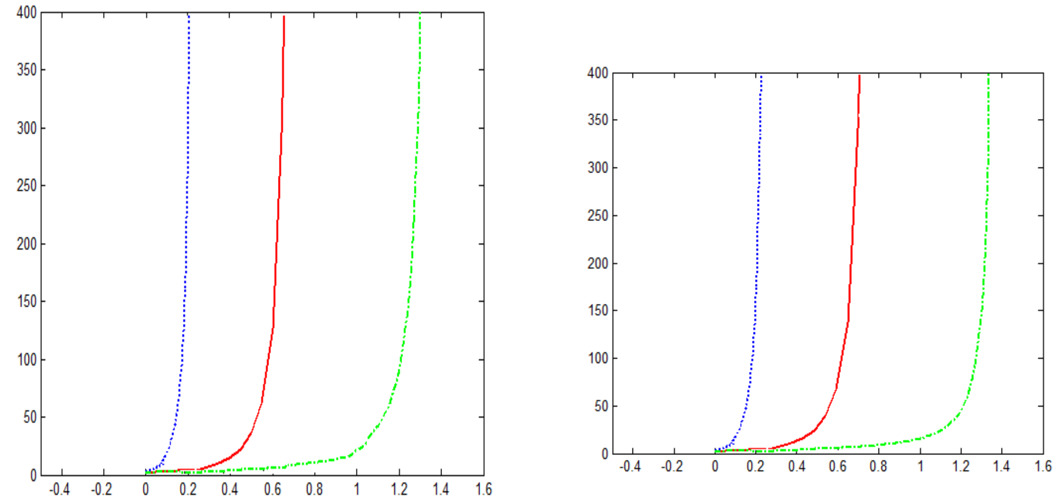

(a) (b)

Figure 2.1: Solution curves for $p = 1.5, q = 2,\ \alpha = 0.75, \beta = 0.5,\ u_0 = 3, v_0 = 2$ (a) Solution curves $u(t)$ for the systems (FDS), (ODS) and (ODSL) (b) Solution curves $v(t)$ for the systems (FDS), (ODS) and (ODSL).

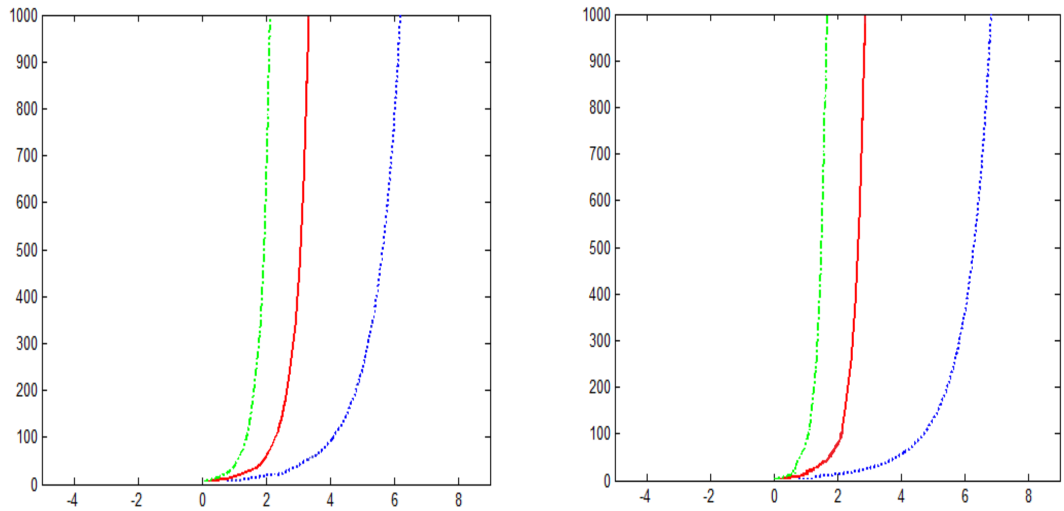

(a) (b)

Figure 2.2: Solution curves for $p = 1.1, q = 1.4,\ \alpha = 0.5,\ \beta = 0.5,\ u_0 = 3, v_0 = 3$ (a) Solution curves $u(t)$ for the systems (FDS), (ODS) and (ODSL) (b) Solution curves $v(t)$ for the systems (FDS), (ODS) and (ODSL).

Example 3:
For Figure 2.3, we set $p = 1.1, q = 1.8, \alpha = 0.25, \beta = 0.4$; the initial conditions are $u_0 = 5, v_0 = 1$. The profile of the solution (u, v), for the system (FDS) is given by the system (ODS) with $\lambda = 1$ and the system (ODSL).

As expected, our simulations show a dependance between the parameters $(\alpha, \beta, u_0, v_0, p, q)$ and the calculated blow up.

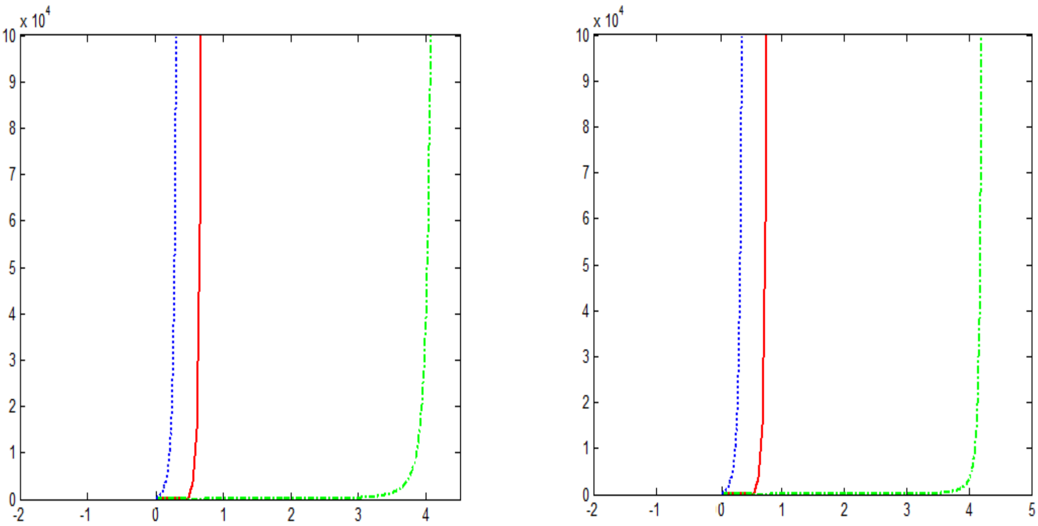

(a) (b)

Figure 2.3: Solution curves for $p = 1.1, q = 1.8,\ \alpha = 0.25, \beta = 0.4,\ u_0 = 5, v_0 = 1$ (a) Solution curves $u(t)$ for the systems (FDS), (ODS) and (ODSL) (b) Solution curves $v(t)$ for the systems (FDS), (ODS) and (ODSL).

2.5 Conclusion and perspectives

We have presented a strategy for getting the profile of blowing-up solutions of a nonlinear system of fractional differential equations with power nonlinearities. We believe that the strategy works for the exponential type nonlinearities.

It would be an interesting task to extend the analysis for the systems

- $$\begin{array}{rcll} u_1'(t) + \rho_1 D_{0+}^{\alpha_1}(u_1 - u_1(0))(t) &=& u_1^{p_{11}} u_2^{p_{12}} ... u_n^{p_{1n}}, & t > 0, \quad \rho_1 > 0, \\ u_2'(t) + \rho_2 D_{0+}^{\alpha_2}(u_2 - u_2(0))(t) &=& u_1^{p_{21}} u_2^{p_{22}} ... u_n^{p_{2n}}, & t > 0, \quad \rho_1 > 0, \\ ... & & ... & \\ u_n'(t) + \rho_n D_{0+}^{\alpha_n}(u_n - u_n(0))(t) &=& u_1^{p_{n1}} u_2^{p_{n2}} ... u_n^{p_{nn}}, & t > 0, \quad \rho_n > 0, \end{array}$$

with $0 < \alpha_i < 1$, $p_{ij} > 1$ for $i, j = 1, 2, ..., n$ and subject to the initial conditions

$$u_i(0) = u_{i0} > 0, \qquad i = 1, 2, ..., n.$$

- $$\begin{aligned} u_1'(t) + \sum_{i=1}^{N} \rho_{1i} D_{0_+}^{\alpha_{1i}}(u_i - u_i(0))(t) &= f_1(u_1, u_2, ..., u_n), \qquad t > 0, \\ u_2'(t) + \sum_{i=1}^{N} \rho_{2i} D_{0_+}^{\alpha_{2i}}(u_i - u_i(0))(t) &= f_2(u_1, u_2, ..., u_n), \qquad t > 0, \\ \cdots \qquad & \qquad \cdots \\ u_n'(t) + \sum_{i=1}^{N} \rho_{ni} D_{0_+}^{\alpha_{ni}}(u_i - u_i(0))(t) &= f_n(u_1, u_2, ..., u_n), \qquad t > 0, \end{aligned}$$

subject to the initial conditions

$$u_i(0) = u_{i0} > 0, \qquad i = 1, 2, ..., N,$$

where $0 < \alpha_{ij} < 1$, $\rho_{ij} > 0$ for $i = 1, 2, ..., N$, $j = 1, 2, ..., n$ and f_i are real valued functions satisfy some conditions for example condition (2.63).

- $$\begin{aligned} \sum_{i=0}^{N} D_{0_+}^{\alpha_i}(u^{m_i} - u_0^{m_i})(t) &+ \sum_{i=0}^{M} D_{0_+}^{\delta_i}(v^{l_i} - v_0^{l_i})(t) = f_1(t, u, v), \\ \sum_{i=0}^{K} D_{0_+}^{\beta_i}(v^{n_i} - v_0^{n_i})(t) &+ \sum_{i=0}^{L} D_{0_+}^{\delta_i}(u^{k_i} - u_0^{k_i})(t) = f_2(t, u, v), \end{aligned}$$

for $m_i > 0, n_i > 0, l_i > 0, k_i > 0$ and, for example

$$\begin{aligned} f_1(t, u, v) &\geq c_1 t^{\theta_1} |u(t)|^{p_1} + c_2 t^{\theta_2} |v(t)|^{p_2}, \\ f_2(t, u, v) &\geq c_3 t^{\theta_3} |u(t)|^{p_3} + c_4 t^{\theta_4} |v(t)|^{p_4}, \end{aligned} \tag{2.63}$$

where $p_1 > 1, p_2 > 1, p_3 > 1, p_4 > 1$ are real numbers and $c_2 > 0, c_3 > 0, c_1 \in \mathbb{R}, c_4 \in \mathbb{R}$ are constants.

Determination of an unknown source term and the temperature distribution for the linear heat equation involving fractional derivative in time

Purpose of the paper:

The purpose of this paper [65] is to determine the pair of functions $\{u(x,t), f(x)\}$ i.e., the temperature distribution and the source term for the following fractional diffusion equation

$$\begin{aligned} D^{\alpha}_{0+}(u(x,t)-u(x,0)) - \varrho u_{xx}(x,t) &= f(x), \qquad (x,t)\in Q_T, && (2.64)\\ u(x,0)=\varphi(x) \quad u(x,T) &= \psi(x), \qquad x\in[0,1], && (2.65)\\ u(1,t)=0, \quad u_x(0,t) &= u_x(1,t), \quad t\in[0,T], && (2.66) \end{aligned}$$

where $\varrho > 0$, D^{α}_{0+} stands for the Riemann-Liouville fractional derivative of order $0 < \alpha < 1$, $\varphi(x)$ and $\psi(x)$ are the initial and final temperatures respectively.

The problem:

The problem in solving the inverse problem is due to the nonlocal boundary conditions (2.66). The underlying spectral problem for (2.64)-(2.66) is non-self-adjoint and we are unable to write the solution as sum of eigenfunctions. The difficulty for solving the inverse problem also arise due to the presence of fractional derivative in time.

Strategy:

For the solution of the inverse problem we shall get the two basis for the space $L^2(0,1)$, which form the biorthogonal system (see V. A. Il'in [49] and M. V. Keldysh [60]). Due to this biorthogonal system we are able to expand the solution in terms of the biorthogonal system. We show the existence and uniqueness of the the inverse problem using properties of the Mittag-Leffler function.

Nonlocal boundary conditions

The nonlocal boundary conditions considered in Chapter 3 and Chapter 4 are known as Bitsadze-Smaraskii boundary conditions. In 1969 A. V. Bitsadze and A. A. Samaraskii considered the nonlocal boundary conditions for the elliptic problem arising in plasma theory.

The nonlocal boundary conditions has the following physical sense: to find the stationary distribution of temperature in plasma such that the temperature on the part of the boundary is equal to the temperature on some manifold inside the domain or other part of the boundary.

Apart from plasma theory nonlocal boundary-value problems have important applications to modern aircraft technology see [105], to the theory of multidimensional diffusion processes see [31, 32] etc. W. Feller in [32] completely characterized the analytic structure of one-dimensional diffusion processes. He proved that if a second-order ordinary differential operator is a generator of a nonnegative contractive strongly continuous semigroup (Feller semigroup), then its domain consists of functions satisfying nonlocal boundary conditions. Conversely, if a second-order ordinary differential operator is defined on the set of sufficiently smooth functions satisfying such nonlocal boundary conditions, then the closure of this operator is a generator of a Feller semigroup.

Let us mention that the general form of the boundary conditions for an infinitesimal generator of Feller semigroup was studied by Venttsel in [110].

Chapter 3

Determination of an unknown source term and the temperature distribution for the linear heat equation involving fractional derivative in time

Abstract

We consider the inverse problem of finding the temperature distribution and the heat source whenever the temperatures at the initial time and the final time are given. The problem considered is one dimensional and the unknown heat source is supposed to be space dependent only. The existence and uniqueness results are proved.

Keywords: Inverse problem, fractional derivative, heat equation, integral equations, biorthogonal system of functions, Fourier series

MSC [2010]: 80A23, 65N21, 26A33, 45J05, 34K37, 42A16.

Contents

3.1 Introduction

In this paper, we are concerned with the problem of finding $u(x,t)$ (the temperature distribution) and $f(x)$ (the source term) in the domain $Q_T = (0,1)\times(0,T)$ for the following system

$$\begin{aligned} D^{\alpha}_{0_+}(u(x,t)-u(x,0)) - \varrho u_{xx}(x,t) &= f(x), \qquad (x,t)\in Q_T, &(3.1)\\ u(x,0)=\varphi(x) \quad u(x,T) &= \psi(x), \qquad x\in[0,1], &(3.2)\\ u(1,t)=0, \quad u_x(0,t) &= u_x(1,t), \qquad t\in[0,T], &(3.3)\end{aligned}$$

where $\varrho > 0$, $D^{\alpha}_{0_+}$ stands for the Riemann-Liouville fractional derivative of order $0<\alpha<1$, $\varphi(x)$ and $\psi(x)$ are the initial and final temperatures respectively. Our choice of the term $D^{\alpha}_{0_+}(u(x,.)-u(x,0))(t)$ rather then the usual term $D^{\alpha}_{0_+}u(x,.)(t)$ is to avoid not only the singularity at zero but also to impose meaningful initial condition.

The problem of determination of temperature at interior points of a region when the initial and boundary conditions along with heat source term are specified are known as direct heat conduction problems. In many physical problems, determination of coefficients or right hand side (the source term, in case of the heat equation) in a differential equation from some available information is required; these problems are known as *inverse problems*. These kind of problems are ill posed in the sense of Hadamard. A number of articles address the solvability problem of the inverse problems (see [5, 8, 54, 56, 69, 104, 98] and references therein).

From last few decades fractional calculus grabbed great attention of not only mathematicians and engineers but also of many scientists from all fields. Indeed fractional calculus tools have numerous applications in nanotechnology, control theory, viscoplasticity flow, biology, signal and image processing etc, see the latest monographs, [7, 62, 70, 101, 102] articles [21, 71] and reference therein. The mathematical analysis of initial and boundary value problems (linear or nonlinear) of fractional differential equations has been studied extensively by many authors, we refer to , [2], [68], [64] and references therein.

In the next section we recall some definitions and notations from fractional calculus. Section 3 is devoted to our main results; we provide the expressions for the temperature distribution and the source term for the problem (3.1)-(3.3). Furthermore, we proved the existence and uniqueness of the inverse problem.

3.2 Preliminaries and notations

In this section, we recall basic definitions, notations from fractional calculus (see [62], [70], [102]).

For an integrable function $f:\mathbb{R}^+\to\mathbb{R}$ the left sided Riemann-Liouville fractional integral of order $0 < \alpha < 1$ is defined by

$$J^{\alpha}_{0_+} f(t) := \frac{1}{\Gamma(\alpha)} \int\limits_0^t \frac{f(\tau)}{(t-\tau)^{1-\alpha}} d\tau, \quad t > 0, \tag{3.4}$$

where $\Gamma(\alpha)$ is the Euler Gamma function. The integral (6.7) can be written as a convolution

$$J^{\alpha}_{0_+} f(t) = (\phi_\alpha \star f)(t), \tag{3.5}$$

where

$$\phi_\alpha := \begin{cases} t^{\alpha-1}/\Gamma(\alpha), & t > 0, \\ 0 & t \leq 0. \end{cases} \tag{3.6}$$

The Riemann-Liouville fractional derivative of order $0 < \alpha < 1$ is defined by

$$D^{\alpha}_{0_+} f(t) := \frac{d}{dt} J^{1-\alpha}_{0_+} f(t) = \frac{1}{\Gamma(1-\alpha)} \frac{d}{dt} \int\limits_0^t \frac{f(\tau)}{(t-\tau)^{\alpha}} d\tau. \tag{3.7}$$

In particular, when $\alpha = 0$ and $\alpha = 1$ then $D^0_{0_+} f(t) = f(t)$ and $D^1_{0_+} f(t) = f'(t)$ respectively; notice that the Riemann-Liouville fractional derivative of a constant is not equal to zero.

The Laplace transform of the Riemann-Liouville integral of order $0 < \alpha < 1$ of a function with at most exponentially growth is

$$\mathcal{L}\{J^{\alpha}_{0_+} f(t) : s\} = \mathcal{L}\{f(t) : s\}/s^{\alpha}.$$

Also, for $0 < \alpha < 1$ we have

$$J^{\alpha}_{0_+} D^{\alpha}_{0_+} \Big(f(t) - f(0) \Big) = f(t) - f(0). \tag{3.8}$$

The Mittag-Leffler function plays an important role in the theory of fractional differential equations, for any $z \in \mathbb{C}$ the Mittag-Leffler function with parameter ξ is

$$E_\xi(z) = \sum_{k=0}^{+\infty} \frac{z^k}{\Gamma(\xi k + 1)} \qquad (Re(\xi) > 0). \tag{3.9}$$

In particular, $E_1(z) = e^z$

The Mittag-Leffler function of two parameters $E_{\xi,\beta}(z)$ which is a generalization of (3.9) is defined by

$$E_{\xi,\beta}(z) = \sum_{k=0}^{+\infty} \frac{z^k}{\Gamma(\xi k + \beta)} \qquad (z, \beta \in \mathbb{C}; \;\; Re(\xi) > 0). \tag{3.10}$$

3.3 Main Results

Let $e_\xi(t,\mu) := E_\xi(-\mu t^\xi)$ where $E_\xi(t)$ is the Mittag-Leffler function with one parameter ξ as defined in (3.9) and μ is a positive real number. Let us state and prove the

Lemma 3.3.1. *Let $g : \mathbb{R}^+ \to \mathbb{R}$ be a differentiable function such that $g \in L^1(\mathbb{R})$. The solution of equation*

$$v(t) + \mu J^{\alpha}_{0_+} v(t) = g(t) \tag{3.11}$$

for $\mu \in \mathbb{R}^+$ satisfies the integral equation

$$v(t) = \int_0^t g'(t-\tau)e_\alpha(\tau,\mu)d\tau + g(0)e_\alpha(t,\mu), \tag{3.12}$$

Proof. Taking the Laplace transform of both sides of the equation (3.11), it follows

$$\mathcal{L}\{v(t) : s\} = \frac{s^\alpha \mathcal{L}\{g(t) : s\}}{s^\alpha + \mu}. \tag{3.13}$$

There are different ways for getting the solution from the equation (3.13) by the inverse Laplace transform.

Writing the equation (3.13) as

$$\mathcal{L}\{v(t); s\} = \frac{s^{\alpha-1}}{s^\alpha + \mu}\Big(s\mathcal{L}\{g(t) : s\} - g(0)\Big) + \frac{s^{\alpha-1}}{s^\alpha + \mu} g(0);$$

and using the inverse Laplace transform, we obtain

$$v(t) = \int_0^t g'(t-\tau)e_\alpha(\tau,\mu)d\tau + g(0)e_\alpha(t,\mu),$$

which is (3.12). □

3.3.1 Solution of the inverse problem

The key factor in determination of the temperature distribution and the unknown source term for the system (3.1)-(3.3) is the specially chosen basis for the space $L^2(0,1)$ which is

$$\{2(1-x), \quad \{4(1-x)\cos 2\pi nx\}_{n=1}^\infty, \quad \{4\sin 2\pi nx\}_{n=1}^\infty\}. \tag{3.14}$$

In [53], it is proved that the set of functions in (3.14) forms a Riesz basis for the space $L^2(0,1)$, hence the set is closed, minimal and spans the space $L^2(0,1)$.

The set of functions (3.14) is not orthogonal and it forms a biorthogonal set of functions with the set of functions given by

$$\{1, \quad \{\cos 2\pi nx\}_{n=1}^\infty, \quad \{x \sin 2\pi nx\}_{n=1}^\infty\}, \tag{3.15}$$

see [86].

The solution of the inverse problem for the linear system (3.1)-(3.3) can be written in the form

$$u(x,t) = 2u_0(t)(1-x) + \sum_{n=1}^{\infty} u_{1n}(t)4(1-x)\cos 2\pi nx + \sum_{n=1}^{\infty} u_{2n}(t)4\sin 2\pi nx \quad (3.16)$$

$$f(x) = 2f_0(1-x) + \sum_{n=1}^{\infty} f_{1n}4(1-x)\cos 2\pi nx + \sum_{n=1}^{\infty} f_{2n}4\sin 2\pi nx \quad (3.17)$$

where $u_0(t), u_{1n}(t), u_{2n}(t), f_0, f_{1n}$ and f_{2n} are to be determined. By plugging the expressions of $u(x,t)$ and $f(x)$ from (3.16) and (3.17) into the equation (3.1), the following system of fractional differential equations is obtained

$$\begin{aligned} D_{0+}^{\alpha}(u_{2n}(t) - u_{2n}(0)) - 4\pi n\varrho u_{1n}(t) + 4\pi^2 n^2 \varrho u_{2n}(t) &= f_{2n}, & (3.18)\\ D_{0+}^{\alpha}(u_{1n}(t) - u_{1n}(0)) + 4\pi^2 n^2 \varrho u_{1n}(t) &= f_{1n}, & (3.19)\\ D_{0+}^{\alpha}(u_0(t) - u_0(0)) &= f_0. & (3.20) \end{aligned}$$

Since $J_{0+}^{\alpha}1 = t^{\alpha}/\Gamma(1+\alpha)$ and for $0<\alpha<1$, $J_{0+}^{\alpha}D_{0+}^{\alpha}(u_0(t)-u_0(0)) = u_0(t)-u_0(0)$ then the solution of equation (3.20) is

$$u_0(t) = \frac{f_0 t^{\alpha}}{\Gamma(1+\alpha)} + u_0(0). \quad (3.21)$$

Setting $\lambda := 4\pi^2 n^2 \varrho$, $F(t) := f_{1n}t^{\alpha}/\Gamma(1+\alpha) + u_{1n}(0)$ then equation (3.19) can be written as

$$u_{1n}(t) + \lambda J_{0+}^{\alpha} u_{1n}(t) = F(t),$$

and using lemma (3.3.1), the solution of the equation (3.19) is given by

$$u_{1n}(t) = \frac{f_{1n}\alpha}{\Gamma(1+\alpha)} \int_0^t (t-\tau)^{\alpha-1} e_{\alpha}(\tau,\lambda)d\tau + u_{1n}(0)e_{\alpha}(t,\lambda). \quad (3.22)$$

Noticing that equation (3.18) can be written as

$$u_{2n}(t) + \lambda J_{0+}^{\alpha} u_{2n}(t) = h(t) \quad (3.23)$$

where $h(t) := J_{0+}^{\alpha}\Big(f_{2n} + 4\pi n\varrho u_{1n}(t)\Big) + u_{2n}(0)$, so its solution by virtue of lemma (3.3.1) is

$$u_{2n}(t) = \int_0^t h'(t-\tau)e_{\alpha}(\tau,\lambda)d\tau + h(0)e_{\alpha}(t,\lambda). \quad (3.24)$$

As $h(0) = u_{2n}(0)$ and

$$\begin{aligned} h'(t) &= \frac{d}{dt}\Big[J_{0+}^{\alpha}(f_{2n} + 4\pi n\varrho u_{1n}(t)) - u_{2n}(0)\Big] \\ &= D_{0+}^{1-\alpha}\Big(f_{2n} + 4\pi n\varrho u_{1n}(t)\Big). \end{aligned}$$

From equation (3.22), we have

$$D_{0_+}^{1-\alpha}u_{1n}(t) = \frac{f_{1n}\alpha}{\Gamma(1+\alpha)}D_{0_+}^{1-\alpha}[t^{\alpha-1}\star e_\alpha(t,\lambda)] + u_{1n}(0)D_{0_+}^{1-\alpha}e_\alpha(t,\lambda),$$

since $D_{0_+}^{1-\alpha}e_\alpha(t,\lambda) = e_{\alpha,\alpha}(t,\lambda)$, where $e_{\alpha,\beta}(t,\lambda) := t^{\beta-1}E_{\alpha,\beta}(-\lambda t^\alpha)$; consequently the equation (3.24) becomes

$$u_{2n}(t) = \int_0^t s(t-\tau)e_\alpha(\tau,\lambda)d\tau + u_{2n}(0)e_\alpha(t,\lambda). \tag{3.25}$$

where we have set

$$s(t) := 4\pi n\varrho\left(\frac{\alpha f_{1n}}{\Gamma(1+\alpha)}t^{\alpha-1}\star e_{\alpha,\alpha}(t,\lambda) + u_{1n}(0)e_{\alpha,\alpha}(t,\lambda)\right) + f_{2n}\frac{t^{\alpha-1}}{\Gamma(\alpha)}.$$

The unknown constants are $u_{2n}(0), u_{1n}(0), u_0(0), f_{2n}, f_{1n}$ and f_0. In order to get these unknowns, we use the initial and final temperatures as given in (3.2)

$$\begin{aligned} 2u_0(0)(1-x) &+ \sum_{n=1}^\infty u_{1n}(0)4(1-x)\cos 2\pi nx + \sum_{n=1}^\infty u_{2n}(0)4\sin 2\pi nx = 2\varphi_0(1-x) \\ &+ \sum_{n=1}^\infty \varphi_{1n}4(1-x)\cos 2\pi nx + \sum_{n=1}^\infty \varphi_{2n}4\sin 2\pi nx, \end{aligned}$$

$$\begin{aligned} 2u_0(T)(1-x) &+ \sum_{n=1}^\infty u_{1n}(T)4(1-x)\cos 2\pi nx + \sum_{n=1}^\infty u_{2n}(T)4\sin 2\pi nx = 2\psi_0(1-x) \\ &+ \sum_{n=1}^\infty \psi_{1n}4(1-x)\cos 2\pi nx + \sum_{n=1}^\infty \psi_{2n}4\sin 2\pi nx. \end{aligned}$$

By identification we get

$$u_{2n}(0) = \varphi_{2n}, \quad u_{1n}(0) = \varphi_{1n}, \quad u_0(0) = \varphi_0, \tag{3.26}$$

$$u_{2n}(T) = \psi_{2n}, \quad u_{1n}(T) = \psi_{1n}, \quad u_0(T) = \psi_0, \tag{3.27}$$

where $\{\varphi_0,\varphi_{1n},\ \varphi_{2n}\}$ and $\{\psi_0,\psi_{1n},\ \psi_{2n}\}$ are the coefficients of the series expansion in the basis (3.14)of the functions $\varphi(x)$ and $\psi(x)$, respectively. In terms of the biorthogonal basis (3.15) these are

$$\varphi_0 = \int_0^1 \varphi(x)dx, \quad \varphi_{1n} = \int_0^1 \varphi(x)\cos 2\pi nxdx, \quad \varphi_{2n} = \int_0^1 \varphi(x)x\sin 2\pi nxdx,$$

$$\psi_0 = \int_0^1 \psi(x)dx, \quad \varphi_{1n} = \int_0^1 \psi(x)\cos 2\pi nxdx, \quad \psi_{2n} = \int_0^1 \psi(x)x\sin 2\pi nxdx.$$

By virtue of (3.21), (3.22), (3.25), and conditions (3.27) we have the expressions of unknowns f_0, f_{1n} and f_{2n} as

$$f_0 = \Gamma(1+\alpha)\left[\frac{\psi_0-\varphi_0}{T^\alpha}\right], \tag{3.28}$$

$$f_{1n} = \Gamma(1+\alpha)\left[\frac{\psi_{1n}-\varphi_{1n}e_\alpha(T,\lambda)}{\alpha\int\limits_0^T (T-\tau)^{\alpha-1}e_\alpha(\tau,\lambda)d\tau}\right], \tag{3.29}$$

$$\frac{f_{2n}}{\Gamma(\alpha)} = \left[\frac{\psi_{2n}-\varphi_{2n}e_\alpha(T,\lambda)-\int\limits_0^T \mathcal{S}(T-\tau)e_\alpha(\tau,\lambda)d\tau}{\int\limits_0^T (T-\tau)^{\alpha-1}e_\alpha(\tau,\lambda)d\tau}\right], \tag{3.30}$$

where

$$\mathcal{S}(t) = 4\pi n\varrho\left(\frac{\alpha f_{1n}}{\Gamma(1+\alpha)}t^{\alpha-1}\star e_{\alpha,\alpha}(t,\lambda)+u_{1n}(0)e_{\alpha,\alpha}(t,\lambda)\right).$$

The unknown source term and the temperature distribution for the problem (3.1)-(3.3) are given by the series (3.17) and (3.16), where the unknowns $u_0(0), u_{1n}(0), u_{2n}(0)$ are calculated from (3.26), while f_0, f_{1n}, f_{2n} are given by (3.28)-(3.30). In the next subsection we will show the uniqueness of the solution.

3.3.2 Uniqueness of the solution

Suppose $\{u_1(x,t), f_1(x)\}$, $\{u_2(x,t), f_2(x)\}$ are two solution sets of the inverse problem for the system (3.1)-(3.3). Define $\overline{u}(x,t) = u_1 - u_2$ and $\overline{f}(x) = f_1 - f_2$ then the function $\overline{u}(x,t)$ satisfies the following equation and boundary conditions

$$\begin{aligned} D_{0+}^\alpha\overline{u}(x,t) - \varrho\overline{u}_{xx}(x,t) &= \overline{f}(x), && (x,t)\in Q_T, && (3.31)\\ \overline{u}(x,0)=0 \quad \overline{u}(x,T) &= 0, && x\in[0,1], && (3.32)\\ \overline{u}(1,t)=0, \quad \overline{u}_x(0,t) &= \overline{u}_x(1,t), && t\in[0,T]. && (3.33) \end{aligned}$$

Using the properties of biorthogonal system (3.14)-(3.15), we have

$$\overline{u}_0(t) = \int_0^1 \overline{u}(x,t)dx, \tag{3.34}$$

$$\overline{u}_{1n}(t) = \int_0^1 \overline{u}(x,t)\cos 2\pi nx dx, \quad (n=1,2,...), \tag{3.35}$$

and

$$\overline{u}_{2n}(t) = \int_0^1 \overline{u}(x,t)x\sin 2\pi nx dx \quad (n=1,2,...). \tag{3.36}$$

Alike,

$$\overline{f}_0 = \int\limits_0^1 \overline{f}(x)dx, \tag{3.37}$$

$$\overline{f}_{1n} = \int\limits_0^1 \overline{f}(x)\cos 2\pi nx dx, \quad (n = 1, 2, ...), \tag{3.38}$$

and

$$\overline{f}_{2n} = \int\limits_0^1 \overline{f}(x)x\sin 2\pi nx dx \quad (n = 1, 2, ...). \tag{3.39}$$

Taking the fractional derivative D_{0+}^{α} under the integral sign of equation (3.34), using (3.31), (3.37) and integration by parts, we get

$$D_{0+}^{\alpha}\overline{u}_0(t) = \overline{f}_0, \tag{3.40}$$

with the boundary conditions

$$\overline{u}_0(0) = 0, \quad \overline{u}_0(T) = 0. \tag{3.41}$$

The solution of the problem (3.40) is

$$\overline{u}_0(t) = \frac{t^{\alpha}}{\Gamma(1+\alpha)}\overline{f}_0;$$

taking into account the boundary conditions (3.41), we get

$$\overline{f}_0 = 0 \qquad \Rightarrow \qquad \overline{u}_0(t) = 0. \tag{3.42}$$

Taking the fractional derivative D_{0+}^{α} under the integral sign of equation (3.35) then by using (3.31), (3.32), (3.38) and integration by parts, we obtain

$$D_{0+}^{\alpha}\overline{u}_{1n}(t) + \lambda\overline{u}_{1n}(t) = \overline{f}_{1n}; \tag{3.43}$$

the associated boundary conditions are

$$\overline{u}_{1n}(0) = 0, \quad \overline{u}_{1n}(T) = 0. \tag{3.44}$$

The solution of the problem (3.43) is

$$\overline{u}_{1n}(t) = e_{\alpha,\alpha}(t,\lambda) \star \overline{f}_{1n}.$$

Using (3.44) we have

$$\overline{f}_{1n} = 0 \qquad \Rightarrow \qquad \overline{u}_{1n}(t) = 0, \quad (n = 1, 2, ...).$$

In the same manner from (3.36), we obtain the equation

$${}^{C}D_{0+}^{\alpha}\overline{u}_{2n}(t) + 4\pi^2 n^2\overline{u}_{2n}(t) = \overline{f}_{2n}; \tag{3.45}$$

the associated boundary conditions are

$$\overline{u}_{2n}(0) = 0, \quad \overline{u}_{2n}(T) = 0. \tag{3.46}$$

Taking account of $\overline{u}_{1n}(t) = 0$ then the solution of the equation (3.45) satisfies

$$\overline{u}_{2n}(t) = e_{\alpha,\alpha}(t, \lambda) \star \overline{f}_{2n};$$

using (3.46) we have

$$\overline{f}_{2n} = 0 \qquad \Rightarrow \qquad \overline{u}_{2n}(t) = 0, \quad (n = 1, 2, ...).$$

For every $t \in [0, T]$, the functions $\overline{u}(x, t)$ and $\overline{f}(x)$ are orthogonal to the system of functions given in (3.15), which form a basis of the space $L^2(0, 1)$, consequently,

$$\overline{u}(x, t) = 0, \quad \overline{f}(x) = 0.$$

3.3.3 Existence of the solution

Suppose $\varphi \in C^4[0, 1]$ be such that $\varphi(1) = 0, \varphi'(0) = \varphi'(1), \varphi''(1) = 0$ and $\varphi'''(0) = \varphi'''(1)$. As φ_{1n} is the coefficient of the cosine Fourier expansion of the function $\varphi(x)$ with respect to basis (3.15), from (3.26) the expression for $u_{1n}(0)$ can be written as

$$u_{1n}(0) = \int_0^1 \varphi(x) \cos 2\pi n x dx$$

which integrated by parts four times gives

$$\begin{aligned} u_{1n}(0) &= \frac{1}{16\pi^4 n^4} \int_0^1 \varphi^4(x) \cos 2\pi n x dx, \\ &= \frac{1}{16\pi^4 n^4} \varphi_{1n}^{(4)}, \end{aligned}$$

where $\varphi_{1n}^{(4)}$ is the coefficient of the cosine Fourier expansion of the function $\varphi^{(4)}(x)$ with respect to the basis (3.15).

Alike, we obtain

$$u_{2n}(0) = \frac{1}{16\pi^4 n^4} \varphi_{2n}^{(4)} + \frac{1}{4\pi^4 n^4} \varphi_{1n}^{(4)}, \tag{3.47}$$

where φ_{2n}^4 is the coefficient of sine Fourier transform of the function φ^4 with respect to the basis (3.15).

The set of functions $\{\varphi_{1n}^{(4)}, \varphi_{2n}^{(4)} \; n = 1, 2, ...\}$ is bounded as by supposition we have $\varphi \in C^4[0, 1]$, and due to the inequality

$$\sum_{n=1}^{\infty} (\varphi_{in}^{(4)})^2 \leq C \parallel \varphi^{(4)}(x) \parallel^2_{L^2(0,1)}, \quad i = 1, 2$$

which is true by the Bessel inequality of the trigonometric series. Similarly, we have for $\psi \in C^4[0,1]$ the set of functions $\{\psi_{1n}^{(4)}, \psi_{2n}^{(4)}\ n = 1,2,...\}$ is bounded and

$$\sum_{n=1}^{\infty} (\psi_{in}^{(4)})^2 \leq C \parallel \psi^{(4)}(x) \parallel_{L^2(0,1)}^2, \quad i = 1,2.$$

The Mittag-Leffler functions $e_\alpha(t;\mu)$ and $e_{\alpha,\beta}(t;\mu)$ for $\mu > 0$ and $0 < \alpha \leq 1$, $0 < \alpha \leq \beta \leq 1$ respectively, are completely monotone functions (see [38] page 268). Furthermore, we have

$$E_{\alpha,\beta}(\mu t^\alpha) \leq M, \quad t \in [a,b], \tag{3.48}$$

where $[a,b]$ is a finite interval with $a \geq 0$, and

$$\int_0^t (t-\tau)^{\alpha-1} E_{\alpha,\beta}(\lambda t^\alpha) d\tau < \infty,$$

(see [96] page 9).

The solution $u(x,t)$ becomes

$$\begin{aligned} u(x,t) \quad &= \quad 2(1-x)\Big(f_0 t^\alpha / \Gamma(1+\alpha) + \varphi_0\Big) \\ &+ \quad \sum_{n=1}^{\infty} \left(\frac{f_{1n}\alpha}{\Gamma(1+\alpha)} t^{\alpha-1} \star e_\alpha(t,\lambda) + \frac{\varphi_{1n}^{(4)}}{16\pi^4 n^4} e_\alpha(t,\lambda) \right) 4(1-x)\cos 2\pi n x \\ &+ \quad \sum_{n=1}^{\infty} \left(\frac{f_{1n}\alpha}{\Gamma(1+\alpha)} t^{\alpha-1} \star e_{\alpha,\alpha}(t,\lambda) + \frac{\varphi_{1n}^4}{4\pi^3 n^3} e_{\alpha,\alpha}(t,\lambda) + f_{2n} \frac{t^{\alpha-1}}{\Gamma(\alpha)} \star e_\alpha(t,\lambda) \right. \\ &\left. + \frac{\varphi_{2n}^{(4)}}{16\pi^4 n^4} e_\alpha(t,\lambda) \right) 4 \sin 2\pi n x \end{aligned} \tag{3.49}$$

Setting $M = \max\{M_1, M_2\}$ where

$$|e_\alpha| \leq M_1, \quad |e_{\alpha,1-\alpha}| \leq M_2 \quad t \in [0,T], T \text{ is finite.}$$

Taking into account the values of f_0, f_{1n}, f_{2n} from (3.28)-(3.30) and the properties of Mittag-Leffler function, the series (3.49) is bounded above by

$$\begin{aligned} & 2(1-x)\left(|\psi_0| + (1 - \frac{t^\alpha}{T^\alpha})|\varphi_0| \right) \\ + \quad & \sum_{n=1}^{\infty} \left(\left\{ \frac{\psi_{1n}^{(4)} - \varphi_{1n}^{(4)} M}{16\pi^4 n^4} \right\} \frac{t^\alpha}{T^\alpha} + \frac{\varphi_{1n}^{(4)}}{16\pi^4 n^4} M \right) 4(1-x)\cos 2\pi n x \\ + \quad & \sum_{n=1}^{\infty} \left(\frac{\varphi_{1n}^{(4)} M}{4\pi^3 n^3} + \frac{t^{1-\alpha}}{T^{1-\alpha}} \left\{ \frac{\psi_{2n}^{(4)} - \varphi_{2n}^{(4)} M}{16\pi^4 n^4} \right\} - \frac{\varphi_{1n}^{(4)} M}{16\pi^4 n^4} \right. \\ & \left. + \frac{\varphi_{2n}^{(4)} M}{16\pi^4 n^4} \right) 4 \sin 2\pi n x. \end{aligned} \tag{3.50}$$

For every $(x,t) \in Q_T$ the series (3.50) is bounded above by the uniformly convergent series

$$\sum_{n=1}^{\infty}\Big(\frac{|\psi_{1n}^{(4)}|+|\varphi_{1n}^{(4)}|2M}{16\pi^4n^4}\Big)+\sum_{n=1}^{\infty}\Big(\frac{(4\pi n-1)|\varphi_{1n}^{(4)}|M}{16\pi^4n^4}+\frac{|\psi_{2n}^{(4)}|-|\varphi_{2n}^{(4)}|2M}{16\pi^4n^4}\Big). \quad (3.51)$$

By the Weierstrass M-test, the series (3.49) is uniformly convergent in the domain Q_T. Hence, the solution $u(x,t)$ is continuous in the domain Q_T.

The uniformly convergent series doesn't provide any information about the convergence of the series obtained from its term by term differentiation. Now take the D_{0+}^{α} derivative from the series expression of $u(x,t)$ given by (3.49)

$$\begin{aligned}\sum_{n=1}^{\infty} D_{0+}^{\alpha}\mathcal{U}_n(x,t) \quad &= \quad 2(1-x)\Big(f_0+\varphi_0\frac{t^{-\alpha}}{\Gamma(1-\alpha)}\Big)\\ &+\sum_{n=1}^{\infty}\Big(\frac{\varphi_{1n}^{(4)}}{16\pi^4n^4}e_{\alpha,1-\alpha}(t,\lambda)\Big)4(1-x)\cos 2\pi nx\\ &+\sum_{n=1}^{\infty}\Big(\frac{\varphi_{1n}^{(4)}}{2\pi^2n^2}e_{\alpha,\alpha}(t,\lambda)+f_{2n}\frac{t^{-\alpha}}{\Gamma(1-\alpha)}\star e_{\alpha,1-\alpha}(t,\lambda)\\ &+\frac{\varphi_{2n}^{(4)}}{16\pi^4n^4}e_{\alpha,1-\alpha}(t,\lambda)\Big)4\sin 2\pi nx, \end{aligned} \quad (3.52)$$

we have used $D_{0+}^{\alpha}t^{\alpha-1}=0$, $D_{0+}^{\alpha}e_{\alpha}(t,\lambda)=e_{\alpha,1-\alpha}(t,\lambda)$, $D_{0+}^{\alpha}e_{\alpha,\alpha}(t,\lambda)=-\lambda e_{\alpha,\alpha}(t,\lambda)$ and $\mathcal{U}_n(x,t)$ is defined by the right hand side of the series (3.16).

The series (3.52) is bounded above by the uniformly convergent series

$$\sum_{n=1}^{\infty}\Big(\frac{|\psi_{2n}^{(4)}|+(4\pi n+1)|\varphi_{1n}^{(4)}|M}{16\pi^4n^4}\Big),$$

hence it converges uniformly, so $D_{0+}^{\alpha}u_n(x,t)=\sum\limits_{n=1}^{\infty}D_{0+}^{\alpha}\mathcal{U}_n(x,t)$.

Take the x-derivative of the series expression of $u(x,t)$ from (3.49), we obtain

$$\begin{aligned}\sum_{n=1}^{\infty}\mathcal{U}_{n,x}(x,t) \quad &:= \quad -2\Big(f_0t^{\alpha}/\Gamma(1+\alpha)+\varphi_0\Big)-\sum_{n=1}^{\infty}\Big(\frac{f_{1n}\alpha}{\Gamma(1+\alpha)}t^{\alpha-1}\star e_{\alpha}(t,\lambda)\\ &+\frac{\varphi_{1n}^{(4)}}{16\pi^4n^4}e_{\alpha}(t,\lambda)\Big)\Big(8\pi n\sin 2\pi nx+4\cos 2\pi nx\Big)\\ &-\sum_{n=1}^{\infty}\Big(\frac{\varphi_{1n}^{(4)}}{4\pi^3n^3}e_{\alpha,1-\alpha}(t,\lambda)+f_{2n}\frac{t^{-\alpha}}{\Gamma(1-\alpha)}\star e_{\alpha}(t,\lambda)\\ &+\frac{\varphi_{2n}^{(4)}}{16\pi^4n^4}e_{\alpha}(t,\lambda)\Big)8\pi n\sin 2\pi nx. \end{aligned} \quad (3.53)$$

$$\begin{aligned}\sum_{n=1}^{\infty}\mathcal{U}_{n,xx}(x,t) \quad := \quad & \sum_{n=1}^{\infty}\Big(\frac{f_{1n}\alpha}{\Gamma(1+\alpha)}t^{\alpha-1}\star e_\alpha(t,\lambda)+\frac{\varphi_{1n}^{(4)}}{16\pi^4n^4}e_\alpha(t,\lambda)\Big)\\ & \Big(16\pi^2n^2\sin 2\pi nx-16\pi^2n^2(1-x)\cos 2\pi nx\Big)\\ & -\sum_{n=1}^{\infty}\Big(\frac{\varphi_{1n}^{(4)}}{4\pi^3n^3}e_{\alpha,1-\alpha}(t,\lambda)+f_{2n}\frac{t^{-\alpha}}{\Gamma(1-\alpha)}\star e_\alpha(t,\lambda)\\ & +\frac{\varphi_{2n}^{(4)}}{16\pi^4n^4}e_\alpha(t,\lambda)\Big)16\pi^2n^2\sin 2\pi nx. \end{aligned} \tag{3.54}$$

The series (3.53) and (3.54) are bounded above by the uniformly convergent series

$$\sum_{n=1}^{\infty}\Big(\frac{(1+2\pi n)|\psi_{1n}^{(4)}|+2\pi n|\psi_{2n}^{(4)}|+(4\pi^2n^2+6\pi n+2)M|\varphi_{1n}^{(4)}|+(1+M)2\pi n|\varphi_{2n}^{(4)}|}{4\pi^4n^4}\Big),$$

$$\sum_{n=1}^{\infty}\Big(\frac{|\psi_{1n}^{(4)}|+2|\psi_{2n}^{(4)}|+(1+TM)M|\varphi_{1n}^{(4)}|+M|\varphi_{2n}^{(4)}|}{\pi^2n^2}\Big),$$

respectively, then $\sum\limits_{n=1}^{\infty}\mathcal{U}_{n,x}(x,t)$ and $\sum\limits_{n=1}^{\infty}\mathcal{U}_{n,xx}(x,t)$ converges uniformly; consequently

$$u_{xx}(t,x)=\sum_{n=1}^{\infty}\mathcal{U}_{n,xx}(x,t),$$

is uniformly convergent.

Hence the term by term differentiation of the series (3.49) with respect to time t and x is valid. Similarly we can show that $f(x)$ obtained by series (3.17) is continuous.

Remark 3.3.2. *The above analysis remains valid if the boundary conditions given by (3.3) are replaced by*

$$\begin{aligned} u(0,t)=u(1,t), \quad u_x(0,t) &= u_x(1,t), \quad t\in[0,T],\\ & \textit{or}\\ u(1,t)=0, \quad u_x(0,t) &= 0, \quad t\in[0,T]. \end{aligned}$$

3.4 Conclusion and perspective

We have presented a strategy for the solution of the inverse problem of determination of a source term for a linear heat equation involving fractional derivative in time. The problem considered has nonlocal boundary conditions and a biorthogonal system is used to expand the solution of the inverse problem. The source term is supposed to be independent of time variable. A natural question arises;

Can we apply the same strategy for determination of a source term which depends on time variable?

The answer is yes. In [66] we have considered the determination of a source term for the following problem

$$D_{0+}^{\alpha}(u(x,t) - \varrho u(x,0)) - u_{xx}(x,t) = a(t)f(x,t), \qquad (x,t) \in Q_T, \tag{3.55}$$

with initial and nonlocal boundary conditions

$$u(x,0) = \varphi(x), \qquad x \in [0,1], \tag{3.56}$$

$$u(0,t) = u(1,t), \quad u_x(1,t) = 0, \qquad t \in [0,T], \tag{3.57}$$

where $Q_T = (0,1) \times (0,T)$, $\varrho > 0$, D_{0+}^{α} stands for the Riemann-Liouville fractional derivative of order $0 < \alpha < 1$, $\varphi(x)$ is the initial temperature.

The inverse problem of unique determination of the source term $a(t)$ and the temperature distribution $u(x,t)$ from initial temperature $\varphi(x)$ and boundary conditions (3.57) is not uniquely solvable; we propose an overdetermination condition of the type

$$\int_0^1 u(x,t)dx = g(t), \qquad t \in [0,T], \tag{3.58}$$

where $g \in AC([0,T],\mathbb{R})$ (the space of absolutely continuous functions). For the solvability of inverse problems such type of integral overdetermination condition has been considered in the literature (see for example [59]).

We show the existence and uniqueness of the solution of the inverse problem using properties of biorthogonal system and the Mittag-Leffler function. The result about the continuous dependence of solution of the inverse problem to the data is proved.

An inverse source problem for a two dimensional time fractional diffusion equation with nonlocal boundary conditions

Purpose of the paper:

Can we extend the results obtained in Chapter 3 to a two dimensional problem? What about the stability of the solution of the inverse problem?

The purpose of this paper is to answer above questions, so we are interested in determination of the temperature distribution $u(x, y, t)$, and a source term (independent of time variable) $f(x, y)$ for the following fractional diffusion equation

$$D^{\alpha}_{0+}(u(x, y, t) - u(x, y, 0)) - \varrho \Delta u(x, t) = f(x, y), \qquad (x, y, t) \in Q_T, \quad (3.59)$$

$$u(x, y, 0) = \varphi(x, y), \quad u(x, y, T) = \psi(x, y), \qquad (x, y) \in \Omega, \quad (3.60)$$

$$u(0, y, t) = u(1, y, t), \quad \frac{\partial u}{\partial x}(1, y, t) = 0, \qquad (y, t) \in D, \quad (3.61)$$

$$u(x, 0, t) = u(x, 1, t) = 0, \qquad (x, t) \in D, \quad (3.62)$$

where $Q_T := \Omega \times [0, T]$, $\Omega := [0, 1] \times [0, 1]$, $D := [0, 1] \times [0, T]$ and D^{α}_{0+} stands for the Riemann-Liouville fractional derivative of order $0 < \alpha < 1$, $\varphi(x, y)$ and $\psi(x, y)$ are the initial and final temperatures respectively.

The problem:

The problem in solving the inverse source problem is due to the nonlocal boundary conditions (3.59)-(3.62). As for the one dimensional problem the underlying spatial spectral problem for the homogeneous problem of (3.59)-(3.62) is non-self-adjoint. We are unable to write the solution as sum of eigenfunctions. The difficulty for solving the inverse problem also arise due to the presence of fractional derivative in time, which are nonlocal operators.

Strategy:

We shall follow the same strategy as adopted in [65] i.e., for the solution of the inverse problem we shall get the two basis for the space $L^2(\Omega)$, which form the biorthogonal system (see V. A. Il'in [49] and M. V. Keldysh [60]). We show the existence and uniqueness of the inverse problem using properties of the biorthogonal system. The result about the continuous dependance of the solution on the data is presented.

Chapter 4

An inverse source problem for a two dimensional time fractional diffusion equation with nonlocal boundary conditions

Abstract

We consider the inverse source problem for a time fractional diffusion equation. The unknown source term is supposed to be independent of the time variable, and the problem is considered in two dimensions. A biorthogonal system of functions consisting of two Riesz basis of the space $L^2[(0,1)\times(0,1)]$, obtained from eigenfunctions and associated functions of the spectral problem and its adjoint problem is used to represent the solution of the inverse problem. Using the properties of the biorthogonal system of functions we show the existence and uniqueness of the solution of the inverse problem and its continuous dependence on the data is given.

Keywords: Inverse problem, fractional derivative, diffusion equation, integral equations, biorthogonal system of functions, Fourier series.

MSC [2010]: 80A23, 65N21, 26A33, 45J05, 34K37, 42A16.

Contents

4.1 Introduction

In this paper, we are concerned with two problems related to the linear diffusion equation

$$D^{\alpha}_{0+}(u(x,y,t)-u(x,y,0))-\varrho\Delta u(x,y,t)=f(x,y,t), \qquad (x,y,t)\in Q_T, \quad (4.1)$$

$$u(x,y,0)=\varphi(x,y), \qquad (x,y)\in\Omega, \quad (4.2)$$

where D^{α}_{0+} stands for the Riemann-Liouville fractional derivative of order $0<\alpha<1$, ϱ is a positive constant, f is the source term, $\Delta=\partial^2/\partial x^2+\partial^2/\partial y^2$, $Q_T:=\Omega\times(0,T]$, $\Omega:=(0,1)\times(0,1)$ and $\varphi(x,y)$ is the initial temperature.

The first problem is the direct problem for equations (4.1)-(4.2) supplemented with nonlocal boundary conditions

$$u(0,y,t)=u(1,y,t), \quad \frac{\partial u}{\partial x}(1,y,t)=0, \qquad (y,t)\in D, \quad (4.3)$$

$$u(x,0,t)=u(x,1,t)=0, \qquad (x,t)\in D, \quad (4.4)$$

where $D:=[0,1]\times[0,T]$. Notice that the initial temperature, i.e., $\varphi(x,y)$ satisfies the consistency relations corresponding to the boundary conditions (4.3) and (4.4).

The solution of the direct problem (4.1)-(4.4) is the unique determination of $u(x,y,t)$ in $\bar{Q}_T$ such that $u(.,.,t)\in C^2[\Omega,\mathbb{R}]$, $D^{\alpha}_{0+}(u(x,y,.)-u(x,y,0))\in C([0,T],\mathbb{R})$, when the initial temperature $\varphi(x,y)$ and the source term $f(x,y,t)$ are given.

The second problem we consider is the inverse source problem, where we suppose that the source term f is independent of time, i.e., in equation (4.1) we have $f(x,y)$. The inverse problem is not uniquely solvable with initial and boundary conditions (4.2)-(4.4), so we consider as a supplementary condition the final temperature $u(x,y,T)=\psi(x,y)$, i.e., we are looking for the map

$$u(x,y,T)\to\{f(x,y),u(x,y,t)\}, \quad t<T.$$

By a solution of the inverse problem we mean a pair of functions $\{u(x,y,t),f(x,y)\}$ such that $u(.,.,t)\in C^2(\Omega,\mathbb{R}), D^{\alpha}_{0+}(u(x,y,.)-u(x,y,0))\in C([0,T],\mathbb{R})$, $f\in C(\Omega,\mathbb{R})$ which satisfy equations (4.1)-(4.4) and $u(x,y,T)=\psi(x,y)$.

Most authors consider the fractional derivative defined in the sense of Caputo by imposing initial conditions without fractional integrals. The definition of fractional derivative in the sense of Caputo requires absolutely continuous functions. By considering $D^{\alpha}_{0+}(u(x,y,.)-u(x,y,0))$ rather than the usual term $D^{\alpha}_{0+}u(x,y,.)$ we not only avoid the possible singularity at zero but also impose meaningful initial condition (without fractional integrals). The boundary conditions (4.3)-(4.4) are nonlocal and not standard boundary conditions, as these boundary conditions relate the values of the solution at the boundaries of the domain $\bar{\Omega}$.

When we want to solve both problems using separation of variables (Fourier's method), we have to consider the spectral problem

$$-\frac{\partial^2 S}{\partial x^2}-\frac{\partial^2 S}{\partial y^2} = \mu S, \qquad (x,y)\in\Omega, \tag{4.5}$$

$$S(0,y)=S(1,y), \quad S(x,0) = S(x,1)=0, \quad \frac{\partial S}{\partial x}(1,y)=0, \quad x,y\in[0,1] \tag{4.6}$$

The boundary value problem (4.5)-(4.6) is non-self-adjoint. Our approach for the solvability of the direct and inverse problem is based on the expansion of the solution $u(x,y,t)$ using a biorthogonal system of functions obtained from the eigenfunctions and associated eigenfunctions of the spectral problem (4.5)-(4.6) and its adjoint problem.

Before we present our results, let us dwell on the literature concerning the time fractional diffusion equation and its related inverse problems. It is well known (see [46], [52] and references therein) that reaction diffusion equation and transport equation, commonly used to explain physical phenomena of diffusion show, in some situations, a disagreement with experimental data. This experimentally observed nonstandard behavior is known as anomalous non Gaussian diffusion. One way to explain this type of diffusion is to introduce fractional derivative in time or space, or both in the equation. There is a vast literature available on this subject (see [52] and references therein). Nonlocal boundary conditions arise from many important applications in heat conduction and thermoelasticity (see [18], [19]).

There are few articles which consider the inverse problem of differential equations involving a fractional derivative in time, in particular for the diffusion equation. In [65] the inverse problem of finding the temperature distribution and a source term independent of time for the one-dimensional fractional diffusion equation with nonlocal boundary conditions

$$D^{\alpha}_{0+}(u(x,t)-u(x,0))-\varrho u_{xx}(x,t) = f(x), \qquad (x,t)\in(0,1)\times(0,T], \tag{4.7}$$

$$u(x,0)=\varphi(x) \quad u(x,T) = \psi(x), \qquad x\in(0,1), \tag{4.8}$$

$$u(1,t)=0, \quad u_x(0,t) = u_x(1,t), \quad t\in(0,T), \tag{4.9}$$

was considered. The authors proved the existence and uniqueness for the solution of the inverse problem.

In [17], the authors consider the inverse problem of determining the order of the fractional derivative and the diffusion coefficient for a one-dimensional diffusion equation (here the fractional time derivative is defined in the sense of Caputo). In [118], the inverse problem of the determination of the source term (which is independent of the time variable) for the fractional diffusion equation is considered. The authors proved the unique determination of the source term by using analytic continuation along with Duhamel's principle. Recently, a few articles have addressed the inverse problem for the fractional diffusion equation by proposing different regularization techniques (see [117], [79]).

Let us mention that in [115], the authors consider the two-dimensional inverse problem of determining heat flux for a homogenous time fractional diffusion equation from a measured temperature history at a fixed point in the domain. Under some assumptions they establish the stability of the solution of the inverse problem and propose a so called Fourier regularizing technique.

The rest of this paper is structured as follows: in section 4.2, for the sake of clarity we give some basic definitions and results needed in the sequel. In section 4.3, we present our main results. First, we establish the existence and uniqueness of the solution of the direct problem based on the expansion of the solution in the biorthogonal system. Second, we consider the inverse problem and present the results about the existence, uniqueness and stability of the solution of the inverse problem. Section 4.4 concludes by describing the results obtained in this paper.

4.2 Preliminaries and notations

In this section, we recall basic definitions and notations from fractional calculus (see [102]). For an integrable function $f : \mathbb{R}^+ \to \mathbb{R}$, the left sided Riemann-Liouville fractional integral of order $0 < \alpha < 1$ is defined by

$$J^{\alpha}_{0_+} f(t) := \frac{1}{\Gamma(\alpha)} \int_0^t \frac{f(\tau)}{(t-\tau)^{1-\alpha}}\, d\tau, \quad t > 0, \tag{4.10}$$

where $\Gamma(\alpha)$ is the Euler Gamma function. We write

$$J^{\alpha}_{0_+} f(t) = (\phi_\alpha * f)(t), \tag{4.11}$$

where

$$\phi_\alpha := \begin{cases} t^{\alpha-1}/\Gamma(\alpha), & t > 0, \\ 0 & t \le 0. \end{cases} \tag{4.12}$$

The Riemann-Liouville fractional derivative of order $0 < \alpha < 1$ is defined by

$$D^{\alpha}_{0_+} f(t) := \frac{d}{dt} J^{1-\alpha}_{0_+} f(t) = \frac{1}{\Gamma(1-\alpha)} \frac{d}{dt} \int_0^t \frac{f(\tau)}{(t-\tau)^{\alpha}}\, d\tau. \tag{4.13}$$

In particular, $D^0_{0_+} f(t) = f(t)$ and when $\alpha \to 1$, $D^{\alpha}_{0_+} f(t) \to f'(t)$. Note that the Riemann-Liouville fractional derivative of a constant is not equal to zero.

For $0 < \alpha < 1$, we also have

$$J^{\alpha}_{0_+} D^{\alpha}_{0_+} \Big(f(t) - f(0) \Big) = f(t) - f(0). \tag{4.14}$$

The Laplace transform of the Riemann-Liouville integral of order $0 < \alpha < 1$ of a function with at most exponential growth is

$$\mathcal{L}\{J^{\alpha}_{0_+} f(t) : s\} = \mathcal{L}\{f(t) : s\}/s^{\alpha}.$$

The Mittag-Leffler function plays an important role in the theory of fractional differential equations; for any $z \in \mathbb{C}$ the Mittag-Leffler function with one parameter ξ is defined by the series

$$E_\xi(z) = \sum_{k=0}^{+\infty} \frac{z^k}{\Gamma(\xi k + 1)} \qquad (Re(\xi) > 0). \tag{4.15}$$

In particular, $E_1(z) = e^z$. The Mittag-Leffler function with two parameters $E_{\xi,\beta}(z)$, which is a generalization of (4.15), is defined by

$$E_{\xi,\beta}(z) = \sum_{k=0}^{+\infty} \frac{z^k}{\Gamma(\xi k + \beta)} \qquad (z, \beta \in \mathbb{C};\ \ Re(\xi) > 0). \tag{4.16}$$

Let $e_\xi(t,\mu) := E_\xi(-\mu t^\xi)$ and $e_{\alpha,\beta}(t,\mu) := t^{\beta-1}E_{\alpha,\beta}(-\mu t^\alpha)$, where μ is a positive real number. Recall that Mittag-Leffler functions $e_\alpha(t;\mu)$ and $e_{\alpha,\beta}(t;\mu)$ for $\mu > 0$ and $0 < \alpha \leq 1$, $0 < \alpha \leq \beta \leq 1$ respectively, are completely monotone functions, i.e., we have

$$(-1)^n[e_\alpha(t,\mu)]^{(n)} \geq 0 \quad \text{and} \quad (-1)^n[e_{\alpha,\beta}(t,\mu)]^{(n)} \geq 0, \quad n \in \mathbb{N} \cup \{0\}.$$

Furthermore, we have

$$E_{\alpha,\beta}(\mu t^\alpha) \leq \mathcal{C}, \qquad 0 \leq a \leq t \leq b < \infty, \tag{4.17}$$

where $\mathcal{C} > 0$ is a constant, and

$$\int_0^t (t-\tau)^{\alpha-1} E_{\alpha,\beta}(\mu t^\alpha)\, d\tau < \infty,$$

(see [96] page 9).

Let H be a Hilbert space of functions equipped with a scalar product $<,>$. Recall that a set $\mathcal{S}$ of functions in H is called complete if there exists no function $f \in H$, different from zero, which is orthogonal to all functions of the set $\mathcal{S}$.

Two sets $\mathcal{S}_1$ and $\mathcal{S}_2$ of functions of H form a biorthogonal system of functions if a one-to-one correspondence can be established between them such that the scalar product of two corresponding functions is equal to unity and the scalar product of two non-corresponding functions is equal to zero, i.e.,

$$< f_i, g_j > = \delta_{ij} := \begin{cases} 1 & \text{if } i = j, \\ 0 & \text{if } i \neq j, \end{cases}$$

where $f_i \in \mathcal{S}_1$ and $g_i \in \mathcal{S}_2$. The biorthogonal system is complete in H if the sets $\mathcal{S}_1$ and $\mathcal{S}_2$ forming a biorthogonal system are complete in H.

The following result is proved in [65]

Lemma 4.2.1. *Let $g : \mathbb{R} \to \mathbb{R}$ be a differentiable function in $L^1(\mathbb{R})$. The solution of the integral equation*

$$v(t) + \mu J^{\alpha}_{0+} v(t) = g(t) \tag{4.18}$$

for $\mu \in \mathbb{R}^+$ can be represented by

$$v(t) = \int_0^t g'(t-\tau) e_\alpha(\tau, \mu)\, d\tau + g(0) e_\alpha(t, \mu). \tag{4.19}$$

4.3 Main Results

4.3.1 Solution of the direct problem

First we present the result about the existence and uniqueness of the classical solution of the problem

$$D^{\alpha}_{0+}(u(x,y,t) - u(x,y,0)) - \varrho \Delta u(x,y,t) = f(x,y,t), \qquad (x,y,t) \in Q_T, \tag{4.20}$$

$$u(x,y,0) = \varphi(x,y), \qquad (x,y) \in \Omega, \tag{4.21}$$

$$u(0,y,t) = u(1,y,t), \quad \frac{\partial u}{\partial x}(1,y,t) = 0, \qquad (y,t) \in D, \tag{4.22}$$

$$u(x,0,t) = u(x,1,t) = 0, \qquad (x,t) \in D. \tag{4.23}$$

Problem (4.20)-(4.23) is linear and its solution can be written as

$$u(x,y,t) = w(x,y,t) + v(x,y,t),$$

where $w(x,y,t)$ is the solution of the boundary value problem

$$D^{\alpha}_{0+}(w(x,y,t) - w(x,y,0)) - \varrho \Delta w(x,y,t) = 0, \qquad (x,y,t) \in Q_T, \tag{4.24}$$

$$w(x,y,0) = \varphi(x,y), \qquad (x,y) \in \Omega, \tag{4.25}$$

$$w(0,y,t) = w(1,y,t), \quad \frac{\partial w}{\partial x}(1,y,t) = 0, \qquad (y,t) \in D, \tag{4.26}$$

$$w(x,0,t) = w(x,1,t) = 0, \qquad (x,t) \in D, \tag{4.27}$$

and $v(x,y,t)$ is the solution of the problem

$$D^{\alpha}_{0+}(v(x,y,t) - v(x,y,0)) - \varrho \Delta v(x,y,t) = f(x,y,t), \qquad (x,y,t) \in Q_T, \tag{4.28}$$

$$v(x,y,0) = 0, \qquad (x,y) \in \Omega, \tag{4.29}$$

$$v(0,y,t) = v(1,y,t), \quad \frac{\partial v}{\partial x}(1,y,t) = 0, \qquad (y,t) \in D, \tag{4.30}$$

$$v(x,0,t) = v(x,1,t) = 0, \qquad (x,t) \in D. \tag{4.31}$$

Problem (4.20)-(4.23) has nonlocal boundary conditions and its spectral problem, i.e., the problem (4.5)-(4.6), is non-self-adjoint. In [50] a biorthogonal system of functions is constructed

$$\begin{array}{ccc} \{\underbrace{Z_{0k} := X_0(x)V_k(y)}, & \underbrace{Z_{(2m-1)k} := X_m(x)V_k(y)}, & \underbrace{Z_{2mk} := X_{2mk}(x)V_k(y)}\}, \\ \downarrow & \downarrow & \downarrow \\ \{W_{0k} := \tilde{X}_0(x)V_k(y), & W_{(2m-1)k} := \tilde{X}_m(x)V_k(y), & W_{2mk} := \tilde{X}_{2mk}(x)V_k(y)\}, \end{array}$$

for $m, k \in \mathbb{N}$, where

$$\begin{aligned} X_0(x) &= 2, \quad V_k(y) = \sqrt{2}\sin(\pi k y), \quad X_m(x) = 4\cos(2\pi m x), \\ X_{2mk}(x) &= 4(1-x)\sin(2\pi m x), \quad \tilde{X}_0(x) = x, \quad \tilde{X}_m(x) = x\cos(2\pi m x), \\ \tilde{X}_{2mk}(x) &= \sin(2\pi m x), \quad m, k \in \mathbb{N}. \end{aligned}$$

The set of functions $\{Z_{0k}, Z_{(2m-1)k}, Z_{2mk}\}$ and $\{W_{0k}, W_{(2m-1)k}, W_{2mk}\}$ are obtained as the eigenfunctions and associated eigenfunctions of the spatial spectral problem (4.5)-(4.6) and its adjoint (conjugate) problem respectively, see [50] as a key reference for this fact.

At this stage let us recall

Lemma 4.3.1. *[50] Each set of functions $\{Z_{0k}, Z_{(2m-1)k}, Z_{2mk}\}$ and $\{W_{0k}, W_{(2m-1)k}, W_{2mk}\}$ for $m, k \in \mathbb{N}$ is a basis for the space $L^2(\Omega)$. Moreover, if ϕ is any function in $L^2(\Omega)$ whose expansion coefficients in the basis Z_{mk} are*

$$\phi_{mk} =< \phi, W_{mk} >, \qquad m \in \mathbb{N} \cup \{0\}, \quad k \in \mathbb{N}, \tag{4.32}$$

then we have the bilateral estimates

$$\frac{1}{16}\|\phi\|^2_{L^2(\Omega)} \leq \sum_{k=1}^{\infty}\sum_{m=0}^{\infty} \phi^2_{mk} \leq \frac{1}{2}\|\phi\|^2_{L^2(\Omega)}. \tag{4.33}$$

Theorem 4.3.2. *Let $f \in L^2(\Omega)$, $\varphi \in C^2(\bar{\Omega})$ be such that $\varphi(0,y) = \varphi(1,y), \partial\varphi(1,y)/\partial x = 0$, and $\varphi(x,0) = \varphi(x,1) = 0$. Then there exist a unique classical solution of the problem (4.24)-(4.27).*

Proof. Let us expand the solution of the problem (4.24)-(4.27) using the biorthogonal system

$$\begin{aligned} w(x,y,t) &= \sum_{k=1}^{\infty} C^w_{0k}(t) Z_{0k}(x,y) + \sum_{m,k=1}^{\infty} C^w_{(2m-1)k}(t) Z_{(2m-1)k}(x,y) \\ &\quad + \sum_{m,k=1}^{\infty} C^w_{2mk}(t) Z_{2mk}(x,y), \end{aligned} \tag{4.34}$$

where $C^w_{0k}(t), C^w_{(2m-1)k}(t)$ and $C^w_{2mk}(t)$ for $m, k \in \mathbb{N}$ are to be determined.

Using properties of the biorthogonal system we have

$$C^w_{0k}(t) =< w(x,y,t), W_{0k}(x,y) >, \quad k \in \mathbb{N}, \tag{4.35}$$

where $< f, g >:= \int_0^1\int_0^1 f(x,y)g(x,y)\,dxdy$ is the scalar product in $L^2(\Omega)$. By virtue of (4.35), we have

$$D^{\alpha}_{0+}(C^w_{0k}(t) - C^w_{0k}(0)) =< D^{\alpha}_{0+}(w(x,y,t) - w(x,y,0)), W_{0k}(x,y) >, \quad k \in \mathbb{N}.$$

Using (4.24) we can write

$$D^{\alpha}_{0+}(C^w_{0k}(t) - C^w_{0k}(0)) =< \varrho\Delta w, W_{0k}(x,y) >, \quad k \in \mathbb{N},$$

whereupon

$$D^{\alpha}_{0+}(C^w_{0k}(t) - C^w_{0k}(0)) = -\varrho\pi^2k^2C^w_{0k}(t), \quad k \in \mathbb{N}. \tag{4.36}$$

Similarly, we obtain the following linear fractional differential equations

$$\begin{aligned} D^{\alpha}_{0+}(C^w_{(2m-1)k}(t) - C^w_{(2m-1)k}(0)) &= -C^w_{(2m-1)k}(t)\varrho(4\pi^2m^2 + \pi^2k^2) \\ &\quad -4\varrho\pi m C^w_{2mk}(t), \ m, k \in \mathbb{N}, \qquad (4.37) \\ D^{\alpha}_{0+}(C^w_{2mk}(t) - C^w_{2mk}(0)) &= -C^w_{2mk}(t)\varrho(4\pi^2m^2 + \pi^2k^2), \qquad (4.38) \end{aligned}$$

for $m, k \in \mathbb{N}$.

Setting $\lambda_{mk} := \varrho(4\pi^2m^2 + \pi^2k^2)$, $\mu_m := 4\varrho\pi^2m^2$ for $m \in \mathbb{N} \cup \{0\}$ and $k \in \mathbb{N}$, then equations (4.36)-(4.38) can be written as

$$\begin{aligned} C^w_{0k}(t) + \lambda_{0k}J^{\alpha}_{0+}C_{0k}(t) &= C^w_{0k}(0), \qquad (4.39) \\ C^w_{(2m-1)k}(t) + \lambda_{mk}J^{\alpha}_{0+}C^w_{(2m-1)k}(t) &= C^w_{(2m-1)k}(0) - 2\sqrt{\mu_m}J^{\alpha}_{0+}C^w_{2mk}(t), (4.40) \\ C^w_{2mk}(t) + \lambda_{mk}J^{\alpha}_{0+}C^w_{2mk}(t) &= C^w_{2mk}(0). \qquad (4.41) \end{aligned}$$

Using Lemma 4.2.1, the solutions of the linear integral equations (4.39)-(4.41) are

$$\begin{aligned} C^w_{0k}(t) &= C^w_{0k}(0)e_{\alpha}(t, \lambda_{0k}), \\ C^w_{(2m-1)k}(t) &= -2\sqrt{\mu_m}C^w_{2mk}(0)\int_0^t D^{1-\alpha}_{0+}e_{\alpha}(t-\tau, \lambda_{mk})e_{\alpha}(\tau, \lambda_{mk})\, d\tau \\ &\quad +C^w_{(2m-1)k}(0)e_{\alpha}(t, \lambda_{mk}), \\ C^w_{2mk}(t) &= C^w_{2mk}(0)e_{\alpha}(t, \lambda_{mk}). \end{aligned}$$

The unknowns $C^w_{0k}(0), C^w_{(2m-1)k}(0), C^w_{2mk}(0)$ are determined by using initial condition (4.25). They are

$$C^w_{0k}(0) = \varphi_{0k}, \quad C^w_{(2m-1)k}(0) = \varphi_{(2m-1)k}, \quad C^w_{2mk}(0) = \varphi_{2mk},$$

where

$$\varphi_{mk} =< \varphi, W_{mk} >, \qquad m \in \mathbb{N} \cup \{0\}, \ k \in \mathbb{N}.$$

Existence of the solution: The solution is formally given by (4.34); so we need to prove that the series corresponding to $w(x, y, t), w_{xx}(x, y, t), w_{yy}(x, y, t)$ and $D^{\alpha}_{0+}(w(x, y, t) - w(x, y, 0))$ are uniformly convergent in Q_T.

First, notice that

$$\begin{aligned} D^{1-\alpha}_{0+}e_{\alpha}(t, \lambda_{mk}) &= e_{\alpha,\alpha}(t, \lambda_{mk}), \quad D^{\alpha}_{0+}e_{\alpha}(t, \lambda_{mk}) = e_{\alpha,1-\alpha}(t, \lambda_{mk}), \\ \frac{\partial^2 Z_{0k}}{\partial x^2} = 0, \quad \frac{\partial^2 Z_{0k}}{\partial y^2} &= -\pi^2k^2Z_{0k}, \quad \frac{\partial^2 Z_{(2m-1)k}}{\partial x^2} = -4\pi^2m^2Z_{(2m-1)k}, \\ \frac{\partial^2 Z_{(2m-1)k}}{\partial y^2} &= -\pi^2k^2Z_{(2m-1)k}, \quad \frac{\partial^2 Z_{2mk}}{\partial x^2} = -4\pi m Z_{(2m-1)k} - 4\pi^2m^2Z_{2mk}, \\ \frac{\partial^2 Z_{2mk}}{\partial y^2} &= -\pi^2k^2Z_{2mk}, \quad k, m \in \mathbb{N}. \end{aligned}$$

By setting

$$\mathcal{W}_{0k} = \varphi_{0k} e_\alpha(t, \lambda_{0k}) Z_{0k}, \tag{4.42}$$

$$\mathcal{W}_{(2m-1)k} = \left[\varphi_{(2m-1)k} e_\alpha(t, \lambda_{mk}) - 2\sqrt{\mu_m}\varphi_{2mk} \int\limits_0^t e_{\alpha,\alpha}(t-\tau, \lambda_{mk}) e_\alpha(\tau, \lambda_{mk})\, d\tau\right] Z_{(2m-1)k}, \tag{4.43}$$

$$\mathcal{W}_{2mk} = \varphi_{2mk} e_\alpha(t, \lambda_{mk}) Z_{2mk}, \tag{4.44}$$

we can write

$$w(x,y,t) = \sum_{k=1}^{\infty} \mathcal{W}_{0k} + \sum_{m,k=1}^{\infty} \mathcal{W}_{(2m-1)k} + \sum_{m,k=1}^{\infty} \mathcal{W}_{2mk}. \tag{4.45}$$

We shall show that for any $\varepsilon > 0$ and $t \in [\varepsilon, T]$ the series in (4.45) are uniformly convergent in $[\varepsilon, T]$. Since $\varphi(x,y)$ is continuous in $\bar{\Omega}$, so $|\varphi(x,y)| \le M$ for all $(x,y) \in \bar{\Omega}$, where $M > 0$ is a constant. Also, for $m, k \in \mathbb{N}$, $|Z_{mk}| \le 4\sqrt{2}$, $|W_{mk}| \le \sqrt{2}$ and $|\varphi_{mk}| \le \sqrt{2}M$.

The Mittag-Leffler function $E_\alpha(-\sigma t^\alpha)$, for $0 < \alpha \le 1$ and σ positive, is monotonically decreasing function. Furthermore, the Mittag-Leffler function satisfies

$$E_\alpha(-\sigma t^\alpha) \simeq e^{-\sigma t^\alpha/\Gamma(\alpha+1)}, \qquad t \ll 1, \tag{4.46}$$

and

$$E_\alpha(-\sigma t^\alpha) \simeq \frac{1}{\Gamma(1-\alpha)\sigma t^\alpha}, \qquad t \gg 1,$$

see [52], [95] and references therein.

We have the following estimates

$$|\lambda_{mk} t^{\alpha-1} E_{\alpha,\alpha}(-\lambda_{mk} t^\alpha)| \le \frac{N}{t} \frac{t^\alpha \lambda_{mk}}{1 + \lambda_{mk} t^\alpha} \le \frac{N}{t} \le C,$$

$$|\mathcal{W}_{0k}| \le 8M e_\alpha(\varepsilon, \lambda_{0k}), \qquad |\mathcal{W}_{2mk}| \le 8M e_\alpha(\varepsilon, \lambda_{mk}),$$

$$|\mathcal{W}_{(2m-1)k}| \le (8M + 16MCT) e_\alpha(\varepsilon, \lambda_{mk}),$$

for all $m, k \in \mathbb{N}$, where $C > 0$, $M > 0$, $N > 0$ are constants independent of m and k.

We set

$$\mathcal{M} = 8M + 16MCT, \qquad \mathcal{N} = \frac{4\varrho\pi^2\varepsilon^\alpha}{\Gamma(1+\alpha)}.$$

Using (4.46) we can write

$$|\mathcal{W}_{0k}| \le \mathcal{M} e^{-\lambda_{0k}\varepsilon^\alpha/\Gamma(1+\alpha)}, \qquad |\mathcal{W}_{2mk}| \le \mathcal{M} e^{-\lambda_{mk}\varepsilon^\alpha/\Gamma(1+\alpha)}$$

and

$$|\mathcal{W}_{(2m-1)k}| \le \mathcal{M} e^{-\lambda_{mk}\varepsilon^\alpha/\Gamma(1+\alpha)}.$$

The double series

$$\sum_{m,k=1}^{\infty} e^{-\mathcal{N}(m^2+k^2)} = \left(\sum_{k=1}^{\infty} e^{-k^2\mathcal{N}}\right)\left(\sum_{m=1}^{\infty} e^{-m^2\mathcal{N}}\right)$$

is convergent by d'Alembert's ratio test.

The series in (4.45) are dominated by absolutely convergent numerical series

$$\sum_{k=1}^{\infty} e^{-\mathcal{N}k^2/4}, \qquad \sum_{m,k=1}^{\infty} e^{-\mathcal{N}(m^2+k^2)}.$$

By the Weierstrass M-test the series in (4.45) are uniformly convergent on $[\varepsilon, T]$.

In order to show that the the series for $w_{xx}(x,y,t)$, and $w_{yy}(x,y,t)$ represent continuous functions we need to prove that the following series

$$\sum_{m,k=1}^{\infty}\left(\frac{\partial \mathcal{W}_{(2m-1)k}}{\partial x^2} + \frac{\partial \mathcal{W}_{2mk}}{\partial x^2}\right), \tag{4.47}$$

$$\sum_{k=1}^{\infty}\frac{\partial \mathcal{W}_{0k}}{\partial y^2}, \qquad \sum_{m,k=1}^{\infty}\left(\frac{\partial \mathcal{W}_{(2m-1)k}}{\partial y^2} + \frac{\partial \mathcal{W}_{2mk}}{\partial y^2}\right), \tag{4.48}$$

are uniformly convergent on $[\varepsilon, T]$.

We have the estimates

$$\begin{aligned}
\left|\frac{\partial^2 \mathcal{W}_{(2m-1)k}}{\partial x^2}\right| &\leq \left(32\pi^2 m^2 M + 32 m^2 TMC\right) e_\alpha(\varepsilon, \lambda_{mk}),\\
\left|\frac{\partial^2 \mathcal{W}_{2mk}}{\partial x^2}\right| &\leq \left(32\pi m M + 32\pi^2 m^2\right) e_\alpha(\varepsilon, \lambda_{mk}),\\
\left|\frac{\partial^2 \mathcal{W}_{(2m-1)k}}{\partial y^2}\right| &\leq 8\pi^2 k^2 M e_\alpha(\varepsilon, \lambda_{0k}),\\
\left|\frac{\partial^2 \mathcal{W}_{(2m-1)k}}{\partial y^2}\right| &\leq \left(16\pi^2 k^2 M + 8\pi^2 k^2 TMC\right) e_\alpha(\varepsilon, \lambda_{mk}),\\
\left|\frac{\partial^2 \mathcal{W}_{2mk}}{\partial y^2}\right| &\leq 8\pi^2 k^2 M e_\alpha(\varepsilon, \lambda_{mk}).
\end{aligned}$$

By using (4.46) and the convergence of the series $\sum_{m=1}^{\infty} m^2 e^{-m^2}$, $\sum_{m=1}^{\infty} m e^{-m^2}$, we conclude that the series (4.47) and (4.48) are bounded above by absolutely convergent numerical series. Thus, by the Weierstrass M-test the series (4.47) and (4.48) are uniformly convergent on $[\varepsilon, T]$.

Thus for $\varepsilon > 0$ the series (4.45), (4.47), (4.48) corresponding to $w(x,y,t)$, $w_{xx}(x,y,t)$, $w_{yy}(x,y,t)$ respectively, represent continuous functions on $\Omega \times [\varepsilon, T]$. To show that the series (4.45) is α differentiable we will rely on the following Lemma from [102].

Lemma 4.3.3. *Let f_i, $i \in \mathbb{N}$ be a sequence of functions defined on the interval $(a, b]$. Suppose the following conditions are fulfilled:*

- *for a given* $\alpha > 0$ *the fractional derivative* $D^{\alpha}_{0+} f_i(t)$ *exists for all* $i \in \mathbb{N}$, $t \in (a, b]$;
- *both series* $\sum\limits_{i=1}^{\infty} f_i(t)$ *and* $\sum\limits_{i=1}^{\infty} D^{\alpha}_{0+} f_i(t)$ *are uniformly convergent on the interval* $[a+\varepsilon, b]$ *for any* $\varepsilon > 0$.

Then the function defined by the series $\sum\limits_{i=1}^{\infty} f_i(t)$ *is* α *differentiable and satisfies*

$$D^{\alpha}_{0+} \sum_{i=1}^{\infty} f_i(t) = \sum_{i=1}^{\infty} D^{\alpha}_{0+} f_i(t).$$

We shall show that the series

$$\left.\begin{array}{c} \sum\limits_{k=1}^{\infty} D^{\alpha}_{0+}\Big(\mathcal{W}_{0k}(t) - \mathcal{W}_{0k}(0)\Big), \\ \sum\limits_{m,k=1}^{\infty} D^{\alpha}_{0+}\Big(\mathcal{W}_{(2m-1)k}(t) - \mathcal{W}_{(2m-1)k}(0)\Big), \\ \sum\limits_{m,k=1}^{\infty} D^{\alpha}_{0+}\Big(\mathcal{W}_{2mk}(t) - \mathcal{W}_{2mk}(0)\Big), \end{array}\right\} \tag{4.49}$$

are uniformly convergent on $[\varepsilon, T]$. We have

$$\begin{aligned} D^{\alpha}_{0+}\Big(\mathcal{W}_{0k}(t) - \mathcal{W}_{0k}(0)\Big) &= -\lambda_{0k}\varphi_{0k} e_{\alpha}(t, \lambda_{0k}) Z_{0k}, \\ D^{\alpha}_{0+}\Big(\mathcal{W}_{(2m-1)k}(t) - \mathcal{W}_{(2m-1)k}(0)\Big) &= \Big[2\lambda_{mk}\sqrt{\mu_m}\varphi_{2mk} \\ &\quad \int\limits_0^t e_{\alpha,\alpha}(t-\tau, \lambda_{mk}) e_{\alpha}(\tau, \lambda_{mk})\, d\tau \\ &\quad -\lambda_{mk}\varphi_{(2m-1)k} e_{\alpha}(t, \lambda_{mk})\Big]\ Z_{(2m-1)k}, \\ D^{\alpha}_{0+}\Big(\mathcal{W}_{2mk}(t) - \mathcal{W}_{2mk}(0)\Big) &= -\lambda_{mk}\varphi_{2mk} e_{\alpha}(t, \lambda_{0k}) Z_{2mk}, \quad m, k \in \mathbb{N}, \end{aligned}$$

where we have used the following relations

$$D^{\alpha}_{0+}\Big(e_{\alpha}(t, \mu) - e_{\alpha}(0, \mu)\Big) = -\mu e_{\alpha}(t, \mu), \quad D^{\alpha}_{0+}\Big(f * g\Big) = (D^{\alpha}_{0+} f) * g$$

and

$$D^{\alpha}_{0+} e_{\alpha,\alpha}(t, \mu) = -\mu e_{\alpha,\alpha}(t, \mu).$$

For any $\varepsilon > 0$, we have the following estimates of the fractional derivatives

$$\begin{aligned} \left|D^{\alpha}_{0+}\Big(\mathcal{W}_{0k}(t) - \mathcal{W}_{0k}(0)\Big)\right| &\le 8M\lambda_{0k} e_{\alpha}(\varepsilon, \lambda_{0k}), \\ \left|D^{\alpha}_{0+}\Big(\mathcal{W}_{(2m-1)k}(t) - \mathcal{W}_{(2m-1)k}(0)\Big)\right| &\le (16M\sqrt{\mu_m}T + 8M\lambda_{mk}) e_{\alpha}(\varepsilon, \lambda_{mk}), \\ \left|D^{\alpha}_{0+}\Big(\mathcal{W}_{2mk}(t) - \mathcal{W}_{2mk}(0)\Big)\right| &\le 8M\lambda_{mk} e_{\alpha}(\varepsilon, \lambda_{mk}), \quad m, k \in \mathbb{N}, \end{aligned}$$

which by using (4.46) lead to

$$\begin{aligned}
\left|D^{\alpha}_{0+}\Big(\mathcal{W}_{0k}(t)-\mathcal{W}_{0k}(0)\Big)\right| &\le 8M\lambda_{0k}e^{-\lambda_{0k}\varepsilon^{\alpha}/\Gamma(1+\alpha)},\\
\left|D^{\alpha}_{0+}\Big(\mathcal{W}_{(2m-1)k}(t)-\mathcal{W}_{(2m-1)k}(0)\Big)\right| &\le (16MT\lambda_{mk}+8M\lambda_{mk})e^{-\lambda_{mk}\varepsilon^{\alpha}/\Gamma(1+\alpha)},\\
\left|D^{\alpha}_{0+}\Big(\mathcal{W}_{2mk}(t)-\mathcal{W}_{2mk}(0)\Big)\right| &\le 8M\lambda_{mk}e^{-\lambda_{mk}\varepsilon^{\alpha}/\Gamma(1+\alpha)}, \quad m,k\in\mathbb{N}.
\end{aligned}$$

The double series

$$\begin{aligned}
\sum_{m,k=1}^{\infty}\lambda_{mk}e^{-\mathcal{N}(m^2+k^2)} &= \sum_{m,k=1}^{\infty}(4\varrho\pi^2m^2+\varrho\pi^2k^2)e^{-\mathcal{N}(m^2+k^2)}\\
&= 4\varrho\pi^2\sum_{m,k=1}^{\infty}m^2e^{-\mathcal{N}(m^2+k^2)}+\varrho\pi^2\sum_{m,k=1}^{\infty}k^2e^{-\mathcal{N}(m^2+k^2)}\\
&= 4\varrho\pi^2\left(\sum_{m=1}^{\infty}m^2e^{-\mathcal{N}m^2}\right)\left(\sum_{k=1}^{\infty}e^{-\mathcal{N}k^2}\right)\\
&\quad+\varrho\pi^2\left(\sum_{m=1}^{\infty}e^{-\mathcal{N}m^2}\right)\left(\sum_{k=1}^{\infty}k^2e^{-\mathcal{N}k^2}\right)
\end{aligned}$$

is convergent by d'Alembert's ratio test.

The series (4.49) are uniformly convergent on $[\varepsilon,T]$ by the Weierstrass M-test; they represent continuous function.

Now, we show that the solution series given by (4.45) is uniformly convergent in $\bar{Q}_T$. In this domain we have

$$|\mathcal{W}_{0k}| \le 4\sqrt{2}|\varphi_{0k}|, \tag{4.50}$$
$$|\mathcal{W}_{(2m-1)k}| \le 4\sqrt{2}(|\varphi_{(2m-1)k}|+8MT|\varphi_{2mk}|), \tag{4.51}$$
$$|\mathcal{W}_{2mk}| \le 4\sqrt{2}|\varphi_{2mk}|, \quad m,k\in\mathbb{N}. \tag{4.52}$$

The set of functions

$$\{\sqrt{2}\cos(\pi ky), \quad 2\sin(2\pi mx)\,\cos(\pi ky), \quad 2\cos(2\pi mx)\,\cos(\pi ky)\} \tag{4.53}$$

is orthonormal in the space $L^2(\Omega)$. We have the following estimates

$$|\varphi_{0k}|\le 0.5\left(\frac{1}{\pi^2k^2}+\eta_{0k}^2\right), \quad |\varphi_{(2m-1)k}|\le 0.5\left(\frac{1}{8\pi^4k^2m^2}+\zeta_{mk}^2\right),$$

$$|\varphi_{2mk}|\le 0.5\left(\frac{1}{\pi^2k^2}+\eta_{mk}^2\right), \quad m,k\in\mathbb{N},$$

where $\{\eta_{0k}, \eta_{mk}\}$, ζ_{mk} are the Fourier coefficients of the functions $\partial\varphi/\partial y$, $\partial^2\varphi/\partial y\partial x$, respectively, given by

$$\eta_{0k} = \sqrt{2}\int_0^1\int_0^1 \frac{\partial\varphi}{\partial y}\cos\pi ky\, dx\, dy, \quad \eta_{mk} = 2\int_0^1\int_0^1 \frac{\partial\varphi}{\partial y}\sin(2\pi mx)\cos(\pi ky)\, dx\, dy,$$

$$\zeta_{mk} = 2\int_0^1\int_0^1 \frac{\partial^2\varphi}{\partial y\partial x}\sin(2\pi mx)\cos(\pi ky)\, dx\, dy.$$

By virtue of Bessel's inequality, we have

$$\sum_{k=1}^{\infty}\eta_{0k}^2 \le \|\partial\varphi/\partial y\|_{L^2(\Omega)}, \qquad \sum_{m,k=1}^{\infty}\zeta_{mk}^2 \le \|\partial^2\varphi/\partial y\partial x\|_{L^2(\Omega)},$$
$$\sum_{m,k=1}^{\infty}\eta_{mk}^2 \le \|\partial\varphi/\partial y\|_{L^2(\Omega)}.$$

Using $\sum\limits_{k=1}^{\infty} 1/k^2 = \pi^2/6$, we obtained

$$\sum_{k=1}^{\infty}|\varphi_{0k}| \le \mathcal{N}_1, \quad \sum_{m,k=1}^{\infty}|\varphi_{(2m-1)k}| \le \mathcal{N}_2, \quad \sum_{m,k=1}^{\infty}|\varphi_{2mk}| \le \mathcal{N}_3, \quad m,k\in\mathbb{N},$$

where

$$\mathcal{N}_1 = 0.5\left(\frac{1}{6} + \|\partial\varphi/\partial y\|_{L^2(\Omega)}\right), \quad \mathcal{N}_2 = 0.5\left(\frac{1}{288} + \|\partial^2\varphi/\partial y\partial x\|_{L^2(\Omega)}\right),$$
$$\mathcal{N}_3 = 0.5\left(\frac{1}{6} + \|\partial\varphi/\partial y\|_{L^2(\Omega)}\right).$$

Consequently, the series in (4.45) are uniformly convergent in $\bar{Q}_T$; their sum represents a continuous function.

Uniqueness of the solution: Let $w_1(x,y,t)$, and $w_2(x,y,t)$ be two solutions of the problem (4.24)-(4.27). Then $\bar{w}(x,y,t) = w_1(x,y,t) - w_2(x,y,t)$ satisfies

$$D_{0+}^{\alpha}\bar{w}(x,y,t) - \varrho\Delta\bar{w}(x,y,t) = 0, \qquad (x,y,t)\in Q_T, \tag{4.54}$$
$$\bar{w}(x,y,0) = 0, \qquad (x,y)\in\Omega, \tag{4.55}$$
$$\bar{w}(0,y,t) = \bar{w}(1,y,t), \quad \frac{\partial\bar{w}}{\partial x}(1,y,t) = 0, \qquad (y,t)\in D, \tag{4.56}$$
$$\bar{w}(x,0,t) = \bar{w}(x,1,t) = 0, \qquad (x,t)\in D. \tag{4.57}$$

Proceeding as previously we have the following system of linear fractional differential equation

$$D_{0+}^{\alpha}(C_{0k}^{\bar{w}}(t) - C_{0k}^{\bar{w}}(0)) = -\lambda_{0k}C_{0k}^{\bar{w}}(t), \tag{4.58}$$
$$D_{0+}^{\alpha}(C_{(2m-1)k}^{\bar{w}}(t) - C_{(2m-1)k}^{\bar{w}}(0)) = -\lambda_{mk}C_{(2m-1)k}^{\bar{w}}(t) - 2\sqrt{\mu_m}C_{2mk}^{\bar{w}}(t), \tag{4.59}$$
$$D_{0+}^{\alpha}(C_{2mk}^{\bar{w}}(t) - C_{2mk}^{\bar{w}}(0)) = -\lambda_{mk}C_{2mk}^{\bar{w}}(t). \tag{4.60}$$

We have $C^{\bar{w}}_{0k}(0) = 0,\ C^{\bar{w}}_{(2m-1)k}(0) = 0,\ C^{\bar{w}}_{2mk}(0) = 0$ for $m, k \in \mathbb{N}$ because of the initial condition (4.55), which in turn lead to

$$C^{\bar{w}}_{0k}(t) = 0, \quad C^{\bar{w}}_{(2m-1)k}(t) = 0, \quad C^{\bar{w}}_{2mk}(t) = 0.$$

We have shown that $\bar{w}(x, y, t) = 0$ for all $t \in (0, T]$, and this means that $\bar{w}(x, y, t)$ is orthogonal to the set of functions $\{Z_{0k}, Z_{(2m-1)k}, Z_{2mk}\}$ for $m, k \in \mathbb{N}$, which is complete and forms a basis for the space $L^2(\Omega)$. Hence $\bar{w}(x, y, t) = 0$ for all $(x, y, t) \in Q_T$. □

The solution of the problem (4.28)-(4.31) is given by

$$\begin{aligned} v(x,y,t) &= \sum_{k=1}^{\infty} \int_0^t f_{0k}(\tau) e_\alpha(t-\tau, \lambda_{0k})\, d\tau Z_{0k} + \sum_{m,k=1}^{\infty} \Bigg[\int_0^t f_{(2m-1)k}(\tau) e_\alpha(t-\tau, \lambda_{mk}) \\ &\quad -2\sqrt{\mu_m} \int_0^t f_{2mk}(\tau) \int_0^{t-\tau} D^{1-\alpha}_{0+} e_\alpha(t-\tau-s, \lambda_{mk}) e_\alpha(s, \lambda_{mk}) ds\, d\tau \Bigg] Z_{(2m-1)k} \\ &\quad + \sum_{m,k=1}^{\infty} \int_0^t f_{2mk}(\tau) e_\alpha(t-\tau, \lambda_{mk})\, d\tau Z_{2mk}, \end{aligned} \tag{4.61}$$

where

$$f_{mk} = < f(x, y, t), W_{mk} >, \quad \text{for} \quad m \in \mathbb{N} \cup \{0\}, k \in \mathbb{N},$$

are the coefficients of the series expansion of the function $f(x, y, t)$ in the basis Z_{mk}, $m \in \mathbb{N} \cup \{0\}, k \in \mathbb{N}$.

Remark 4.3.4. *It is worth noting that by taking $\varrho = 1, \alpha = 1$ in the solution (4.34) and (4.61) we obtain*

$$\begin{aligned} w(x,y,t) &= \sum_{k=1}^{\infty} \varphi_{0k} e^{-\lambda_{0k} t} Z_{0k} + \sum_{m,k=1}^{\infty} \left[\varphi_{(2m-1)k} e^{-\lambda_{mk} t} - 2\sqrt{\mu_m} \varphi_{(2m-1)k} t e^{-\lambda_{mk} t} \right] \\ &\quad Z_{(2m-1)k} + \sum_{m,k=1}^{\infty} \varphi_{2mk} e^{-\lambda_{mk} t} Z_{2mk}, \end{aligned} \tag{4.62}$$

$$\begin{aligned} v(x,y,t) &= \sum_{k=1}^{\infty} \int_0^t f_{0k}(\tau) e^{-\lambda_{0k}(t-\tau)}\, d\tau Z_{0k} + \sum_{m,k=1}^{\infty} \Bigg[\int_0^t f_{(2m-1)k}(\tau) e^{-\lambda_{mk}(t-\tau)}\, d\tau \\ &\quad -2\sqrt{\mu_m} \int_0^t f_{2mk}(\tau)(t-\tau) e^{-\lambda_{mk}(t-\tau)}\, d\tau \Bigg] Z_{(2m-1)k} \\ &\quad + \sum_{m,k=1}^{\infty} \int_0^t f_{2mk}(\tau) e^{-\lambda_{mk}(t-\tau)}\, d\tau Z_{2mk}. \end{aligned} \tag{4.63}$$

The expressions given by (4.62) and (4.63) are the same as those obtained in [50] for $\alpha = 1$.

4.3.2 Solution of the inverse problem

To solve the inverse problem we expand the functions $u(x,y,t)$ and $f(x,y)$ using the biorthogonal system. Thus

$$\begin{aligned} u(x,y,t) &= \sum_{k=1}^{\infty} C_{0k}^u(t)Z_{0k}(x,y) + \sum_{m,k=1}^{\infty} C_{(2m-1)k}^u(t)Z_{(2m-1)k}(x,y) \\ &\quad + \sum_{m,k=1}^{\infty} C_{2mk}^u(t)Z_{2mk}(x,y), \end{aligned} \tag{4.64}$$

and

$$f(x,y) = \sum_{k=1}^{\infty} f_{0k}Z_{0k}(x,y) + \sum_{m,k=1}^{\infty} f_{(2m-1)k}Z_{(2m-1)k}(x,y) + \sum_{m,k=1}^{\infty} f_{2mk}Z_{2mk}(x,y), \tag{4.65}$$

where $C_{0k}^u(t), C_{(2m-1)k}^u(t)$, $C_{2mk}^u(t)$, $f_{0k}, f_{(2m-1)k}$ and f_{2mk} for $m,k \in \mathbb{N}$ are to be determined.

By the property of the biorthogonal system we have

$$\begin{aligned} C_{0k}^u(t) &= < u(x,y,t), W_{0k} >, \\ C_{(2m-1)k}^u(t) &= < u(x,y,t), W_{(2m-1)k} >, \\ C_{2mk}^u(t) &= < u(x,y,t), W_{2mk} >, \qquad \text{for } m,k \in \mathbb{N}. \end{aligned}$$

Hence

$$\begin{aligned} D_{0+}^{\alpha}(C_{0k}^u(t) - C_{0k}^u(0)) &= < D_{0+}^{\alpha}(u(x,y,t) - u(x,y,0)), W_{0k} >, \\ D_{0+}^{\alpha}(C_{(2m-1)k}^u(t) - C_{(2m-1)k}^u(0)) &= < D_{0+}^{\alpha}(u(x,y,t) - u(x,y,0)), W_{(2m-1)k} >, \\ D_{0+}^{\alpha}(C_{2mk}^u(t) - C_{2mk}^u(0)) &= < D_{0+}^{\alpha}(u(x,y,t) - u(x,y,0)), W_{2mk} >, \end{aligned}$$

for $m,k \in \mathbb{N}$.

Using (4.1) we obtain the following system of linear fractional differential equations

$$D_{0+}^{\alpha}(C_{0k}^u(t) - C_{0k}^u(0)) = -\lambda_{0k}C_{0k}^u(t) + f_{0k}, \tag{4.66}$$

$$\begin{aligned} D_{0+}^{\alpha}(C_{(2m-1)k}^u(t) - C_{(2m-1)k}^u(0)) &= -\lambda_{mk}C_{(2m-1)k}^u(t) - 2\sqrt{\mu_m}C_{2mk}^u(t) \\ &\quad + f_{(2m-1)k}, \end{aligned} \tag{4.67}$$

$$D_{0+}^{\alpha}(C_{2mk}^u(t) - C_{2mk}^u(0)) = -\lambda_{mk}C_{2mk}^u(t) + f_{2mk}. \tag{4.68}$$

By virtue of relation (4.14) and Lemma 4.2.1, the solutions of equations (4.66)-

(4.68) are

$$
\begin{aligned}
C^u_{0k}(t) &= \int\limits_0^t g'_{0k}(t-\tau)e_\alpha(\tau,\lambda_{0k})\,d\tau + g_{0k}(0)e_\alpha(t,\lambda_{0k}),\\
C^u_{(2m-1)k}(t) &= \int\limits_0^t g'_{(2m-1)k}(t-\tau)e_\alpha(\tau,\lambda_{mk})\,d\tau + g_{(2m-1)k}(0)e_\alpha(t,\lambda_{mk}),\\
C^u_{2mk}(t) &= \int\limits_0^t g'_{2mk}(t-\tau)e_\alpha(\tau,\lambda_{mk})\,d\tau + g_{2mk}(0)e_\alpha(t,\lambda_{mk}),
\end{aligned}
$$

where

$$
\begin{aligned}
g_{0k}(t) &= C^u_{0k}(0) + \frac{f_{0k}t^\alpha}{\Gamma(1+\alpha)} \quad \Rightarrow \quad g'_{0k}(t) = \frac{f_{0k}t^{\alpha-1}}{\Gamma(\alpha)},\\
g_{(2m-1)k}(t) &= C^u_{(2m-1)k}(0) - 2\sqrt{\mu_m}J^\alpha_{0+}C^u_{2mk}(t) + \frac{f_{(2m-1)k}t^\alpha}{\Gamma(1+\alpha)}\\
\Rightarrow \quad & g'_{(2m-1)k}(t) = -2\sqrt{\mu_m}f_{2mk}\left(\frac{t^{2\alpha-2} * e_\alpha(t,\lambda_{mk})}{\Gamma(2\alpha-1)}\right)\\
& +C^u_{2mk}(0)e_{\alpha,\alpha}(t,\lambda_{mk}) + f_{(2m-1)k}\frac{t^{\alpha-1}}{\Gamma(\alpha)},\\
g_{2mk}(t) &= C^u_{2mk}(0) + \frac{f_{2mk}t^\alpha}{\Gamma(1+\alpha)} \quad \Rightarrow \quad g'_{2mk}(t) = \frac{f_{2mk}t^{\alpha-1}}{\Gamma(\alpha)}.
\end{aligned}
$$

In the above calculation of $g'_{(2m-1)k}(t)$ we used the following facts

$$
D^\alpha_{0+}(f*g) = (D^\alpha_{0+}f*g) = (f*D^\alpha_{0+}g), \quad D^{1-\alpha}_{0+}t^{1-\alpha} = \frac{\Gamma(\alpha)t^{2\alpha-2}}{\Gamma(2\alpha-1)},
$$

$$
D^{1-\alpha}_{0+}e_\alpha(t,\lambda_{mk}) = t^{\alpha-1}E_{\alpha,\alpha}(-\lambda_{mk}t^\alpha) =: e_{\alpha,\alpha}(t,\lambda_{mk}).
$$

Using the initial and final temperatures, we obtain

$$
C^u_{0k}(0) = \varphi_{0k}, \quad C^u_{(2m-1)k}(0) = \varphi_{(2m-1)k}, \quad C^u_{2mk}(0) = \varphi_{2mk},
$$

$$
C^u_{0k}(T) = \psi_{0k}, \quad C^u_{(2m-1)k}(T) = \psi_{(2m-1)k}, \quad C^u_{2mk}(T) = \psi_{2mk}, \tag{4.69}
$$

where $\psi_{mk} = <\psi, W_{mk}>$ for $m \in \mathbb{N}\cup\{0\}$, $k \in \mathbb{N}$.

The unknowns f_{0k}, $f_{(2m-1)k}$ and f_{2mk}, obtained from the relations (4.69), are

$$
f_{0k} = \frac{\psi_{0k} - \varphi_{0k}e_\alpha(T,\lambda_{0k})}{\int\limits_0^T \frac{(T-\tau)^{\alpha-1}}{\Gamma(\alpha)}e_\alpha(\tau,\lambda_{0k})\,d\tau}, \tag{4.70}
$$

$$
f_{(2m-1)k} = \frac{\psi_{(2m-1)k} - \varphi_{(2m-1)k}e_\alpha(T,\lambda_{mk}) + s_1(T) + s_2(T)}{\int\limits_0^T \frac{(T-\tau)^{\alpha-1}}{\Gamma(\alpha)}e_\alpha(\tau,\lambda_{mk})\,d\tau}, \tag{4.71}
$$

$$f_{2mk} = \frac{\psi_{2mk} - \varphi_{2mk} e_\alpha(T, \lambda_{mk})}{\int\limits_0^T \frac{(T-\tau)^{\alpha-1}}{\Gamma(\alpha)} e_\alpha(\tau, \lambda_{mk})\, d\tau}, \tag{4.72}$$

where we have set

$$\begin{aligned} s_1(T) &= \varphi_{2mk} \int\limits_0^T e_{\alpha,\alpha}(T-\tau, \lambda_{mk}) e_\alpha(\tau, \lambda_{mk})\, d\tau, \\ s_2(T) &= 2\sqrt{\mu_m} f_{2mk} \int\limits_0^T \left(\frac{(T-\tau)^{2\alpha-2}}{\Gamma(2\alpha-1)} * e_\alpha(T-\tau, \lambda_{mk}) \right) e_\alpha(\tau, \lambda_{mk})\, d\tau. \end{aligned}$$

Theorem 4.3.5. *Let $\varphi(x,y), \psi(x,y)$ be defined in $\bar{\Omega}$ such that $\varphi, \psi \in C^2(\bar{\Omega})$, $\varphi(0,y) = \varphi(1,y), \partial\varphi(1,y)/\partial x = 0$, $\varphi(x,0) = \varphi(x,1) = 0$ and $\psi(0,y) = \psi(1,y), \partial\psi(1,y)/\partial x = 0$, $\psi(x,0) = \psi(x,1) = 0$. Then there exists a unique solution of the inverse problem (4.1)-(4.4).*

Proof. In order to show the existence of the solution of the inverse problem given by series (4.64) and (4.65), we need to prove that the functions $u(x,y,t), u_{xx}(x,y,t), u_{yy}(x,y,t)$, $D^\alpha_{0+}(u(x,y,t) - u(x,y,0))$ and $f(x,y)$ are continuous in Q_T, i.e., we have to prove that the corresponding series are uniformly convergent in Q_T. By using properties of the Mittag-Leffler function and the biorthogonal system we can show that the series are uniformly convergent as we did in subsection 4.3.1.

Uniqueness of the solution: Let $\{u_1(x,y,t), f_1(x,y)\}$ and $\{u_2(x,y,t), f_2(x,y)\}$ be two solution sets of the inverse problem, then $\bar{u}(x,y,t) = u_1(x,y,t) - u_2(x,y,t)$ and $\bar{f}(x,y) = f_1(x,y) - f_2(x,y)$ satisfy

$$D^\alpha_{0+}(\bar{u}(x,y,t) - \bar{u}(x,y,0)) - \varrho\Delta\bar{u}(x,y,t) = \bar{f}(x,y), \qquad (x,y,t) \in Q_T, \tag{4.73}$$

$$\bar{u}(x,y,0) = 0, \quad \bar{u}(x,y,T) = 0, \qquad (x,y) \in \Omega, \tag{4.74}$$

$$\bar{u}(0,y,t) = \bar{u}(1,y,t), \quad \frac{\partial\bar{u}}{\partial x}(1,y,t) = 0, \qquad (y,t) \in D, \tag{4.75}$$

$$\bar{u}(x,0,t) = \bar{u}(x,1,t) = 0, \qquad (x,t) \in D. \tag{4.76}$$

Following the same procedure, i.e., expanding the $\bar{u}(x,y,t)$ into the basis $\{Z_{0k}, Z_{(2m-1)k}, Z_{2mk}\}$ for $m, k \in \mathbb{N}$ and using the property of the biorthogonal system, we obtain

$$D^\alpha_{0+}(C^{\bar{u}}_{0k}(t) - C^{\bar{u}}_{0k}(0)) = -\lambda_{0k} C^{\bar{u}}_{0k}(t) + \bar{f}_{0k}, \tag{4.77}$$

$$D^\alpha_{0+}(C^{\bar{u}}_{(2m-1)k}(t) - C^{\bar{u}}_{(2m-1)k}(0)) = -\lambda_{mk} C^{\bar{u}}_{(2m-1)k}(t) - 2\sqrt{\mu_m} C^{\bar{u}}_{2mk}(t) + \bar{f}_{(2m-1)k}, \tag{4.78}$$

$$D^\alpha_{0+}(C^{\bar{u}}_{2mk}(t) - C^{\bar{u}}_{2mk}(0)) = -\lambda_{mk} C^{\bar{u}}_{2mk}(t) + \bar{f}_{2mk}. \tag{4.79}$$

In view of (4.74), we have

$$\begin{aligned} C^{\bar{u}}_{0k}(0) &= 0 = C^{\bar{u}}_{0k}(T), \quad C^{\bar{u}}_{(2m-1)k}(0) = 0 = C^{\bar{u}}_{(2m-1)k}(T), \\ C^{\bar{u}}_{2mk}(0) &= 0 = C^{\bar{u}}_{2mk}(T), \end{aligned}$$

for $m,k\in\mathbb{N}$.

Whereupon

$$\bar{f}_{0k}=0,\quad \bar{f}_{(2m-1)k}=0,\quad \bar{f}_{2mk}=0.$$

Consequently, we have

$$(\bar{f}(x,y)=0\quad\text{and}\quad \bar{u}(x,y,t)=0)\quad\Rightarrow\quad(u_1=u_2\quad\text{and}\quad f_1=f_2).$$

□

Before we proceed to show the stability of the solution $\{f(x,y),u(x,y,t)\}$ of the inverse problem, let us recall the following estimates:

First recall that the Mittag-Leffler functions (4.15) and (4.16) are entire functions.

We have

$$e_\alpha(T,\mu_{0k})\le M_1,\qquad \frac{1}{\int\limits_0^T\frac{(T-\tau)^{\alpha-1}}{\Gamma(\alpha)}e_\alpha(\tau,\lambda_{0k})\,d\tau}\le M_2,$$

$$\frac{1}{\int\limits_0^T\frac{(T-\tau)^{\alpha-1}}{\Gamma(\alpha)}e_\alpha(\tau,\lambda_{mk})\,d\tau}\le M_3,$$

$$e_\alpha(T,\lambda_{mk})\le M_4,\quad \int\limits_0^T e_{\alpha,\alpha}(T-\tau,\lambda_{mk})e_\alpha(\tau,\lambda_{mk})\,d\tau\le M_5,$$

$$\mu_m\int\limits_0^T e_{\alpha,\alpha}(T-\tau,\lambda_{mk})e_\alpha(\tau,\lambda_{mk})\,d\tau\le\lambda_{mk}\int\limits_0^T e_{\alpha,\alpha}(T-\tau,\lambda_{mk})e_\alpha(\tau,\lambda_{mk})\,d\tau\le M_6,$$

for all $m\in\mathbb{N}\cup\{0\}$, $k\in\mathbb{N}$, where M_i, $i=1,...,6$, are constants independent of m and k.

Theorem 4.3.6. *For any $\varphi,\psi\in L^2(\Omega)$ the solution of the inverse problem (4.1)-(4.4) depends continuously on the given data.*

Proof. Let $\{u(x,t),f(x,y)\}$, $\{\tilde{u}(x,t),\tilde{f}(x,y)\}$ be solution sets of the inverse problem, corresponding to the data $\{\varphi,\psi\}$, $\{\tilde{\varphi},\tilde{\psi}\}$, respectively.

Due to the estimate (4.33) we have

$$\|f-\tilde{f}\|_{L^2(\Omega)}\le 16\sum_{m=0}^{\infty}\sum_{k=1}^{\infty}(f_{mk}-\tilde{f}_{mk})^2,$$

where f_{mk}, $\tilde{f}_{mk}$, for $m\in\mathbb{N}\cup\{0\},k\in\mathbb{N}$ given by (4.70)-(4.72) correspond to the data $\{\varphi,\psi\}$, $\{\tilde{\varphi},\tilde{\psi}\}$.

Furthermore, we have

$$\begin{aligned}\sum_{m=0}^{\infty}\sum_{k=1}^{\infty}(f_{mk}-\tilde{f}_{mk})^2 &\leq N_1\sum_{m=0}^{\infty}\sum_{k=1}^{\infty}\Big((\varphi_{mk}-\tilde{\varphi}_{mk})^2+(\psi_{mk}-\tilde{\psi}_{mk})^2\Big),\\ &\leq \frac{3N_1}{2}\Big(\|\varphi-\tilde{\varphi}\|_{L^2(\Omega)}+\|\psi-\tilde{\psi}\|_{L^2(\Omega)}\Big), \qquad (4.80)\end{aligned}$$

where we use $ab \leq 1/2(a^2+b^2)$ and Lemma 4.3.1 with

$$\begin{aligned}N_1 &= \max\{2M_2^2, 2M_1^2M_2^2, 4M_3^2, 2M_3^2+16M_4^2M_6^2M_3^2, 16M_4^2M_6^2M_3^2\\ &\quad +4M_3^2M_5^2+2M_3^2M_4\}.\end{aligned}$$

Finally, we have

$$\|f-\tilde{f}\|_{L^2(\Omega)} \leq C_1\Big(\|\varphi-\tilde{\varphi}\|_{L^2(\Omega)}+\|\psi-\tilde{\psi}\|_{L^2(\Omega)}\Big),$$

with $C_1 = 2\sqrt{6N_1}$.

Similarly we can obtain an estimate for $u(x,y,t)$. □

4.4 Conclusion

We have presented the existence and uniqueness of the classical solution of a time fractional diffusion equation posed in two dimensional space with nonlocal boundary conditions. Our method of proof is based on expanding the solution using a biorthogonal set of functions. We choose this technique as the problem considered is not self-adjoint, and therefore the completeness property of eigenfunctions of the spectral problem does not hold.

We have also looked for the map $u(x,y,T) \to \{f(x,y), u(x,y,t)\}$, i.e., the determination of the source term $f(x,y)$ and the temperature distribution whenever the final temperature distribution, the initial and boundary conditions are given. The existence and uniqueness results for the inverse source problem are established, and the stability of the solution of the inverse problem with respect to the data is proved.

Image structure preserving denoising using generalized fractional time integrals

Purpose of the paper:

The purpose of the paper [22] is to remove noise from digital images while preserving salient features of digital images. The process is known as image denoising (simplification, smoothing, restoration or enhancement). The objective is to propose an image denoising model which is well posed and numerical discretization is convergent.

The problem:

In digital images the denoising process seems to have conflicting tasks as one has to remove the noise while preserving the salient features (structure) of images. It is also known that the numerical differentiation in digital images is ill posed problem. In order to have an efficient image denoising model one should have a well posed model and use a numerical scheme which is convergent and preserve the apparent properties of the digital images e.g., positivity of the solution.

Strategy:

We propose a model based on linear heat equation which involve fractional derivative in time of order $1 < \alpha < 2$. The equation has the intermediate properties of linear heat equation and linear wave equation. The diffusion process can be controlled by the order of the fractional derivative (depending on the order of fractional derivative). The denoising process take in account the structure of the digital images, when the proposed equation applied to each pixel of the digital images. The space and time discretizations adopted are convergent.

CHAPTER 5

Image structure preserving denoising using generalized fractional time integrals

Abstract

A generalization of the linear fractional integral equation $u(t) = u_0 + \partial^{-\alpha} Au(t)$, $1 < \alpha < 2$, which is written as a Volterra matrix–valued equation when applied as a pixel–by–pixel technique, is proposed in this paper for image denoising (restoration, smoothing,...). Since the fractional integral equation interpolates a linear parabolic equation and a hyperbolic equation, the solution enjoys intermediate properties. The Volterra equation we propose is well–posed for all $t > 0$, and allows us to handle the diffusion by means of a *viscosity parameter* instead of introducing non–linearities in the equation as in the Perona–Malik and alike approaches. Several experiments showing the improvements achieved by our approach are provided.

Keywords: Image processing, Fractional integrals and derivatives, Volterra equations, Convolution quadrature methods.

MSC [2010]: 44A35, 44K05, 45D05, 65R20, 68U10, 94A08.

Contents

5.1 Introduction

Partial differential equations based methods for image processing (filtering, denoising, restorations, segmentation, edge enhancement/detection,...) have been largely studied in the literature (see [114] and references therein).

In that framework the first, and most investigated equation is the linear heat equation with homogeneous Neumann boundary condition

$$\begin{cases} \partial_t u(t,\mathbf{x}) &= \Delta u(t,\mathbf{x}), & (t,\mathbf{x}) \in [0,T]\times\Omega, \\ u(0,\mathbf{x}) &= u_0(\mathbf{x}), & \mathbf{x}\in\Omega, \\ \dfrac{\partial u}{\partial \eta}(t,\mathbf{x}) &= 0, & (t,\mathbf{x}) \in [0,T]\times\partial\Omega, \end{cases} \tag{5.1}$$

where ∂_t, and Δ stand for the time derivative, and two–dimensional Laplacian operator, respectively, $\Omega \subset \mathbb{R}^2$ is typically a square domain, $\partial\Omega$ represents the boundary of Ω, $\partial/\partial\eta$ stands for the outward normal derivative, and u_0 is the noisy image from which the objective is to restore the original (ideal) image. Let us notice that $u(t,\mathbf{x})$ stands for the restored image at the time level t.

The interest for this model is due to the fact that the solution of (5.1) can be written as a convolution

$$u(t,\mathbf{x}) = \int_{\mathbb{R}^2} G_{\sqrt{2t}}(\mathbf{x}-\mathbf{y})u_0(\mathbf{y})\,\mathrm{d}\mathbf{y},$$

where G is the two–dimensional Gaussian kernel

$$G_\sigma(\mathbf{x}) := \frac{1}{2\pi\sigma^2}e^{-|\mathbf{x}|^2/2\sigma^2}.$$

Since convolution with a positive kernel is the basic tool in linear filtering, computing the solution of (5.1) is equivalent to Gaussian filtering in a classical way.

However, in this equation the diffusion is isotropic which, in the context of image processing, means that smoothing applies uniformly in the whole image and is equivalent in the direction of both coordinates axis, therefore independent of the image structure itself. This yields that in most cases edges and corners are severely blurred disabling this filter for practical applications.

In view of this, an edge–preserving regularization, i.e., a non uniform diffusion model, will require more sophisticated approaches. One of this was proposed by Perona and Malik in [91] and reads as the non–linear heat equation based problem

$$\begin{cases} \partial_t u(t,\mathbf{x}) &= \operatorname{div}\left(c(|\nabla u(t,\mathbf{x})|^2)\nabla u(t,\mathbf{x})\right), \\ u(0,\mathbf{x}) &= u_0(\mathbf{x}), \\ \dfrac{\partial u}{\partial \eta}(t,\mathbf{x}) &= 0, \quad \mathbf{x}\in\partial\Omega, \end{cases} \tag{5.2}$$

for $(t,\mathbf{x}) \in Q = [0,T]\times\Omega$. The diffusion coefficient $c : [0,+\infty) \to [0,+\infty)$, is chosen to be close to zero near edges and corners, that is, pixels where gradient is large. On the contrary, c should be large in pixels with low gradient variation.

Functions satisfying these assumptions are commonly called *edge stopping functions*, and examples of such a function were firstly proposed by Perona and Malik, e.g,

$$c(s) = 1/(1+s) \qquad \text{or} \qquad c(s) = e^{-s}. \tag{5.3}$$

Unfortunately, the *edge stopping functions* lead in general to backward–forward problems that turn out to be ill–posed. Numerical experiments carried out by some authors with these models (involving edge stopping functions) reported that no significant instabilities are observed; moreover, for large final times, restored images seem to preserve and enhance edges (see e.g., [45]). The reason for not observing any instability in Perona-Malik model is that in many cases the numerical scheme used does not correspond to their equation but rather to a time–regularized one which is a well–posed equation as reported by H. Amman [4]. Even in the case of the discretization corresponding to the equation (i.e., without regularizing) the only one artifact usually observed in the numerical experiments is the *staircasing effect*. This occurs when a standard spatial discretization of the equation is considered instead of the continuous one. In that case it has been proved in [112] that (5.2) becomes a well–posed system of nonlinear ordinary differential equations.

In the same way, some other approaches have been proposed as for example the ones based on the total variation of suitable functionals (see [100]). All these works have promoted the idea of replacing (5.2) by nearby equations keeping on the one hand the same image structure, and on the other hand, lying in a *reasonable* functionals space setting where the well–posedness can be guaranteed as well as the bounded variation, and further analytical and numerical properties. The first perturbed model was proposed in [16] where, for a suitable extension of u over $\mathbb{R}^2$ (e.g., by 0) denoted $\tilde{u}$, $c(|\nabla u|)$ is replaced by $c(|\nabla(G_\sigma * \tilde{u})|)$ (G_σ as defined above). In that case, for $u_0 \in L_2(\Omega)$, the regularized problem admits a unique solution in $C([0,T], L_2) \cap L_2((0,T), H^1)$ where H^1 is the Sobolev space defined as $H^1(\mathbb{R}^2) := \{f \in L_2(\mathbb{R}^2), \nabla f \in L_2(\mathbb{R}^2)\}$. Despite of some features of this model, images become uniformly grey (for grey–scale images) in the long run, thus the information gets lost (see [4]). Variants of this approach have been studied by many authors (see e.g., [57, 58] and references therein).

Lately, further approaches have been proposed, e.g., by adding regularizing terms, like $\varepsilon\Delta\partial_t u$, to the diffusion equation in (5.2) (see [11]), or for example higher order partial differential equations based regularization, and in particular fourth order partial differential equations (see [80]). However, despite of the practical results which seem to be quite good in most of the cases, some of them have not been closely studied from the analytical and the numerical view point.

Many image denoising models based on local average (also known as neighborhood filters) have been proposed for controlling the diffusion process. Let us mention some of the neighboring filters: Yaroslavsky neighborhood filter [116], sigma filter [72], bilateral filtering [109] are a few examples. The faster diffusion is obtained in these filters by assigning appropriate weights where the neighborhood pixels have gray scale value close to one another (uniform region) and slower diffusion is obtained across the boundaries of the region, resulting in the preservation of edges in the image. All the local nonlinear filters (neighborhood filters) create artifact boundaries (staircase effect) in the restored images. In [13], the authors justify the phenomena of artifact boundaries by showing that the Yaroslavsky neighborhood filter has exactly the same qualitative behavior as Perona-Malik model [91]. Similar behavior of staircase for the bilateral filter was observed (see [9]).

Finally let us comment that one can face up to diffusion filtering in a more general framework as the one of *anisotropic* models. In fact most of models we mentioned above turn out to be *isotropic* since the diffusion is governed by means of a scalar–valued function c which allows to reflect the structure of the underlying image, but the diffusion turns out to be the same in the two orthogonal directions of coordinate axis. A generalization of such approaches consist in replacing c by a tensor which allows on the one hand to rotate the flux and so the diffusion in orthogonal directions toward a suitable orientation, and on the other hand a suitable choice of the eigenvalues of the tensor can lead to different diffusions on each single direction (see e.g., [3, 10, 113] for more details). In the present work we focus on the scalar approach, i.e., no tensor diffusion is considered, keeping in mind that a tensorial approach in the framework of fractional calculus fits well and will be the topic of our future works.

In this work, we present a new approach based on fractional calculus which allows us to handle the diffusion, i.e., the smoothing in the image terminology, by means of a single parameter which plays the role of "viscosity" parameter in a linear partial differential equation (see Section 5.3 for more details on our main contributions). Besides the satisfactory practical results obtained (see Section 5.6), we mention hereafter the new features of our model. First, the linear model we are proposing here is well–posed; since the final objective is the practical implementation, very efficient numerical discretizations can be applied for the proposed model because a large variety of them have been closely studied by many authors and they are at our disposal for the experiments in Section 5.6. Moreover, the model we propose enjoys the well–posedness for all positive time levels, i.e., for $t > 0$, on the contrary to what typically happens when nonlinear equations are involved, this occurs for example with the Perona-Malik model. However, despite the fact that this model turns out to be a well–posed system of nonlinear equations after discretizing in space as we described earlier, the existence of a unique solution can be guaranteed only locally i.e., for a finite time interval (usually small). Therefore, when using the semidiscrete Perona-Malik model in practical applications some estimation of the acceptable final time should be done. Second, we have to highlight the simplicity of our model for controlling the diffusion process, which has been achieved by choosing a scalar function which allows a suitable choice of the viscosity parameter as we describe in Section 5.5. Moreover, due to the numerical scheme chosen for our experiments, some additional properties are guaranteed, in fact the positivity of the image seen in the continuous setting is also guaranteed in the discrete one (Th. 5.4.1, in Section 5.4).

This paper is organized as follows. In Section 5.2, we recall some facts concerning fractional calculus, and the first approaches to image processing by using fractional calculus. Section 5.3 focusses on a generalized fractional integrals based approach to image processing which is the main novelty of this work. Numerical discretizations are presented in Section 5.4. The discussion on the implementation, and practical experiments, are shown in Sections 5.5 and 5.6, respectively. Finally, we end with conclusions in Section 5.7.

5.2 Fractional calculus

Image filtering by means of fractional calculus was first considered in [21]. In that work, a generalization of the heat equation (5.1) is proposed which reads as

$$\begin{cases} \partial_t^\alpha u(t,\mathbf{x}) &= \Delta u(t,\mathbf{x}), & (t,\mathbf{x}) \in [0,T]\times\Omega \\ u(0,\mathbf{x}) &= u_0(\mathbf{x}), & \mathbf{x}\in\Omega, \\ \partial_t u(0,\mathbf{x}) &= 0, & \mathbf{x}\in\Omega, \\ \dfrac{\partial u}{\partial\eta}(t,\mathbf{x}) &= 0, & (t,\mathbf{x})\in[0,T]\times\partial\Omega, \end{cases} \tag{5.4}$$

where ∂_t^α stands for the fractional time derivative of order $1<\alpha<2$ in the sense of Riemann–Liouville. Integrating in both sides, the problem (5.4) can be expressed as

$$u(t,\mathbf{x}) = u_0(\mathbf{x}) + \frac{1}{\Gamma(\alpha)}\int_0^t (t-s)^{\alpha-1}\Delta u(s,\mathbf{x})\,\mathrm{d}s,$$

also with homogeneous Neumann boundary condition, or in a compact format

$$u(t,\mathbf{x}) = u_0(\mathbf{x}) + \partial^{-\alpha}\Delta u(t,\mathbf{x}), \tag{5.5}$$

where $\partial^{-\beta}$, for $\beta>0$, stands for the fractional integral of order $\beta\in\mathbb{R}^+$, in the sense of Riemann–Liouville.

Let us recall that, for $g:[0,+\infty)\to\mathbb{R}$, $g\in AC[0,+\infty)$ (the space of absolutely continuous functions) the integral of order $\beta\in\mathbb{R}^+$ in the sense of Riemann–Liouville is defined as the convolution integral

$$\partial^{-\beta}g(t) := \int_0^t k_\beta(t-s)g(s)\,\mathrm{d}s, \qquad t\geq 0, \tag{5.6}$$

where $k_\beta(t) := t^{\beta-1}/\Gamma(\beta)$, for $t>0$ (see [62]). Now, the definition of the fractional derivative of order $\beta\geq 0$ is

$$\partial^\beta g(t) := \frac{d^m}{dt^m}\partial^{\beta-m}g(t), \qquad t\geq 0,$$

where $m\in\mathbb{N}$, $m-1<\beta\leq m$.

The interest of our model in the framework of image processing is due to the fact that, for $1<\alpha<2$, the problem (5.4) interpolates the linear (parabolic) heat equation (5.1) corresponding to $\alpha=1$ (with no need of $\partial_t u(0,\mathbf{x})=0$), and the linear (hyperbolic) wave equation

$$\begin{cases} \partial_t^2 u(t,\mathbf{x}) & = & \Delta u(t,\mathbf{x}), & (t,\mathbf{x}) \in [0,T]\times\Omega \\ u(0,\mathbf{x}) & = & u_0(\mathbf{x}), & \mathbf{x}\in\Omega, \\ \partial_t u(0,\mathbf{x}) & = & 0, & \mathbf{x}\in\Omega, \\ \dfrac{\partial u}{\partial \eta}(t,\mathbf{x}) & = & 0, & (t,\mathbf{x}) \in [0,T]\times\partial\Omega, \end{cases} \tag{5.7}$$

corresponding to $\alpha = 2$ (with zero initial velocity). Therefore, some properties of the solution of (5.4) are intermediate between the ones of (5.1) and (5.7) (see e.g., [33, 34]). In particular, it can be easily proved that for the scalar equation (i.e., by replacing Δ in (5.4) with a complex λ with non–positive real part) the solution decays as $1/(1 + t^\alpha|\mathrm{Re}(\lambda)|)$, i.e., the solution is $o(t^{-\alpha})$, as $t \to +\infty$. In that case, the solution decays slower than the one of the scalar heat equation (with the same λ) for which the solution decays exponentially, and faster than the one of the scalar wave equation whose solution does not decay (but oscillates). The diffusion is now handled by the parameter α. We show below that the solution of the model we propose is well behaved.

At the same time, fractional calculus was proposed for edge detection in [84], and later for image denoising in [6]. In these papers, the authors proposed anisotropic equations, where the anisotropy is handled by means of spatial fractional derivatives; however, the papers do neither include the study of the well–posedness of the problem nor the study of the behavior of the fully numerical discretization.

Finally, let us mention [26, 27, 28] where the fractional calculus, also applied to image processing, is understood as the fractional powers of the two–dimensional Laplacian, i.e., $(-\Delta)^\beta$, for $\beta > 0$, therefore in a different framework and with some different features.

5.3 Volterra equations

Despite of the fact that the approach (5.5) in Section 5.2 seems to be very promising, the diffusion (smoothing) is still uniform all over the whole image as in (5.1).

The above idea led us to a refinement which consists in splitting the whole image into sub–images, and apply (5.4) with different values of α for each sub–image (see [20]). However the approach we propose in this paper is more than a slight extension of the one in [20], from a technical viewpoint. Roughly speaking, in [20] the choice of each α is carried out by setting values close to 1 for the sub–images with lower mean gradient variation, and close to 2 for the sub–images with higher mean gradient variation. This approach does not provide satisfactory results as extended in the framework of image denoising despite of the fact that this approach has provided good results in some practical situations such as in satellite image classification (see [99]). It is mainly due to the fact that in most cases the borders of each single sub–image keep clearly sharpened which is undesirable in image denoising.

However this idea suggested us a finer approach which is the main contribution of this work, and which intends to be the limit of the above situation, i.e., the application of the fractional equation (5.4) with a different value of α (i.e., order of derivative) for each single pixel. The values of α are chosen according to the gradient variation at each single pixel as we discuss in Section 5.5.

Hereafter, we will consider gray–scale images since for colored images processing becomes a more difficult task. A naive way for colored images is to perform a similar methodology based on the one we present here but separately for each of the three layers (one per color) e.g., in the case of RGB format.

Let us start by taking a spatial discretization of the Laplacian in (5.4) based on a second order central difference scheme with mesh length $h > 0$. In such a way, Δ transforms into a $M^2 \times M^2$ pentadiagonal matrix Δ_h (see Fig. 5.1), and in the same fashion, $u(t, \mathbf{x})$ is transformed into a $M^2 \times 1$ vector–valued function $\mathbf{u}(t)$ which stands for the vector–arranged image pixels at time level t where M is the length and width of the image.

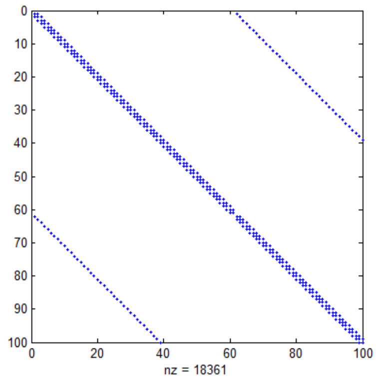

Figure 5.1: Sparsity pattern of the discretized Laplacian

As we commented above, the novelty of our approach consists in replacing the (only one) order derivative α of equation (5.4) with a different value of α for each single pixel of the image. This approach reads now as the linear Volterra matrix–valued equation

$$\mathbf{u}(t) = \mathbf{u}_0 + \int_0^t \mathbf{K}(t-s)\mathbf{u}(s)\, \mathrm{d}s, \qquad 0 \le t \le T, \tag{5.8}$$

where $\mathbf{u}_0$ is the vector–arranged initial data (noisy image), and the convolution kernel $\mathbf{K}$ is defined as

$$\mathbf{K}(t) = I(t) \cdot \Delta_h$$

with

$$I(t) = \begin{bmatrix} \dfrac{t^{\alpha_1}}{\Gamma(\alpha_1+1)} & 0 & \dots & 0 \\ 0 & \dfrac{t^{\alpha_2}}{\Gamma(\alpha_2+1)} & \dots & 0 \\ \vdots & \vdots & \ddots & \vdots \\ 0 & \dots & 0 & \dfrac{t^{\alpha_{M^2}}}{\Gamma(\alpha_{M^2}+1)} \end{bmatrix}$$

and, $1 < \alpha_j < 2$, for $j = 1, 2, \dots, M^2$.

Let us notice that $\mathbf{K}$ is a pentadiagonal matrix valued function, and since the Laplace transform of $\mathbf{K}$ exists, the well–posedness of (5.8) is then guaranteed all over the positive real line (see e.g., [97]).

5.4 Time discretizations

5.4.1 Background

Time discretizations of Volterra equations as (5.8) have been largely studied in literature; let us mention, e.g., the convolution quadrature based methods (see [75, 76, 77]). In particular Runge–Kutta convolution quadrature methods (the convolution quadrature is based on classical Runge–Kutta methods) of that equations provide high order numerical methods jointly with good stability properties. In [78], these discretizations have been studied in the abstract setting of sectorial operators, i.e., for convolution kernels whose Laplace transform is of *sectorial type*. Let us recall that a complex function G is of *sectorial type* if there exist $0 < \theta < \pi/2$, $c \in \mathbb{R}$, and $\mu, M > 0$ such that G is analytic in the sector

$$S_\theta := \{\lambda \in \mathbb{C} : |\arg(\lambda - c)| < \pi - \theta\},$$

and

$$|G(\lambda)| \leq \frac{M}{|\lambda|^\mu}, \qquad \lambda \in S_\theta.$$

Under these assumptions, the inverse Laplace transform of G can be written by means of the Bromwich formula as

$$g(t) = \frac{1}{2\pi i} \int_\gamma e^{\lambda t} G(\lambda)\, \mathrm{d}\lambda,$$

where γ is a complex path connecting $-i\infty$ and $+i\infty$ parallel to the boundary of S_θ with increasing imaginary part.

The convergence of these methods has been recently extended to analytic semigroups (see [14]) where the only one requirement on the kernel is the existence of the Laplace transform (weaker assumption than the assumption of sectorial type). Since the Laplace transform of each function $t^{\alpha_j}/\Gamma(\alpha_j+1)$ in (5.8) exists, and therefore the Laplace transform of $\mathbf{K}$ exists as a matrix–valued function, these methods turn out to be appropriate for our purposes. In this case, if $\tilde{\mathbf{K}}$ denotes the Laplace transform of $\mathbf{K}$, then the inverse Laplace transform can be written as

$$\mathbf{K}(t) = \frac{1}{2\pi i}\int_\gamma e^{\lambda t}\tilde{\mathbf{K}}(\lambda)\,\mathrm{d}\lambda,$$

where $\gamma(r) = a + ri$, $-\infty < r < +\infty$, for $a \in \mathbb{R}^+$. Let us notice that now the whole path γ lies on the right–hand complex plane $\mathrm{Re}(\lambda) \geq a$.

In order to set a suitable Runge–Kutta convolution quadrature method, we must take into account that the time regularity of the solution of (5.8) is constrained by the nature of the convolution kernel, in particular the continuity of their derivatives is guaranteed only up to the first order. Therefore, in this work, we will focus on the backward Euler convolution quadrature method, i.e., avoiding higher order schemes whose convergence will require more regularity on the solutions. This method will be sufficient to show the new features of our approach.

5.4.2 Convolution quadratures

For the sake of the readers convenience, we first recall the definition of the backward Euler convolution quadratures, and for the sake of the simplicity of the explanation we refer the readers to [14, 77] for the definition of Runge–Kutta convolution quadratures in the general case and further references.

Let $\tau > 0$ be the time step of the discretization. The convolution integral in (5.8) reads

$$\begin{aligned}\int_0^t \mathbf{K}(t-s)\mathbf{u}(s)\,\mathrm{d}s &= \int_0^t \frac{1}{2\pi i}\int_\gamma e^{\lambda(t-s)}\tilde{\mathbf{K}}(\lambda)\,\mathrm{d}\lambda\,\mathbf{u}(s)\,\mathrm{d}s \\ &= \frac{1}{2\pi i}\int_\gamma \tilde{\mathbf{K}}(\lambda)Y(\lambda,t)\,\mathrm{d}\lambda,\end{aligned}$$

where $Y(\lambda,t)$ stands for the solution of the ordinary differential equation

$$\mathbf{y}'(t) = \lambda\mathbf{y}(t) + \mathbf{u}(t),\ 0 \leq t \leq T, \quad \text{with} \quad \mathbf{y}(0) = 0. \tag{5.9}$$

The backward Euler convolution quadrature is obtained as

$$\int_0^{t_n} \mathbf{K}(t_n-s)\mathbf{u}(s)\,\mathrm{d}s \approx \frac{1}{2\pi i}\int_\gamma \tilde{\mathbf{K}}(\lambda)Y_n(\lambda)\,\mathrm{d}\lambda,$$

where $t_n = n\tau$, and $Y_n(\lambda)$ stands for the approximation of $Y(\lambda,t_n)$ reached by the backward Euler method applied to (5.9). Therefore, the convolution quadrature reads

$$\int_0^{t_n} \mathbf{K}(t_n-s)\mathbf{u}(s)\,\mathrm{d}s \approx \sum_{j=0}^{n}\mathbf{Q}_{n-j}^{(\alpha)}\mathbf{u}(t_j),$$

where the weights $\mathbf{Q}_j^{(\alpha)}$ are defined in terms of the backward Euler characteristic polynomials quotient $\rho(z)/\delta(z) = z/(z-1)$ evaluated in the variable $\xi = 1/z$. In fact, such weights turn out to be the coefficients of

$$\tilde{\mathbf{K}}\left(\frac{1-\xi}{\tau}\right) = \sum_{j=0}^{+\infty} \mathbf{Q}_j^{(\alpha)} \xi^j.$$

which explicitly written read

$$\mathbf{Q}_j^{(\alpha)} = \tau^{\alpha} \begin{bmatrix} \binom{\alpha_1}{j} & 0 & \dots & 0 \\ 0 & \binom{\alpha_2}{j} & \dots & 0 \\ \vdots & \vdots & \ddots & \vdots \\ 0 & \dots & 0 & \binom{\alpha_{M^2}}{j} \end{bmatrix} \cdot \Delta_h, \tag{5.10}$$

for $j = 0, 1, 2, \ldots$, as $M^2 \times M^2$ matrices. (see [14, 24, 77] for more details).

5.4.3 Numerical method. Convergence

Let $\mathbf{u}_n$ be the approximation of $\mathbf{u}(t_n)$, for $n \geq 0$. Then the time discretization of (5.8) by means of the backward Euler convolution quadrature method reads

$$\mathbf{u}_n = \mathbf{u}_0 + \sum_{j=1}^{n} \mathbf{Q}_{n-j}^{(\alpha)} \mathbf{u}_j, \quad n \geq 1,$$

and keeping in mind the practical implementation, since the matrix Δ_h is not singular, the unique n-th approximation is reached by solving the linear system

$$\left(I - \mathbf{Q}_0^{(\alpha)}\right) \mathbf{u}_n = \mathbf{u}_0 + \sum_{j=1}^{n-1} \mathbf{Q}_{n-j}^{(\alpha)} \mathbf{u}_j, \quad n \geq 1. \tag{5.11}$$

In the abstract setting considered in [14], optimal error bounds are obtained. In particular, for the backward Euler based method, the first order is reached by assuming the existence and boundedness of the second derivative of the solution. However, since the second derivative of the solution of (5.8) is merely integrable but not continuous, these results cannot be directly applied. In our case, if one takes into account the nature of the convolution kernel, then the stability proven in [24] jointly with Theorem 3.1 in [75] allow us to guarantee that the method is convergent of first order.

Besides, in [14] an interesting result is also proven which becomes even more interesting when applications fit into the framework of image processing. For the readers convenience we recall this result in the case of the backward Euler convolution quadrature method we apply in this paper.

Theorem 5.4.1. *If $\mathbf{u}$ is the solution of (5.8), and $\mathbf{u}_n$, for $n \geq 0$, is the numerical solution yielded by (5.11), then there exists a probability density $\rho_{n,\tau} : [0, +\infty) \to \mathbb{R}$ such that*

$$\mathbf{u}_n = \int_0^{+\infty} \mathbf{u}(s) \rho_{n,\tau}(s)\, \mathrm{d}s, \qquad n \geq 1. \tag{5.12}$$

The interest of this theorem is that, since $\rho_{n,\tau}$ is a probability density, i.e., positive and satisfying

$$\int_0^{+\infty} \rho_{n,\tau}(s)\,\mathrm{d}s = 1,$$

if $\mathbf{u}$ is for example positive, then the representation (5.12) guarantees the positivity of $\mathbf{u}_n$. In other words, the numerical solution (5.11) preserves, among other properties, the positivity of the continuous solution.

Moreover, let us point out that in [14] it is proven that the density of probability in (5.12) does not depend on the equation itself but only on the numerical method. In particular, for the method considered here (see [24, 15]), there is an explicit expression for such a density

$$\rho_{n,\tau}(t) = \frac{1}{\tau(n-1)!}\left(\frac{t}{\tau}\right)^{n-1} \mathrm{e}^{-t/\tau}, \qquad n \geq 1.$$

Finally, we can mention some other very efficient methods to discretize (5.8) as for example the ones based on the discretization of the inverse Laplace transform (see [74]), the ones based on the adaptive fast and oblivious convolutions (see [73]), or the collocation methods (see [12] and references therein).

5.5 Implementation

In this section we will discuss some facts concerning the implementation of (5.11) itself.

First of all, the choice of α's should be done according to the idea of preserving edges and corners and removing noise. Therefore, in view of the discussion in Section 5.2, pixels where the gradient is large should be associated with values of α close to 2. On the contrary, pixels with lower gradients should be associated with values of α close to 1. Let us notice that the practical computation of the gradient variation turns out to be very simple in a discrete setting as the one we consider in the spatial variables.

However some remarks have to be taken into account:

- On the one hand, avoiding singular situations can be yielded in both–sides values of α, i.e., $\alpha = 1$ and $\alpha = 2$, at least from the numerical point of view, we will not reach these values when setting α's. In particular, in Section 5.6, for $j = 1, 2, \ldots, M^2$, $\alpha_j \in [1+\varepsilon, 2-\varepsilon]$ with $\varepsilon = 10^{-3}$.

- On the other hand, since extreme situations appear such as *isolated* noisy pixels (see Figure 5.3 where a gray–scale image is shown as a three–dimensional surface), a particular choice of α's is expected; in particular for those pixels, values close to 1 will be associated. On the contrary, near edges and corners (very high gradient variation) no smoothing should be required, therefore α's close to 2 will be set for that pixels.

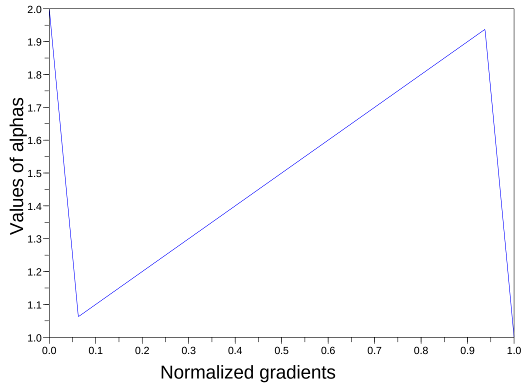

Figure 5.2: Profile distribution of α's.

According to this criterion, in this work, the setting of α values follows a profile distribution as in Figure 5.2.

Notice that this simple and naive procedure allows one to establish different settings of distributions depending, e.g., on the characteristics of each image.

- From a computational point of view, the number of different values of α's should be limited, otherwise if one admits a number of α's as large as the number of pixels, the implementation carries out a very high computational cost in practical cases. In fact, in this work, we set $\alpha \in \{1+j/N, 1 \leq j \leq N\}$, for a fixed integer N which in Section 5.6 turns out to be $N = 100$.

Let us also mention that in (5.10) a fixed number of weights $\mathbf{Q}_j^{(\alpha)}$ are computed once for all for each α_j. Moreover, the practical computation of that weights has been carried out by means of the Fast Fourier Transform as in [14], therefore saving a noticeable *run–time*.

Another fact of interest concerns the measure of quality of filtered/restored images in image filtering, and restoration. Despite of in many cases a visual analysis turn out to be sufficient to determine the quality of a methodology when applied to image processing, in this work, we consider two numerical criteria, SNR and $PSNR$, which have been largely used in literature (see e.g., [25]), and which are commonly applied to determine the quality of a processed image in the sense commented above (filtering, restoration,...). In fact, SNR and $PSNR$ stand for the Signal to Noise Ratio and Peak Signal to Noise Ratio, respectively, and the unit for both of these ratios are decibels (dB). To be more precise, SNR of a restored image R compared to an ideal image I is defined as

$$SNR = 10 \cdot \log_{10}\left(\frac{\text{var}(I)}{\text{var}(I-R)}\right),$$

where $\text{var}(x)$ stands for the variance of the vector x. Here I and R are considered

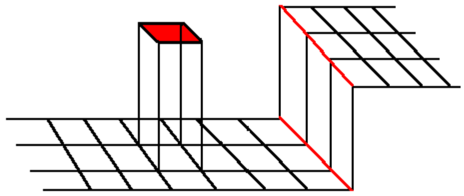

Figure 5.3: Three dimensional representation of (expected) isolated noisy pixels for a gray–scale image.

as vector arranged gray–scale images, as in Section 5.3, with 256 gray levels. In the same way, $PSNR$ is defined as

$$PSNR = 10 \cdot \log_{10}\left(\frac{\sum_{i,j} 255^2}{\sum_{i,j}(I_{i,j} - R_{i,j})^2}\right),$$

where $I_{i,j}$, $R_{i,j}$ are the pixel values of I and R respectively. Notice that in restoration problems, we have a corrupted image, and try to restore the ideal image which in general is not available, but for the calculation of SNR and $PSNR$ (from above formulas) ideal image is required. For the experiments in Section 5.6, we take an image (ideal image) and we perturb that image by adding noise. This image is then used for restoration; therefore SNR and $PSNR$ can be computed for the restored images.

5.6 Practical results

In this section, we show the improvements in the restorations provided by our approach. To this end, we perform some experiments where a noisy image is evolved by using the Perona–Malik model (5.2) with $c(s) = \mathrm{e}^{-s}$ as commented in (5.3) (PM), the contrast parameter (λ) is chosen such that $1.5 * \sigma < \lambda < 2 * \sigma$ as suggested in [39] (where σ is the noise variation) and the model (5.8) we propose (VE).

First experiment:
In the first experiment the six images shown in (Figure 5.4) are considered for the experimental validation of the proposed method. Each original image from the six images (Figure 5.4) has been perturbed by additive Gaussian noise of variance ranging from 10 to 30. In Table 5.1, we show the results (in terms of SNR) yielded by the restoration carried out with the mentioned procedures.

In fact, in view of Table 5.1, it can be observed that similar results are reached with (PM) and (VE). However we should recall that (VE) stands for a linear model whose well–posedness is guaranteed on the contrary to what happens with (PM).

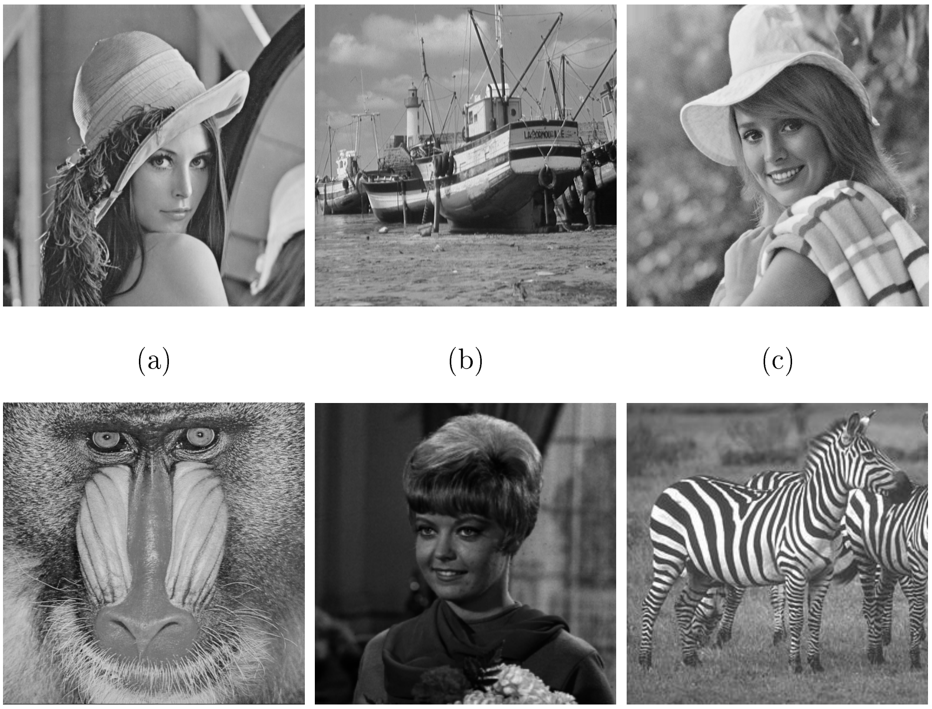

(a) (b) (c)

(d) (e) (f)

Figure 5.4: Images for the first experiment: (a) Lena, (b) Boats, (c) Elaine, (d) Baboon, (e) Lady, (f) Zebra.

For further close observation of the procedures applied to the images of Lena (Figure 5.4.(a)) and Elaine (Figure 5.4.(c)), with $\sigma = 25$ a part of such image is considered for all denoising models; in particular, a 200×200 part of the image has been considered (see Figure 5.5). The restored images by Perona-Malik model for both Lena and Elaine images, preserves edges/corners (Figure 5.5.(c) and Figure 5.5.(g)) but smooths very strongly the *flat* areas which causes lost of information regarding the texture of the image. Also, strong artifacts at the edges and corners has been observed as reported in [13]. The (VE) denoises the image (Figure 5.5.(j) and Figure 5.5.(h)), also by preserving edges/corners of the image; but here smoothing in flat areas is not so strong as with (PM) and it preserves the structure of the image without creating any artifacts.

Table 5.1: First experiment: SNR analysis

σ	10	15	20	25	30
Input SNR	13	10	7	5.6	4
Method	Lena (512×512)				
(PM)	16.81	14.79	13.82	13.32	11.27
(VE)	17.31	15.00	14.46	13.73	12.78
Input SNR	13.3	9.88	7.4	5.5	4
Method	Boats (512×512)				
(PM)	15.07	13.69	12.26	11.32	9.72
(VE)	15.74	14.10	12.65	11.57	10.32
Input SNR	13.2	9.7	7.3	5.3	3.8
Method	Elaine (512×512)				
(PM)	15.60	14.56	13.52	13.01	11.22
(VE)	16.32	14.74	13.71	13.52	11.96
Input SNR	12.5	9	6.5	4.5	3
Method	Baboon (512×512)				
(PM)	13.42	10.09	8.34	7.27	6.15
(VE)	12.88	10.29	8.51	7.49	6.89
Input SNR	12	8.73	6.34	4.5	3.1
Method	Lady (256×256)				
(PM)	16.06	14.23	12.50	11.90	9.94
(VE)	16.49	14.54	13.19	12.00	11.07
Input SNR	13.79	10.25	7.81	5.88	4
Method	Zebra (256×256)				
(PM)	15.18	12.38	10.19	9.13	7.49
(VE)	14.33	11.44	9.63	8.14	7.60

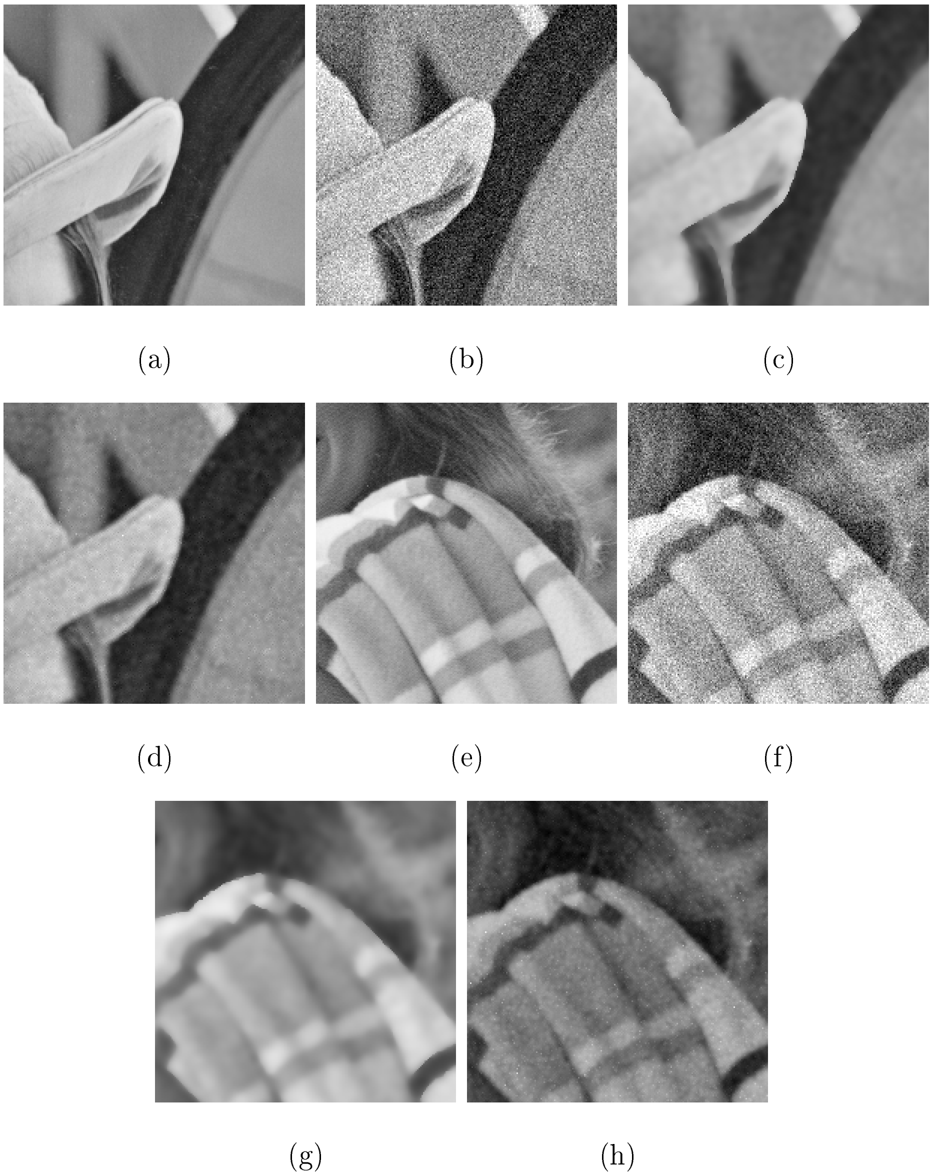

Figure 5.5: Zoomed 200×200 part of the Lena and Elaine images: (a) Original image of Lena, (b) Noisy image perturbed by Gaussian noise ($\sigma = 25$), (c) Restoration by (PM), (d) Restoration by (VE), (e) Original image of Elaine, (f) Noisy image perturbed by Gaussian noise ($\sigma = 25$), (g) Restoration by (PM), (h) Restoration by (VE).

Table 5.2: First experiment: PSNR analysis

σ	10	15	20	25	30
Input PSNR	26.66	24.5	22	20.2	18
Method		Lena (512×512)			
(PM)	28.14	27.40	26.73	26.00	25.15
(VE)	30.00	29.33	28.37	27.08	25.94
Input PSNR	28	24.6	22	20.27	18.7
Method		Boats (512×512)			
(PM)	29.45	28.00	27.12	25.64	24.15
(VE)	30.49	28.42	27.25	26.32	25.02
Input PSNR	28	24.6	22	20.19	18.6
Method		Elaine (512×512)			
(PM)	29.11	28.50	26.73	25.94	23.61
(VE)	30.98	30.19	28.41	28.00	26.08
Input PSNR	28	24.6	22	20.19	18.6
Method		Baboon (512×512)			
(PM)	28.44	24.91	22.62	22.57	21.75
(VE)	29.02	25.92	24.07	22.87	22.34
Input PSNR	28.24	24.88	22.49	20.69	19.23
Method		Lady (256×256)			
(PM)	32.06	30.29	28.46	28.00	27.04
(VE)	32.14	30.78	29.35	27.85	25.76
Input PSNR	28.24	24.7	22.27	20.3	18.78
Method		Zebra (256×256)			
(PM)	29.64	26.83	24.63	22.05	19.95
(VE)	28.00	25.45	22.57	21.45	19.00

In Table 5.2 $PSNR$ analysis for the six images of Figure 5.4 with the variance of noise from 10 to 30 is given. The values of the table shows that the proposed method performs more or less in the same manner. In fact for the images from Figure 5.4.(a) to Figure 5.4.(e) the values of $PSNR$ for the purposed method are slightly larger then the (PM) model. For the image of zebra (PM) model has values of $PSNR$ larger than (VE) model.

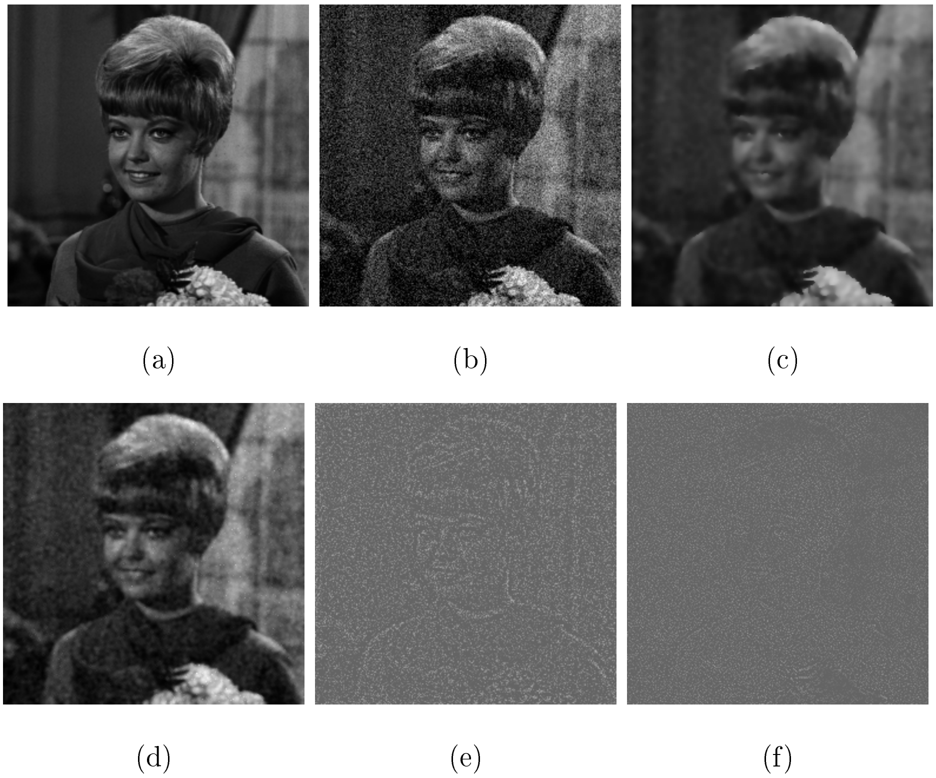

Figure 5.6: Analysis of Lady image: (a) Original image of Lady, (b) Noisy image perturbed by Gaussian noise ($\sigma = 25$), (c) Restoration by (PM), (d) Restoration by (VE), (e) Residual to (PM) restoration, (f) Residual to (VE) restoration.

Consider the image of Lady (Figure 5.4.(e)) perturbed by an additive Gaussian noise of variance $\sigma = 25$ for further investigation. Notice that the size of the image is 256×256 and in Figure 5.6, we provide original image (Figure 5.6.(a)), noisy image (Figure 5.6.(b)), restored images by (PM) and (VE) in (Figure 5.6.(c)-Figure 5.6.(d)), respectively. Figure 5.6.(e) and Figure 5.6.(f) are the residual to (PM) model and (VE) model with the noisy image, i.e, Residual = Noisy image – restored image. The residual figure 5.6.(e) contain more structure part of the image as compare to the figure 5.6.(f), which also hints that the denoising by proposed (VE) method is structure preserving.

Second experiment:
As in the previous discussion of SNR and $PSNR$ for (PM) and (VE), keep very close one to each other, the efficiency of our approach seems to be based on no more than an optical evidence. However, we will show that the efficiency of our approach is more than optical, and to this end, we will consider images where the texture plays a crucial role, and where the restoration procedures can be stressed.

The images we consider in these experiments are a 250×250 size image of wood (Figure 5.7. (a)), and a 512×512 size naive image (Figure 5.7. (e)), both strongly perturbed with gaussian noise (ratios $SNR = 0.014$ and $PSNR = 12$, see Figure 5.7. (b), $SNR = 0.054$ and $PSNR = 16.2$, see Figure 5.7.(f), respectively). In these kind of images, the texture turns out to be more important than edges preservation, and among the numerical results in Table 3, a simple overview shows the goodness of our approach vs. (PM).

However, to be more precise in our analysis, Table 5.3 shows a numerical evidence of the efficiency of our method; in fact it must be highlighted that SNR and $PSNR$ are improved by using (VE) in comparison with (PM).

Table 5.3: Second experiment (textured images).

	SNR	PSNR	Figure
(PM)	1.8	12.1	Fig. 5.7.(c)
(VE)	4	14.4	Fig. 5.7.(d)
(PM)	5	21.2	Fig. 5.7.(g)
(VE)	6.8	22.6	Fig. 5.7.(h)

5.7 Conclusions and outlook

In the present work, we propose a partial differential equation based approach to image processing (filtering, denoising, enhancing,...) whose main novelty is that it fits into the framework of fractional calculus (derivatives and integrals) hence Volterra equations.

The interest of our work is two fold: On the one hand, the model we propose allows us to handle the smoothing by means of certain "viscosity" parameters which define the matrix–valued linear Volterra equation we propose. In other words, the smoothing is now handled by means of a linear partial equation, i.e., without introducing tricky nonlinear terms in the equation as many authors propose.

On the other hand, the model we propose fits into a closed mathematical setting, both from the analytical and the numerical point of view. To be more precise, the well–posedness of the Volterra equation we propose is as we said guaranteed all over the whole positive real line on the contrary what typically happens with non–linear

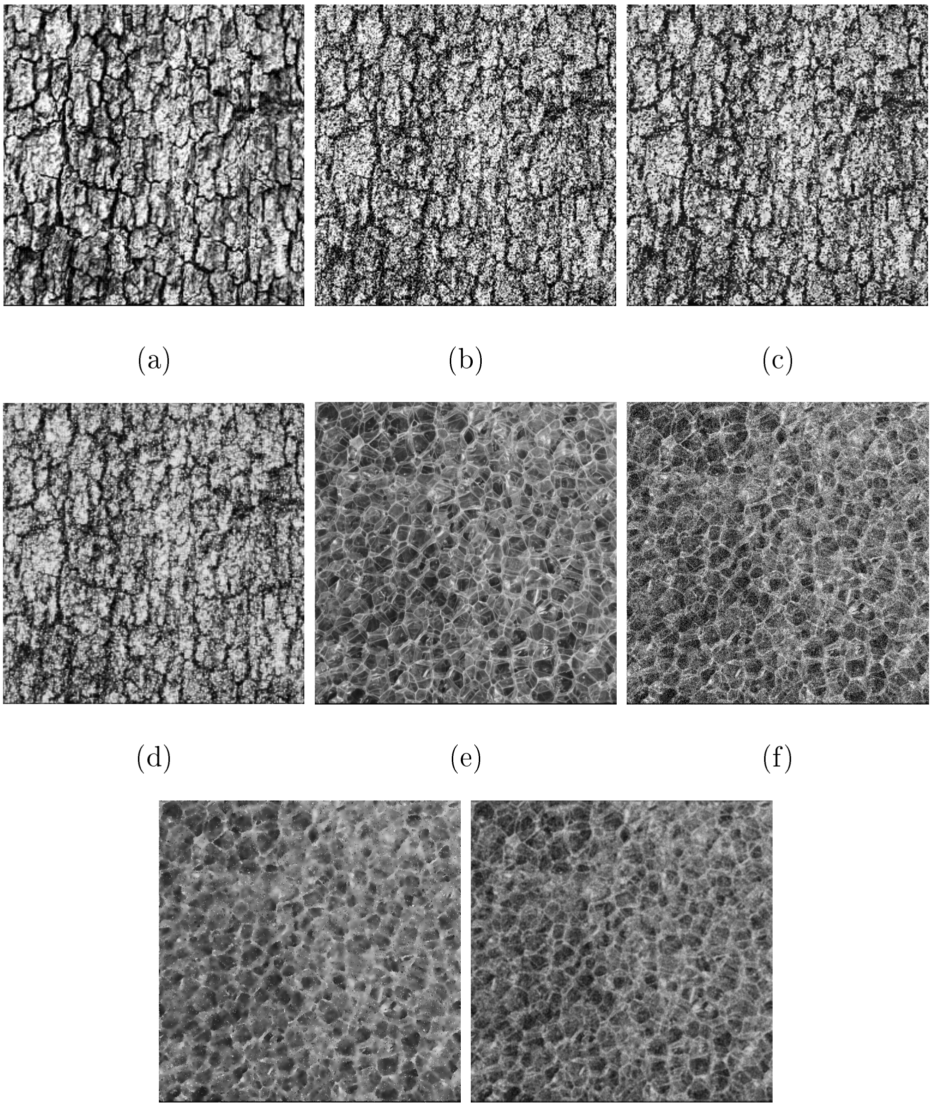

(a) (b) (c)

(d) (e) (f)

(g) (h)

Figure 5.7: Images for the second experiment. Denoising of textured images: (a) Original image of wood, (b) Noisy image perturbed by gaussian noise, (c) (PM), (d) (VE) (e) Original naive image, (f) Noisy image perturbed by gaussian noise, (g) (PM), (h) (VE).

models, and numerical methods for its discretization have been largely studied in the literature.

As an additional interesting property of our proposal is that one can change the *profile* of the filter merely by changing the “viscosity" parameters setting, i.e., the distribution function we use. This allows the user to adapt easily the filter to each single image according to its characteristics.

On the improvement of Volterra equation based filtering for image denoising

Purpose of the paper:

The purpose of the paper [23] is to improve the image denoising model proposed in Chapter 3. The image denoising process has been controlled by the order of fractional derivative in time (linear heat equation). We want to improve the process of determination of order of fractional derivative, which decides the nature of the filter by the linear heat equation with fractional derivative in time.

The problem:

It is difficult to distinguish between the noise and the feature of the image to be preserved. The assignment of order of fractional derivative is an important step in the model proposed in Chapter 3. Some efficient techniques are required to get a better denoising results.

Strategy:

We propose an alternative choice for determination of order of fractional derivative in time by using structure tensor of image. The assignment of the order of fractional derivative has been made by the fact that the eigenvalues are higher on the edges, texture like features as compare to uniform region. The experiments show the improvement in the proposed model visually and in terms of SNR and PSNR.

CHAPTER 6

On the improvement of Volterra equation based filtering for image denoising

Abstract

This paper presents a simple but effective approach for the removal of additive white Gaussian noise from digital images. In our approach, a generalization of a linear heat equation, obtained by replacing time derivative to a fractional time derivative of order between 1 and 2 has been used and a pixel by pixel technique applied. The choice of order of fractional time derivative has been made for each pixel by using *structure tensor* of image, which allows us to control the diffusion process without introducing nonlinearities in equation as in classical approaches. The proposed model is well posed and numerical scheme adopted is stable. Several experiments showing improvement of our approach visually and in terms of SNR, $PSNR$ are also provided.

Keywords: Fractional integrals and derivatives, Volterra equations, Structure tensor, Convolution quadrature methods.

MSC [2010]: 44A35, 44K05, 45D05, 65R20, 68U10, 94A08.

Contents

6.1 Introduction

Among several techniques available, for digital image processing (filtering, denoising, restorations, segmentation, edge enhancement/detection,...), partial differential equations based techniques are one of them, which have been largely studied in the literature (see [114] and references therein). It is well known in signal processing that the convolution of a signal with a Gaussian kernel acts like a low pass filter. The convolution of the signal with a Gaussian is equivalent to computing the solution of the linear heat equation

$$\begin{cases} \partial_t u(t,x) &= \Delta u(t,x), & (t,x) \in [0,T] \times \Omega, \\ u(0,x) &= u_0(x), & x \in \Omega, \\ \dfrac{\partial u}{\partial \eta}(t,x) &= 0, & (t,x) \in [0,T] \times \partial\Omega, \end{cases} \tag{6.1}$$

where Δ denotes the two–dimensional Laplacian, in case of images $\Omega \subset \mathbb{R}^2$ is typically a square domain, $\partial\Omega$ represents the boundary of Ω, $\partial/\partial\eta$ stands for the outward normal derivative, and u_0 the original image. The effect of equation (6.1), on digital images is isotropic, which yields loss of information about edges, textures and corners in practical applications of image restoration (denoising).

An anisotropic model seems to be a suitable approach to guarantee an edge preserving restoration (denoising). This approach was initially proposed by Perona and Malik in [91]; it reads

$$\begin{cases} \partial_t u(t,\mathbf{x}) &= \operatorname{div}\left(c(|\nabla u(t,\mathbf{x})|^2)\nabla u(t,\mathbf{x})\right), (t,\mathbf{x}) \in Q, \\ u(0,\mathbf{x}) &= u_0(\mathbf{x}), \qquad \mathbf{x} \in \Omega, \\ \dfrac{\partial u}{\partial \eta}(t,\mathbf{x}) &= 0, \qquad \partial\Omega, \end{cases} \tag{6.2}$$

for $(t,\mathbf{x}) \in Q = [0,T] \times \Omega$. The diffusion coefficient $c : [0,+\infty) \to [0,+\infty)$, is chosen to preserve the edges and corners meanwhile smooths the uniform regions. Therefore, diffusion coefficient c, defined such that it has values close to zero where we want to preserve the information of the image (normally near edges, corners etc where gradient values of pixels are large). On the contrary, c should be large in pixels with low gradient variation. The choice of such functions lead to backward–forward parabolic problems that are ill–posed (see [61]). But, the implementation of Perona-Malik model doesn't reveal any such property of unstability. The reason as reported by H. Amman [4] is that the numerical scheme used by Perona and Malik does not correspond to their equation but rather to a time–regularized one which is well–posed.

There is a need of regularization of Perona-Malik model such that new model inhibits the same practical results but lying in a *reasonable* functional space setting where the well–posedness can be guaranteed as well as the bounded variation and further analytical and numerical properties. In this regard, several perturbed models proposed (see e.g., [16, 57, 58, 44]).

In this paper, we consider a recent work of authors (see [22]), in which a linear Volterra matrix–valued equation, obtained by pixel by pixel technique has been proposed for image denoising. Volterra matrix–valued equation is a generalization of Volterra equation

$$u(t) = u_0 + \partial^{-\alpha} A u(t), \tag{6.3}$$

where $\partial^{-\alpha}$ is the Riemann–Liouville fractional integral of order $1 < \alpha < 2$. The value of α (between 1 and 2) for each pixel is obtained by a viscosity parameter (defined in [22]). The profile of the viscosity parameter determines the diffusion process on the images, furthermore changing the profile of the viscosity parameter can change the nature of the filter proposed in [22].

The contribution of the present work is the proposal of an alternative approach for the selection of α for each pixel, i.e, a different profile for the viscosity parameter is proposed using the structure tensor of image. Previously, viscosity parameter (see [22]) allows us to handle the diffusion, as it exploits the nature of Volterra equation (6.3), which interpolates the linear heat equation and the linear wave equation (see [33]), for image denoising. Since the choice of α controls the diffusion process so the choice of α is crucial in implementation of the algorithm. The proposed method for choosing α, using structure tensor plays an important role and improve the results as seen in section (5.5). Well–posedness results, and a large variety of numerical discretizations of the proposed model have been closely studied by many authors, and therefore they are at our disposal for the experiments (see [97, 77, 78] and references therein).

The rest of the paper is organized as follows: the next section presents the main idea of the paper i.e., selection of values of $1 < \alpha < 2$ for each pixel by using structure tensor of the image. In section 6.3 we provide the generalized matrix valued Volterra equation and its discritization in space and time. Section 6.4 illustrates the implementation of the proposed model and we provide some practical examples. Finally, section 6.5 concludes the work of this paper.

6.2 Volterra equations

The fractional calculus in image denoising has been firstly proposed in [21], where a generalization of the heat equation (6.1) is proposed which reads

$$\begin{cases} \partial_t^\alpha u(t,\mathbf{x}) &= \Delta u(t,\mathbf{x}), & (t,\mathbf{x}) \in [0,T]\times\Omega \\ u(0,\mathbf{x}) &= u_0(\mathbf{x}), & \mathbf{x}\in\Omega, \\ \dfrac{\partial u}{\partial \eta}(t,\mathbf{x}) &= 0, & (t,\mathbf{x}) \in [0,T]\times\partial\Omega, \end{cases} \tag{6.4}$$

where ∂_t^α stands for the Riemann–Liouville fractional time derivative of order $1 < \alpha < 2$; for an integrable function f is given by (see [62])

$$\partial_t^\alpha f(t) := \frac{1}{\Gamma(2-\alpha)}\frac{d^2}{dt^2}\int_0^t \frac{f(\tau)}{(t-\tau)^{\alpha-1}}d\tau. \tag{6.5}$$

The equation (6.4) is equivalent to the Volterra equation

$$u(t,\mathbf{x}) = u_0(\mathbf{x}) + \partial^{-\alpha}\Delta u(t,\mathbf{x}), \tag{6.6}$$

with homogeneous Neumann boundary condition along with $\partial_t u(0,\mathbf{x}) = 0$ and in equation (6.6), $\partial^{-\alpha}$, for $\alpha > 0$, stands for the Riemann–Liouville fractional integral of order $\alpha \in \mathbb{R}^+$ (see [62]) defined by

$$\partial^{-\alpha} f(t) := \frac{1}{\Gamma(\alpha)} \int_0^t \frac{f(\tau)}{(t-\tau)^{1-\alpha}} d\tau, \quad t > 0. \tag{6.7}$$

The main contribution of this work comes out as an alternative approach for the choice of α for each pixel. The choice of α proposed in [22], by using viscosity parameter, leaves some isolated pixels (see section 5.5) in the restored images. This is because, the noise plays its part while getting the value of α by viscosity parameter. Here, we use structure tensor (see [114]) for getting the eigenvalues of the image and use the well known fact that the eigenvalues near the edges, corners are greater than the eigenvalues of the smooth regions. This fact allows us to assign the value of α near 2 to the pixels which have large eigenvalues and 1 to contrary.

The structure tensor has been used for identifying several structures in images such as texture like flow, corners, T junctions etc, is defined as

$$J_\rho(\nabla u_\sigma) := K_\rho \star (\nabla u_\sigma \otimes \nabla u_\sigma) \qquad \rho \geq 0, \tag{6.8}$$

where K_ρ is the Gaussian kernel, $\star$ represents the convolution operator in space variable, $\nabla u_\sigma \otimes \nabla u_\sigma := \nabla u_\sigma \nabla u_\sigma^t$, ρ is the integration scale, σ is called local or noise scale. It is easy to calculate the expressions for eigenvectors and eigenvalues associated with structure tensor, for more details see [114]. The eigenvalues of the structure tensor provides us information about the edges corners of image, so the choice of α made as described above.

6.3 Space and time discretizations

Before we start spatial discretization of Laplacian, it is worthwhile to notice that $u(t, \mathbf{x})$ is transformed into a $MN \times 1$ vector–valued function $\mathbf{u}(t)$ whose components stand for the vector–arranged image pixels at time level t (M is length and N is the width of the image). Without loss of generality let $M = N$, for discretization of Laplacian in (6.4), a central difference scheme with a step size $h > 0$ has been considered. So, Δ transforms into a $M^2 \times M^2$ five–diagonals sparse matrix Δ_h, with the number of nonzero elements, $5M^2 - 4M$. The sparse nature of discretized Laplacian Δ_h is helpful in implementation as we store only nonzero elements for Δ_h, which makes algorithm robust when applied.

The equation (6.6), applied for the choice of α, for each pixel reads now as the linear Volterra matrix–valued equation given by

$$\mathbf{u}(t) = \mathbf{u}_0 + \int_0^t \mathbf{K}(t-s)\mathbf{u}(s)\,\mathrm{d}s, \qquad 0 \leq t \leq T, \tag{6.9}$$

where $\mathbf{u}_0$ is the initial image, and the convolution kernel $\mathbf{K}$ is defined as

$$\mathbf{K}(t) = I(t) \cdot \Delta_h$$

with $I(t)$ be diagonal matrix with diagonal entries $t^{\alpha_i}/\Gamma(\alpha_i+1)$ for $i=1,2,...,M^2$ and for each i, $1<\alpha_i<2$. Let us notice that $\mathbf{K}$ is a five–diagonal matrix valued function and, since the Laplace transform of $\mathbf{K}$ exists, the well–posedness of (6.9) is then guaranteed (see e.g., [97]).

For the time discretizations of Volterra equation (6.9), Runge–Kutta convolution quadrature method has been adopted, which provide high order numerical methods jointly with good stability properties. These methods have been studied extensively in literature, e.g., the convolution quadrature based methods (see [77, 78] and references therein).

Let $\tau>0$ be the time step of the discretization and $\mathbf{u}_n$ be the approximation of $\mathbf{u}(t_n,\mathbf{x})$, for $n\geq 0$. Then the discretization of (6.9) by means of the backward Euler convolution quadrature method reads

$$\mathbf{u}_n=\mathbf{u}_0+\sum_{j=1}^{n}\mathbf{Q}^{(\alpha)}_{n-j}\mathbf{u}_j,\quad n\geq 1,$$

where, $\mathbf{Q}^{(\alpha)}_j$ is a $M^2\times M^2$ diagonal matrix for each $j=0,1,2,\ldots$, containing convolution quadrature weights. The entries of $\mathbf{Q}^{(\alpha)}_j$ are given by $\binom{\alpha_i}{j}$, $i=0,1,2,\ldots,M^2$ (see [22] and reference therein, for more details). Since the matrix Δ_h is not singular, the unique n-th approximation is reached by solving the linear system

$$\left(I-\mathbf{Q}^{(\alpha)}_0\right)\mathbf{u}_n=\mathbf{u}_0+\sum_{j=1}^{n-1}\mathbf{Q}^{(\alpha)}_{n-j}\mathbf{u}_j,\quad n\geq 1. \tag{6.10}$$

6.4 Implementation and practical results

In discrete setting, for an efficient implementation of (6.10), some facts must be considered. For $\alpha=1$ and $\alpha=2$, singularities may occur from the numerical point of view. In order to avoid these possible singularities for practical purposes, we set $\alpha_j\in[1+\varepsilon,2-\varepsilon]$ with $\varepsilon=10^{-3}$ for $j=1,2,\ldots,M^2$.

For each α_j, a fixed number of convolution quadrature coefficients has been computed. Moreover, the practical computation of that weights has been carried out by means of the Fast Fourier Transform as in [14]. From a computational point of view, the number of different values of α's should be limited, otherwise if one admits number of α's as large as the number of pixels, the implementation becomes unavailable in practical cases.

The quality of processed image has been obtained by calculating signal to noise ratio(SNR) and peak signal to noise ratio($PSNR$). The formula used for the SNR is

$$SNR=10\cdot\log_{10}\left(\frac{\mathrm{var}(I)}{\mathrm{var}(I-R)}\right),$$

where R is the restored image, I is an ideal image, $\mathrm{var}(x)$ stands for the variance of the vector x. The formula for $PSNR$ used is defined as

$$PSNR = 10 \cdot \log_{10}\left(\frac{\sum_{i,j} 255^2}{\sum_{i,j}(I_{i,j} - R_{i,j})^2}\right),$$

where $I_{i,j}$, $R_{i,j}$ are the pixel values of I and R respectively.

(a)

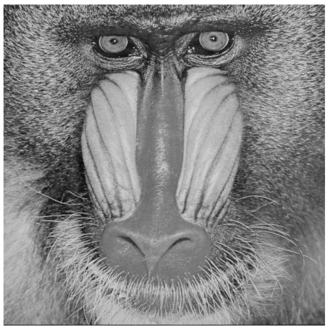

(b)

(c)

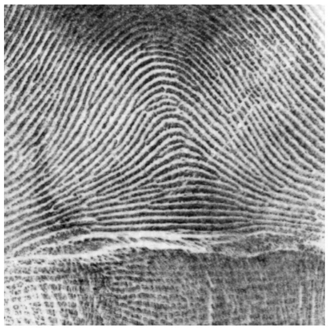

(d)

Figure 6.1: Original image of (a) Barbara, (b) Baboon, (c) Boats, (d) Fingerprint.

We show some experiments where a noisy image is evolved by using the Volterra equation method (viscosity parameter for the choice of α) as in [22] (VEV), Perona–Malik model (6.2) with $c(s) = \mathrm{e}^{-s}$ (PM) and the contrast parameter (λ) is chosen such that $1.5 * \sigma < \lambda < 2 * \sigma$ as suggested in [39] (where σ is the noise variation) and the model (6.9), with structure tensor method for choice of α (VES).

All the four images used for the experiments are of size 512×512, i.e., on the spatial domain $\Omega = [0, 511] \times [0, 511]$ and are shown in Fig 6.1.(a-d). For all images, original (ideal) image has been perturbed by Gaussian white noise of variance ranging from 10 to 35 and resulting noisy images used as input for the evolution process of the three methods. In table 6.1, we show the noise level in terms of SNR, for the restoration of the noisy images yielded out with the above mentioned procedures. Notice that the proposed method (VES) has the best SNR

(in decibels) for all the four images. Table 6.2, shows noise level of the processed images as a function of $PSNR$ (in decibels) level of the input noisy image, as in case of SNR for all four images the proposed method (VES) outperforms the (PM) and (VEV) denoising process.

Table 6.1: SNR analysis

σ	10	15	20	25	30	35
Input SNR	14.74	11.25	8.79	6.90	5.38	4.10
Method	Barbara (512×512)					
(PM)	17.00	14.00	12.25	10.85	10.27	9.7
(VEV)	16.72	14.16	12.00	10.5	9.78	9.60
(VES)	17.31	15.20	13.95	11.85	10.80	10.30
Input SNR	14.00	10.60	8.20	6.30	4.80	3.50
Method	Fingerprint (512×512)					
(PM)	14.80	11.97	10.26	9.10	7.90	8.15
(VEV)	15.00	11.40	10.9	9.50	9.3	8
(VES)	17.00	15.11	13.60	12.59	11.80	10.52
σ	10	15	20	25	30	35
Input SNR	13.30	9.88	7.40	5.50	4.00	2.70
Method	Boats (512×512)					
(PM)	15.07	13.69	12.26	11.57	9.72	9.74
(VEV)	15.74	14.10	12.65	11.32	10.32	9.42
(VES)	16.84	14.88	13.50	12.52	11.81	10.69
Input SNR	12.50	9.00	6.50	4.50	3.00	1.78
Method	Baboon (512×512)					
(PM)	13.42	10.09	8.34	7.27	6.15	5.51
(VEV)	12.88	10.29	8.51	7.49	6.89	6.34
(VES)	13.87	11.01	9.50	8.52	7.65	7.28

The visual inspection for the images of Barbara, boats and fingerprint has been made in Figure 6.2 and Figure 6.3 by considering a zoomed small part of the restored images. The part of Barbara's image of size 100×100 is considered (Figure 6.2(a)). The noisy image with $\sigma = 30$ has been evolved by the three process (PM), (VEV) and (VES) (the proposed method). The zoomed part of noisy image is given in (Figure

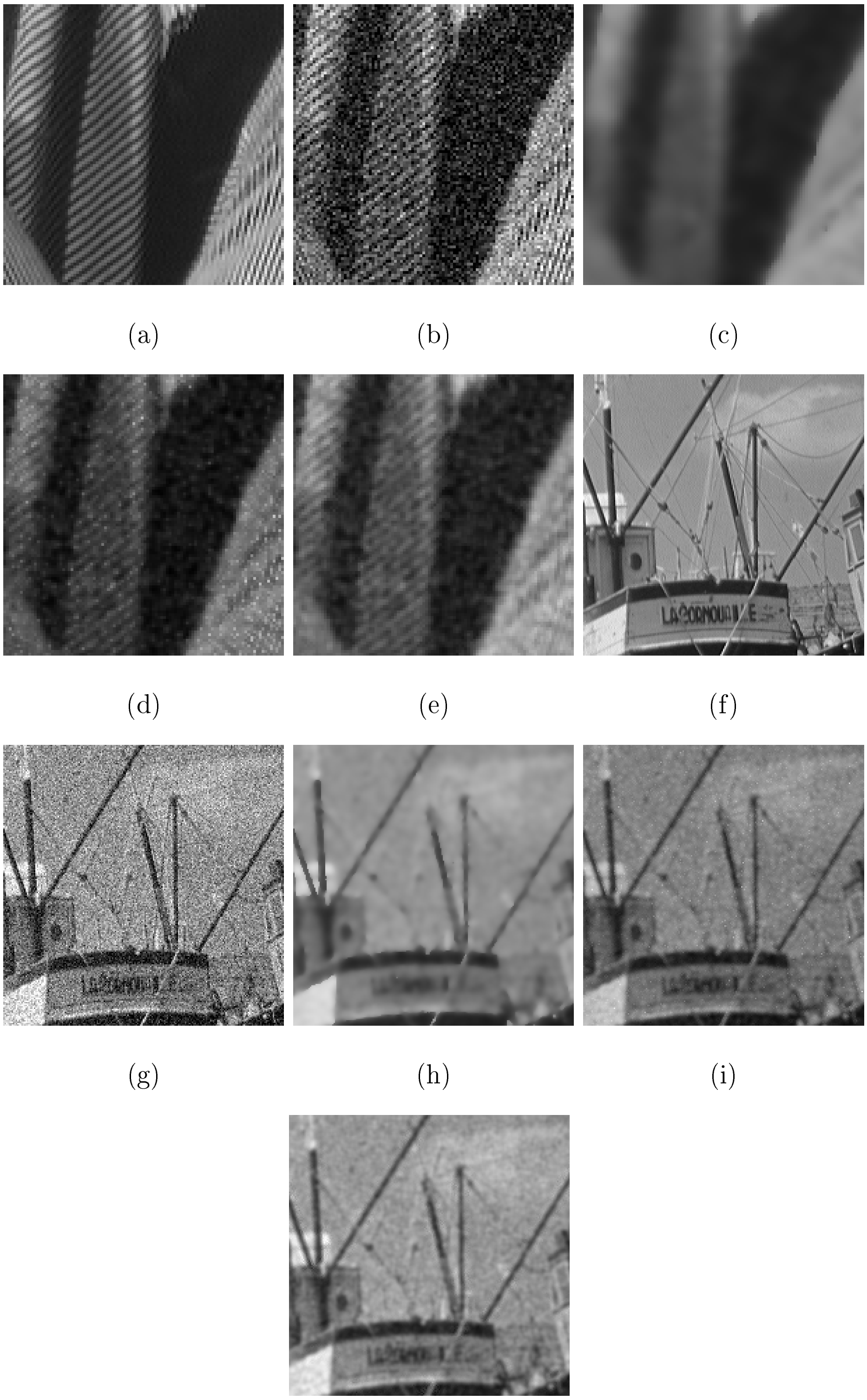

Figure 6.2: (a) 100×100 zoomed part of original Barbara's image, (b) Zoomed part of Barbara's noisy image ($\sigma = 30$), (c) Restored zoomed part by (PM), (d) Restored zoomed part by (VEV), (e) Restored zoomed part by (VES), (f) 200×200 zoomed part of original Boats's image, (g) Zoomed part of Boats's noisy image ($\sigma = 30$), (h) Restored zoomed part by (PM), (i) Restored zoomed part by (VEV), (j) Restored zoomed part by (VES).

Table 6.2: $PSNR$ analysis

σ	10	15	20	25	30	35
Input PSNR	28.12	24.6	22.18	20.29	18.76	17.50
Method			Barbara (512×512)			
(PM)	30.14	26.40	24.60	23.10	22.00	20.54
(VEV)	30.00	27.33	25.08	24.03	23.15	21.26
(VES)	32.00	28.76	26.37	25.00	24.34	23.74
Input PSNR	28.13	24.6	22.2	20.3	19	17
Method			Fingerprint (512×512)			
(PM)	28.81	25.91	24.21	23.05	21.87	20.01
(VEV)	29.17	27.33	25.37	24.00	22.42	20.9
(VES)	31.23	29.01	27.62	26.60	25.8	24.5
σ	10	15	20	25	30	35
Input PSNR	28	24.6	22	20.27	18.7	17.10
Method			Boat (512×512)			
(PM)	29.45	28.00	27.12	25.64	24.15	23.48
(VEV)	30.49	28.42	27.25	26.32	25.02	23.43
(VES)	31.57	29.61	28.14	27.05	25.08	24.00
Input PSNR	28	24.6	22	20.19	18.6	17.18
Method			Baboon (512×512)			
(PM)	28.44	24.91	22.62	22.57	21.75	20.46
(VEV)	29.02	25.92	24.07	22.87	22.34	20.82
(VES)	28.38	25.08	24.05	23.62	22.58	21.67

6.2.(b)) the restoration by (PM) model Figure 6.2.(c) removes the noise by losing the structure of the image. Notice that (PM) very strongly smooths the regions of small pixel value variations corresponding to texture of image, hence losing information regarding texture and structure of the image whereas the denoising results obtained by (VEV) and (VES) preserves the structure of the image. For the image of boats (with $\sigma = 30$), a part of size 200×200 has been zoomed for the visual inspection, the original and noisy images are given in Figure 6.2.(f-g). Notice that (PM) model (Figure 6.2.(h)) not only smooths the region of small variation but also creates the artifact (staircase effect) at the edges. The restoration by (VEV) (Figure 6.2.(i)) doesn't create any staircase effect on edges but leaves some isolated pixels, where as the restoration by the proposed method (VES) (Figure 6.2.(j)) removes the noise by preserving the structure (texture) of the image and without leaving any isolated pixel and without creating any artifacts.

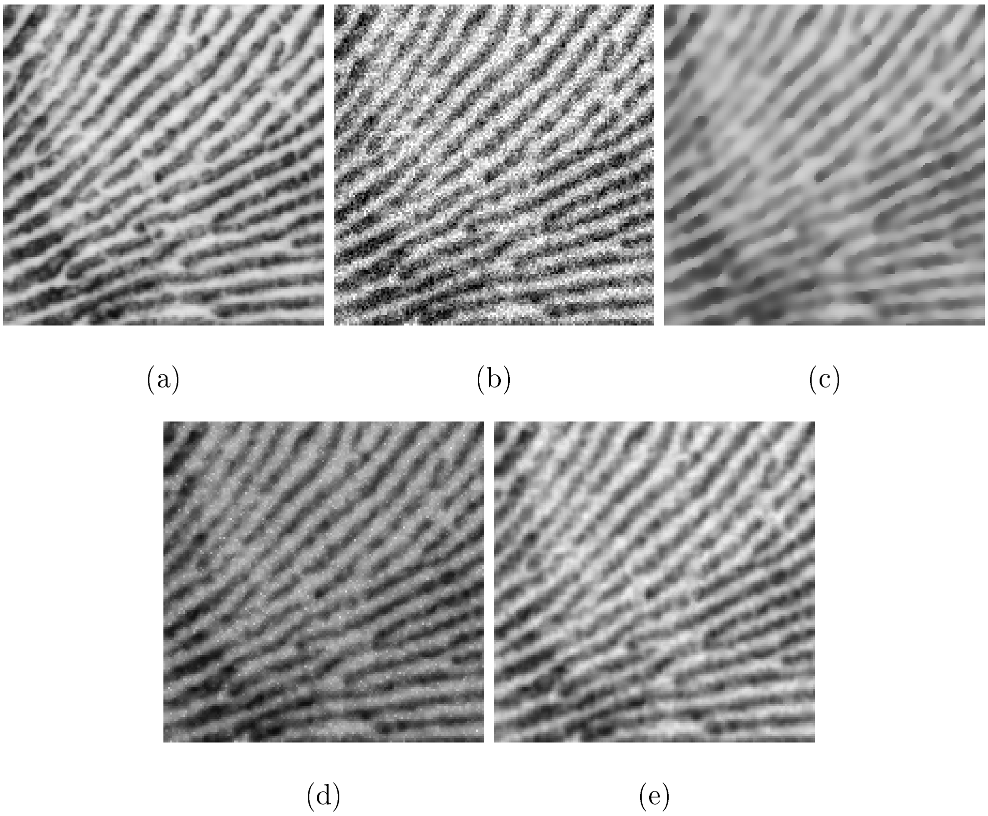

Figure 6.3: (a) 150×150 part of Fingerprint's original image, (b) Zoomed part of Fingerprint's noisy image ($\sigma = 30$), (c) Restored zoomed part by (PM), (d) Restored zoomed part by (VEV), (e) Restored zoomed part by (VES).

It has been reported in [22] that the Volterra equation (Eq. (9)) based filtering removes the noise by preserving the structure of the images and hence works well for the images where texture plays an important role, i.e., textured images. For this we consider the image of fingerprint (Figure 6.1.(d)) and a zoomed part of 150×150 has been investigated for the restoration process (Figure 6.3. (a)-(e)). The restoration by (PM) (Figure 6.3.(c)) as observed for the previous examples creates artifacts at edges and restoration by (VEV) (Figure 6.3.(d)) leave some isolated pixels. The proposed method (VES) (Figure 6.3.(e)) not only outperforms the two methods (PM), (VEV) visually but also in terms of SNR and $PSNR$.

In Figure 6.4.(a) we present the plot of SNR values of first 35 iterations for the restoration of a noisy image of Barbara ($\sigma = 25$) by (VEV) and (VES). Figure 6.4.(b) shows the plot of SNR values of first 45 iterations for the denoising (restoration) process of Baboon's image ($\sigma = 30$) by (VEV) and (VES). From both figures the improvement of the proposed method is evident. The difference of optimal stoping

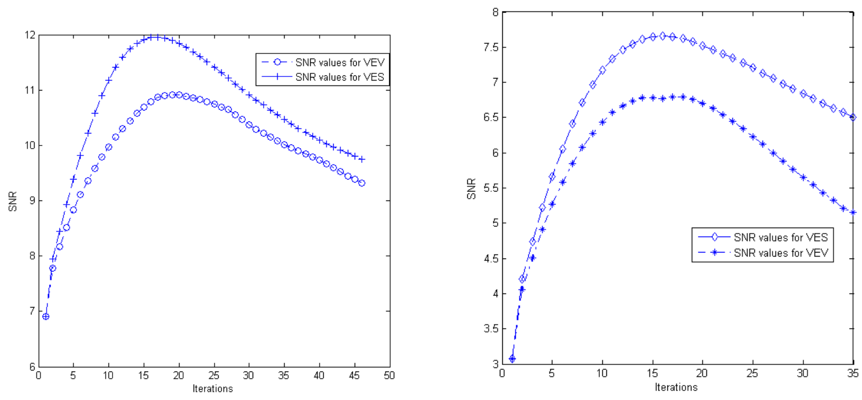

(a) (b)

Figure 6.4: (a) SNR values for the first 35 iterations of (VEV) and (VES) for the noisy image of Barbara with $\sigma = 25$, (b) SNR values for the first 45 iterations of (VEV) and (VES) for the noisy image of Baboon with $\sigma = 30$.

time for nonlinear and linear models restrict us to include SNR values for (PM) in the plots of Figure 6.4 (see [87]).

6.5 Conclusion and future work

We have presented a novel approach for image denoising in the framework of fractional calculus using linear heat equation with fractional derivative in time of order $1 < \alpha < 2$, which is equivalent to matrix–valued Volterra equation. The assignment of α for each pixel of the image, explores the fact that large eigenvalues occur for edges and corner, where as structure tensor of the image has been used for getting the eigenvalues of the image. The practical results show improvements visually and in terms of SNR, $PSNR$ when compared to the nonlinear Perona-Malik model and the model already proposed by authors in [22]. The proposed model is linear and well–posed. The numerical scheme used in discretization is convergent and preserves positivity of the solution. The extension of this work to the nonlinear models, involving structure tensor or fractional Laplacian (as nonlinearity in the model) will be the topic of our forthcoming papers.

CHAPTER 7

Conclusion and perspectives

In this chapter, we conclude the thesis by presenting

- the contributions of the work carried out over the period of this thesis
- a glimpse on the perspective and future directions of the work.

7.1 Contributions

This thesis just unfold some of the problems concerning the nonlinear fractional differential equations, inverse problems involving fractional derivative in time and applications of fractional derivative (integrals) based models to image processing.

The contributions of the thesis falls into three categories.

- *The profile of blowing-up solutions:*
  For the nonlinear system of fractional differential equations (FDS), we propose a method for getting the estimates from above and below for the solution of the nonlinear system (FDS) via properties of Mittag-Leffler function and integral equations. The method can be easily extended to more general systems. Let us provide the American Mathematical Society review about our paper "The profile of blowing-up solutions to a nonlinear system of fractional differential equations".

  "In this paper the authors study the profile of blowing-up solutions to a nonlocal fractional dynamical system. The Riemann-Liouville fractional derivative is used. The authors use a new approach and innovative methods, relying on comparisons of the solution to the original system with solutions of subsystems obtained by dropping either the usual derivatives or the fractional derivatives, to prove the main theorems and lemmas. Finally, an algorithm for the numerical approximation of solutions to fractional dynamical systems is given".

- *Inverse problem of fractional diffusion equation:*
  For a linear heat equation with fractional derivative of order $0 < \alpha < 1$ in time, the inverse problem of finding the source term and temperature distribution is addressed. The method we propose gives the analytical results about the uniqueness and existence of the inverse problem. The inverse problems for fractional differential equations is a new field and there is no general technique to tackle these problems. As expected the proposed method could handle a limited class of problems.

- *Image structure preserving denoising: A framework within fractional calculus*

  A simple but effective approach for the removal of additive white Gaussian noise from digital images has been presented whose main novelty is that it fits into the framework of fractional calculus (derivatives and integrals).

  Among several features of our approach let us mention the two main contribution of our work on image denoising: firstly, the model we propose allows us to handle the smoothing by means of order of fractional derivative in linear heat equation (we call it "viscosity" parameters), i.e., the denoising (diffusion) is handled by means of a linear partial differential equation without introducing nonlinear terms in contrast to classical approaches.

  Secondly, the model we propose fits into a closed mathematical setting, both from the analytical and the numerical point of view. As an additional interesting property of our proposal is that one can change the *profile* of the filter merely by changing the “viscosity" parameters setting, i.e., the distribution function we use (as we have seen in chapter 6). This allows the user to adapt easily the filter to each single image according to its characteristics.

7.2 Perspectives

We have devised a method for getting the profile of solutions to a nonlinear system of fractional differential equations. The question of extension of the study to the reaction diffusion equations with different nonlinearities and with space and time fractional derivatives would be an interesting topic. It is well known that the order of fractional time derivative in fractional diffusion equation has been used to explain the anomalous diffusion. A very interesting question is the determination of the order of fractional time derivative with some given data. Apart from that the inverse problems for the fractional differential equations is a new field and has many attractive and important questions just as extension of the inverse problems of partial differential equations.

The extension of the proposed model for image denoising (for gray scale images) to the colored images treating the three channels of the colored image in a single framework by considering the three channels as a vector field is desired. It is also interesting to extend the method for matrix valued data such as we have in magnetic resonance images used in medical science.

Appendix A

Appendix

A.1 The Profile of blowing-up solutions to a nonlinear system of fractional differential equations

The proof of formula (2.13) is

Proof. By definition

$$D^{\alpha}_{T_-}\varphi(t) = \frac{-1}{\Gamma(1-\alpha)}\frac{d}{dt}\int_t^T \frac{T^{-\lambda}(T-\tau)^{\lambda}}{(\tau-t)^{\alpha}}d\tau. \tag{A.1}$$

Since

$$\frac{d}{dt}(T-t)^{\lambda} = -\lambda(T-t)^{\lambda-1} \text{ and } \varphi(T)=0.$$

Using (2.7), we have

$$D^{\alpha}_{T_-}\varphi(t) = \frac{\lambda T^{-\lambda}}{\Gamma(1-\alpha)}\int_t^T \frac{(T-\tau)^{\lambda-1}}{(\tau-t)^{\alpha}}d\tau. \tag{A.2}$$

By Euler change of variable

$$y = \frac{\tau-t}{T-t},$$

(A.2) becomes

$$\begin{aligned} D^{\alpha}_{T_-}\varphi(t) &= \frac{\lambda}{\Gamma(1-\alpha)}T^{-\lambda}\int_0^1 \frac{(T-t)^{\lambda-1}(1-y)^{\lambda-1}}{(T-t)^{\alpha}y^{\alpha}}(T-t)dy \\ &= \frac{\lambda}{\Gamma(1-\alpha)}T^{-\lambda}(T-t)^{\lambda-\alpha}\int_0^1 \frac{(1-y)^{\lambda-1}}{y^{\alpha}}dy. \end{aligned} \tag{A.3}$$

But the integral

$$\int_0^1 \frac{(1-y)^{\lambda-1}}{y^{\alpha}}dy = B(1-\alpha,\lambda),$$

where B is the beta function, consequently

$$\begin{aligned} D^{\alpha}_{T_-}\varphi(t) &= \frac{\lambda}{\Gamma(1-\alpha)}T^{-\lambda}(T-t)^{\lambda-\alpha}\frac{\Gamma(1-\alpha)\Gamma(\lambda)}{\Gamma(1-\alpha+\lambda)} \\ &= \frac{T^{-\lambda}(T-t)^{\lambda-\alpha}\Gamma(\lambda+1)}{\Gamma(1-\alpha+\lambda)}. \end{aligned} \tag{A.4}$$

Integration gives the required result. □

Lemma A.1.1. *Let the test function $\varphi(t)$ as defined in (2.12) and $p>1$. Then for $\lambda > p-1$*

$$\int_0^T \varphi^{1-p}(t)\left|\varphi'(t)\right|^p dt = C_p T^{1-p}, \qquad C_p = \frac{\lambda^p}{\lambda-\alpha+1}. \tag{A.5}$$

For $\lambda > \alpha p - 1$

$$\int_0^T \varphi^{1-p}(t)\left|D^{\alpha}_{T-}\varphi(t)\right|^p dt = C_{p,\alpha}T^{1-\alpha p}, \qquad C_{p,\alpha} = \frac{1}{\lambda-p\alpha+1}\left[\frac{\Gamma(\lambda+1)}{\Gamma(\lambda+1-\alpha)}\right]^p. \tag{A.6}$$

Proof. We have

$$\begin{aligned} \int_0^T \varphi^{1-p}(t)\left|\varphi'(t)\right|^p dt &= \int_0^T \left[T^{-\lambda}(T-t)^{\lambda}\right]^{1-p}\left|-\lambda T^{\lambda}(T-t)^{\lambda-1}\right|^p dt \\ &= \lambda^p T^{(-\lambda p-\lambda(1-p))}\int_0^T (T-t)^{\lambda(1-p)}(T-t)^{p(\lambda-1)}dt \\ &= \lambda^p T^{-\lambda}\int_0^T (T-t)^{\lambda-p}dt \\ &= -\lambda^p T^{-\lambda}\left[\frac{(T-t)^{\lambda-p+1}}{\lambda-p+1}\bigg|_0^T\right]dt \\ &= \frac{\lambda^p T^{1-p}}{\lambda+1-p}. \end{aligned} \tag{A.7}$$

Take the second integral for the evaluation

$$\begin{aligned}
\int_0^T \varphi^{1-p}(t)\left|D^{\alpha}_{T-}\varphi(t)\right|^p dt &= \int_0^T \left[T^{-\lambda}(T-t)^{\lambda}\right]^{1-p}\left|\frac{T^{-\lambda}(T-t)^{\lambda-\alpha}\Gamma(\lambda+1)}{\Gamma(1-\alpha+\lambda)}\right|^p dt \\
&= T^{(-\lambda p-\lambda(1-p))}\left[\frac{\Gamma(\lambda+1)}{\Gamma(1-\alpha+\lambda)}\right]^p \int_0^T (T-t)^{\lambda(1-p)+p(\lambda-\alpha)}dt \\
&= T^{(-\lambda p-\lambda(1-p))}\left[\frac{\Gamma(\lambda+1)}{\Gamma(1-\alpha+\lambda)}\right]^p \int_0^T (T-t)^{\lambda-p\alpha}dt \\
&= T^{(-\lambda p-\lambda(1-p))}\left[\frac{\Gamma(\lambda+1)}{\Gamma(1-\alpha+\lambda)}\right]^p \left[\left.\frac{(T-t)^{\lambda-p\alpha+1}}{\lambda-p\alpha+1}\right|_T^0\right]dt \\
&= \frac{1}{\lambda-p\alpha+1}\left[\frac{\Gamma(\lambda+1)}{\Gamma(1-\alpha+\lambda)}\right]^p T^{1-p\alpha}. \qquad \text{(A.8)}
\end{aligned}$$

□

For the proof of Theorem 2.3.6, we follow [89, 90]

Proof. It is assumed that blow up occurs simultaneously for each $u(t)$ and $v(t)$, so that we have

$$u(t)\to\infty, \quad v(t)\to\infty, \quad t\to T^{\alpha,\beta}_{max}<\infty,$$

for the investigation of asymptotic behavior the following transformation is considered

$$\rho=(T^{\alpha,\beta}_{max}-t)^{-1}-\rho_0, \quad \rho_0=(T^{\alpha,\beta}_{max})^{-1}, \quad w_1(\rho)=u(t), \quad w_2(\rho)=v(t).$$

The blowing up conditions becomes

$$w_j(\rho)\to\infty \quad \text{as} \quad \rho\to\infty \quad j=1,2,$$

and the Volterra equations in system (2.42) becomes

$$w_j(\rho)=\int_0^{\rho} K_j\{(\rho-\mu)[(\mu+\rho_0)(\rho+\rho_0)]^{-1}\}\Phi_j(\mu)d\mu, \quad j=1,2, \qquad \text{(A.9)}$$

where

$$K_1(t)=\frac{t^{\alpha-1}}{\Gamma(\alpha)}, \quad K_2(t)=\frac{t^{\beta-1}}{\Gamma(\beta)}, \quad \Phi_j(\rho)=(\rho+\rho_0)^{-2}F_j(w_{3-j}),$$

with $F_1(w_2)=v(t)^q$, $F_2(w_1)=u(t)^p$.

By setting $\mu=\rho\tau$ equation (A.9) becomes

$$w_j(\rho)=\rho I_j(\rho)=\rho\left(\frac{\rho}{\rho+\rho_0}\right)^{\eta_j-1}\int_0^1 (1-\tau)^{\eta_j-1}\phi_j(\rho\tau), \quad j=1,2, \qquad \text{(A.10)}$$

where $\eta_1 = \alpha$, $\eta_2 = \beta$, and ϕ_j is defined by

$$\phi_j(\rho\tau) = (\rho\tau + \rho_0)^{1-\eta_j}\Phi_j(\rho\tau), \quad j = 1, 2. \tag{A.11}$$

For asymptotic behavior of $I_j(\rho)$ as $\rho \to \infty$, Parseval formula for the Mellin transform is applied to the equation (A.10) and suitable form of the integral in equation (A.10) is obtained

$$w_j(\rho) \cong \frac{\rho}{2\pi i}\int\limits_{c-i\infty}^{c+i\infty} \rho^{-z}\mathcal{M}(K_j(\tau), 1-z)\mathcal{M}(\phi_j(\tau), z)d\tau, \quad j = 1, 2, \tag{A.12}$$

where c is the vertical path of integration in the complex plane and lies with in the strip of analyticity of the integrand.

The Mellin transform of a function $f(t)$ is defined as

$$\mathcal{M}(f(t), z) = \int\limits_0^\infty t^{z-1}f(t)dt.$$

Since

$$\mathcal{M}(K_j(t), 1-z) = \frac{\Gamma(1-z)}{\Gamma(1-z+\eta_j)},\ j = 1, 2,$$

the equation (A.12) takes the following form

$$w_j(\rho) \cong \frac{\rho^{1-z}\,\Gamma(1-z)}{2\pi i\,\Gamma(1-z+\eta_j)}\int\limits_{c-i\infty}^{c+i\infty} \mathcal{M}(\phi_j(\tau), z)\,dz, \quad j = 1, 2. \tag{A.13}$$

The advantage of writing the integral in (A.10) to the form in (A.13) is that the asymptotic behavior of the integral in equation (A.13) is determined by the asymptotic behavior of the function ϕ_j as $\rho \to \infty$.

We have

$$\phi_j(\rho\tau) = \rho^{-1-\eta_j}F_j(w_{3-j}), \quad j = 1, 2, \quad \rho \to \infty.$$

Without loss of generality we can suppose that $p_1 = q \geq p_2 = p$ and to achieve an asymptotic balance to the leading order in (A.13), assume that

$$w_j(\rho) \cong C_{j,\alpha,\beta}(\rho)^{l_j}, \quad \text{as} \quad \rho \to \infty, \quad j = 1, 2, \tag{A.14}$$

where $C_{j,\alpha,\beta},\ j = 1, 2$ and $l_1 = \delta, l_2 = \xi$ are to be determined.

It follows that

$$\phi_j(\rho) \cong C_{3-j,\alpha,\beta}^{p_j}(\rho)^{p_j\,l_{3-j}-1-\eta_j}, \quad \text{as} \quad \rho \to \infty, \quad j = 1, 2, \tag{A.15}$$

from (A.15) it can be determined that $\mathcal{M}(\phi_j(\rho), z)$ has a simple pole at $z = 1 + \eta_j - p_j\,l_{3-j}$ and

$$\mathcal{M}(\phi_j(\rho), z) \cong -\frac{(C_{3-j,\alpha,\beta})^{p_j}}{z - (1 + \eta_j - p_j\,l_{3-j})}, \quad \text{as} \quad z \to 1 + \eta_j - p_j\,l_{3-j}, \quad j = 1, 2.$$

To compute the asymptotic behavior of the integral in (A.13), the vertical path of integration is displaced to the right. In doing so the pole at $z = 1+\eta_j - p_j\, l_{3-j}$ will be encountered before that of $\Gamma(1-z)$ at $z = 1$ so the condition becomes

$$1+\eta_j - p_j\, l_{3-j} < 1, \quad j = 1, 2,$$

which ensures the leading contribution of the integrand. Thus, for (A.14) the asymptotic equality (A.13) takes the form

$$C_{j,\alpha,\beta}(\rho)^{l_j} \cong \left(\frac{(C_{3-j,\alpha,\beta})^{p_j}\Gamma(p_j l_{3-j} - \eta_j)}{\Gamma(p_j l_{3-j})} \right) \rho^{p_j l_{3-j} - \eta_j}, \quad \rho \to \infty \quad j = 1, 2$$

the asymptotic balance of the above expression gives the values of the constants, which completes the proof. □

For the proof of Theorem 2.3.7, we follow the strategy developed in [90], which can be implemented if we convert the system (PFDS) to its equivalent Volterra integral equations (2.42).

Proof. In order to transform the system (2.42) in appropriate form let $u(t) = u_0(u_1(s)+1)$, $v(t) = v_0(v_1(s)+1)$ and we made the following change of variable

$$t = \left[\frac{\Gamma(\beta)v_0^{q+1}}{\Gamma(\alpha)u_0^{p+1}} \right]^{\frac{1}{\beta-\alpha}} s, \qquad \tau = \left[\frac{\Gamma(\beta)v_0^{q+1}}{\Gamma(\alpha)u_0^{p+1}} \right]^{\frac{1}{\beta-\alpha}} \sigma.$$

The system (2.42) is transformed into

$$u_j(s) = \int_0^s K_j(s-\sigma)[u_{3-j}(\sigma)+1]^{p_j} d\sigma, \quad s > 0, \qquad j = 1, 2, \tag{A.16}$$

where

$$K_j = \gamma t^{\beta_j - 1}, \qquad j = 1, 2, \quad \text{with} \quad \beta_1 = \alpha,\ \beta_2 = \beta, \quad p_1 = q,\ p_2 = p,$$

and γ is given by (2.47).

Lower bound on the blow-up time:

In order to obtain a lower bound on the blow-up time for the integral equations (A.16), we adopt the analysis of [90]. The approach is to show that the integral operator (A.16) is a contraction for $0 \le s \le t^*$ provided that

$$I(t^*) \le \frac{M}{(M+1)^r}, \qquad I(t^*) \le \frac{1}{r(M+1)^{r-1}}, \tag{A.17}$$

for continuous functions $u_j(s)$, $0 \le u_j(s) \le M < \infty$, $j = 1, 2$, where

$$I(t) = \int_0^t K(s) ds,$$

with

$$K(t) := \max\{k_1, k_2\} = \gamma \begin{cases} t^{\beta_1 - 1}, & 0 \le t \le 1, \\ t^{\beta_2 - 1} & 1 \le t < \infty, \end{cases} \tag{A.18}$$

and $r = \max\{p_1, p_2\}$.

A lower bound T_L for the blow-up time T_{max} of the the system (A.16) can be obtained from

$$I(T_L) = \frac{(r-1)^{r-1}}{r^r}, \tag{A.19}$$

where it is assumed that T_L be the maximum value of t^* that satisfy (A.17) and in order to optimize the bounds in (A.17), we take $M = 1/(r-1)$, equation (A.19) gives us T_L as in the Th. 2.3.7.

Upper bound on the blow-up time:

For obtaining an upper bound T_U, the approach in [90] first assumes the existence of continuous solution of (A.16) for $0 \le t \le t^{**}$ and then find a value $T_U < \infty$ which contradicts the assumption.

It is easy to see that

$$k(t) := \min\{k_1(t), k_2(t)\} = \gamma \begin{cases} t^{\beta_2 - 1}, & 0 \le t \le 1, \\ t^{\beta_1 - 1} & 1 \le t < \infty. \end{cases} \tag{A.20}$$

Let us introduce the functional

$$J_j(t) = \int_0^t k(t^{**} - s)[u_{3-j}(s) + 1]^{p_j}, \quad 0 \le t \le t^{**}, \quad j = 1, 2,$$

then we have $u_j \ge J_j$, for $j = 1, 2$. Differentiating the functional J_j gives

$$J_j'(t) \ge k(t^{**} - t)[J_{3-j}(t) + 1]^{p_j}, \quad 0 \le t \le t^{**}, \quad j = 1, 2,$$

to establish a blow-up for J_j the following comparison problem has been introduced

$$V_j'(t) = k(t^{**} - t)[V_{3-j}]^{p_j}, \quad V_j(0) = 1, \quad 0 \le t \le t^{**}, \quad j = 1, 2. \tag{A.21}$$

Notice that $u_j(t) \ge J_j(t) \ge V_j(t)$, hence a blow-up phenomena for V_j ensures the blow-up of $u_j(t)$ and an upper bound on the blow-up time of $V_j(t)$ is also an upper bound on the blow-up time for $u_j(t)$. We try to decouple the equation (A.21), for this notice that we can write

$$\frac{d}{dt}[G_{3-j}(V_j(t))] = k(t^{**} - s)[V_{3-j}(t)]^{p_j}[V_j(t)]^{p_{3-j}}, \quad V_j(0) = 1, \quad j = 1, 2, \tag{A.22}$$

where $G_j(V)$ is the antiderivative of the nonlinearities in the system (A.21). The right hand side of equation (A.22) is invariant for $j = 1, 2$, we can have

$$G_2[V_1(t)] - G_1[V_2(t)] = G_2(1) - G_1(1), \quad 0 \le t \le t^{**},$$

moreover, the positivity of nonlinearities with positive input insures that the antiderivative $G_j(V)$ are strictly increasing and hence invertible so we have

$$V_j(t) = G_{3-j}^{-1}\{G_j[V_{3-j}(t)] - G_j(1) + G_{3-j}(1)\}, \quad j = 1, 2. \tag{A.23}$$

For $j = 2$ the equation (A.23) becomes

$$(p_2 + 1)[V_2(t)]^{p_1+1} = (p_1 + 1)[V_1(t)]^{p_2+1} + p_2 - p_1,$$

it is easily seen that both V_1 and V_2 blows-up simultaneously. Due to (A.23), it is possible to find implicit solution of (A.21) for $V_j(t), j = 1, 2$ in the form

$$\int_1^{V_j(t)} \frac{dy}{R_j(y)} = \tilde{I}(t), \quad j = 1, 2, \quad 0 \leq t \leq t^{**}, \tag{A.24}$$

where

$$R_j(y) = \left[\frac{(p_j + 1)y^{p_{3-j}+1} + p_{3-j} - p_j}{p_{3-j} + 1}\right]^{\frac{p_j}{p_j+1}}, \quad j = 1, 2,$$

and

$$\tilde{I}(t) = \int_0^t k(s)ds.$$

The blow-up by (A.24) is associated with $V_j(t) \to \infty$ as $t \to T_U \leq t^{**}$, where T_U is obtained from

$$\kappa = \min\{\kappa_j\} = \tilde{I}(T_U), \tag{A.25}$$

with

$$\kappa_j = \int_1^\infty \frac{dy}{R_j(y)}, \quad j = 1, 2.$$

Thus, if we replace κ by an upper bound such as

$$\kappa_j \leq \int_1^\infty \left(\frac{1}{y}\right)^{\frac{p_1p_2+r}{1+r}} dy = \frac{r+1}{p_1p_2 - 1}, \quad j = 1, 2,$$

with this value of κ_j and using equation (A.25) given the T_U as in the Theorem 2.3.7. □

A.2 Determination of an unknown source term and the temperature distribution for the linear heat equation involving fractional derivative in time

The underlying spectral problem for problem (3.1)-(3.3) is

$$X'' = -\lambda X, \qquad x \in (0,1), \tag{A.26}$$
$$X(1) = 0, \quad X'(0) = X'(1). \tag{A.27}$$

The boundary value problem (A.26)-(A.27) is non-self-adjoint; it has the following conjugate (adjoint) problem:

$$Y'' = -\lambda Y, \qquad x \in (0,1), \tag{A.28}$$
$$Y'(0) = 0, \quad Y(0) = Y(1). \tag{A.29}$$

In fact

$$\int_0^1 YX'' = X'(0)(Y(0) - Y(1)) + X(0)Y'(0) + \int_0^1 Y''X.$$

It is clear that the right side of this relation vanishes if $Y(0) = Y(1)$ and $Y'(0) = 0$.

The spectral problem (A.26)-(A.27) has the eigenvalues

$$\lambda_n = (2\pi n)^2 \qquad \text{for} \;\; n = 0, 1, 2, ...$$

and the eigenvectors

$$X_0 = (1 - x), \text{ for } \lambda_0 = 0, \text{ and } \; X_n = \sin 2\pi n x, \;\; \text{for } \lambda_n = (2\pi n)^2 \quad n = 1, 2, ...$$

The eigenvectors X_n, for $n > 0$ are not orthogonal to X_0, the set of functions $\{X_0, X_n\}$ do not form a complete system and is not a basis in $L^2(0,1)$.

In order to complete the basis (see [49]), we consider the associated eigenvectors $\tilde{X}$ for the λ_n corresponding to X_n defined as the solution of the problem

$$\tilde{X}'' = -\lambda_n \tilde{X} - X_n, \qquad x \in (0,1), \tag{A.30}$$
$$\tilde{X}(1) = 0, \quad \tilde{X}'(0) = \tilde{X}'(1). \tag{A.31}$$

If $\lambda_0 = 0$ the problem (A.30)-(A.31) has no solution and $\lambda_n = (2\pi n)^2$ for $n = 1, 2, ...$ the problem (A.30)-(A.31) has the eigenvectors

$$\tilde{X}_n = \frac{(1-x)}{4\pi n} \cos 2\pi n,$$

for $n = 1, 2, ...$ Thus

$$S = \{X_0, X_n, \tilde{X}_n\},$$

forms a complete system but not orthogonal.

We need another complete set of functions which together with the set S forms a biorthogonal system for the space $L^2(0,1)$. In order to get the other system, we shall consider the conjugate or adjoint problem (A.28)-(A.29).

Alike, solving (A.28)-(A.29), we obtain the complete set of eigenvectors

$$\tilde{S} = \{Y_0, Y_n, \tilde{Y}_n\},$$

where

$$Y_0 = 1, \quad Y_n = \cos 2\pi n, \quad \tilde{Y}_n = x \sin 2\pi nx.$$

Remark A.2.1. *The set of functions S and $\tilde{S}$ forms a biorthogonal system for the space $L^2(0,1)$. We can normalize the biorthogonal system and its final form is*

$$\{X_0 = 2(1-x), \quad X_n = \{4(1-x)\cos 2\pi nx\}_{n=1}^{\infty}, \quad \tilde{X}_n = \{4\sin 2\pi nx\}_{n=1}^{\infty}\}. \tag{A.32}$$

$$\{Y_0 = 1, \quad Y_n = \{\cos 2\pi nx\}_{n=1}^{\infty}, \quad \tilde{Y}_n = \{x \sin 2\pi nx\}_{n=1}^{\infty}\}, \tag{A.33}$$

A.3 An inverse source problem for a two dimensional time fractional diffusion equation with nonlocal boundary conditions

The adjoint problem for the spectral problem (4.5)-(4.6)

$$\begin{aligned}
\frac{\partial^2 V}{\partial x^2} + \frac{\partial^2 V}{\partial y^2} &= -\mu V, \qquad (x,y) \in \Omega, & \text{(A.34)}\\
V(0,y) = 0, \quad V(x,0) &= V(x,1) = 0, & \text{(A.35)}\\
\frac{\partial V}{\partial x}(0,y) &= \frac{\partial V}{\partial x}(1,y), \quad x,y \in [0,1]. & \text{(A.36)}
\end{aligned}$$

For solving (4.5)-(4.6) let us introduce

$$S(x,y) = X(x)Y(y),$$

then we obtain the following boundary value problems

$$Y''(y) + \lambda Y(y) = 0, \quad Y(0) = Y(1) = 0, \quad y \in (0,1), \tag{A.37}$$

$$X''(x) + \gamma X(x) = 0, \quad X(0) = X(1), \quad X'(1) = 0, x \in (0,1), \tag{A.38}$$

where $\gamma = \mu - \lambda$. The solution of the boundary value problem (A.37) is

$$\lambda_k = \pi^2 k^2, \quad Y_k(y) = \sqrt{2}\sin(\pi k y), \quad k = 1, 2, \ldots.$$

The eigenvalues and eigenfunctions of the boundary value problem (A.38) are

$$\gamma_m = 4\pi^2 m^2, \quad X_0 = 2 \text{ (for } m = 0), \quad X_m(x) = 4\cos(2\pi m x), \quad m = 1, 2, \ldots.$$

Consequently, the eigenvalues and eigenfunctions of the problem (4.5)-(4.6) are

$$\mu_{mk} = 4\pi^2 m^2 + \pi^2 k^2, \quad X_m(x)Y_k(y), \quad m = 0, 1, 2, \ldots, k = 1, 2, \ldots.$$

Let us mention that the constants eigenfunctions and associated eigenfunctions are chosen from normalization conditions.

The set of functions $\{S_{mk} = X_m(x)Y_k(y), \quad m = 0,1,2,...,k = 1,2,...\}$ is not complete in the space $L^2(\Omega)$ and we supplement the this set with the associated eigenfunctions of the problem (see [49])

$$\begin{aligned}
\frac{\partial^2 \tilde{S}_{mk}}{\partial x^2} + \frac{\partial^2 \tilde{S}_{mk}}{\partial y^2} &= -\mu_{mk}\tilde{S}_{mk} - 2\sqrt{\gamma_m}S_{mk}, \qquad (x,y) \in \Omega, && \text{(A.39)}\\
\tilde{S}_{mk}(0,y) &= \tilde{S}_{mk}(1,y), \quad y \in [0,1] && \text{(A.40)}\\
\tilde{S}_{mk}(x,0) &= \tilde{S}_{mk}(x,1), \quad \frac{\partial \tilde{S}_{mk}}{\partial x}(1,y) = 0, \quad x \in [0,1]. && \text{(A.41)}
\end{aligned}$$

The problem (A.39)- (A.41) has no solution for $m = 0$ and $k = 1,2,...$ and for $m,k = 1,2,...$ the associated eigenfunctions i.e., solution of the problem (A.39)-(A.41) are

$$\tilde{S}_{mk} = 4(1-x)\sin(2\pi m x)\sqrt{2}\sin(\pi k y).$$

The set of functions $\{X_0(x)Y_k(y), X_m(x)Y_k(y), \tilde{S}_{mk}\}$ for $m,k = 1,2,...$ is a complete set of functions in $L^2(\Omega)$. Clearly, this set of functions is not orthogonal. The root functions i.e., eigenfunctions and associated eigenfunctions of the problem (A.34)-(A.36) are

$$\{W_{0k} := \tilde{X}_0(x)Y_k(y), \quad W_{(2m-1)k} := \tilde{X}_m(x)Y_k(y), \quad W_{2mk} := \tilde{X}_{2mk}(x)Y_k(y)\},$$

for $m,k = 1,2,...$ and

$$\tilde{X}_0(x) = x, \quad \tilde{X}_m(x) = x\cos(2\pi m x)\tilde{X}_{2mk}(x) = \sin(2\pi m x).$$

A.4 Image structure preserving denoising using generalized fractional integrals

The following lemma describes the apparent properties of heat equation when applied to images.

Lemma A.4.1. *Let T_t, $t > 0$, be the family of scale operators defined by $(T_t u_0)(\mathbf{x}) = u(t,\mathbf{x})$, where $u(t,\mathbf{x})$ is the unique solution of system (1.76) given by equation (1.77); T_t is a family of linear operators which have the following properties:*

- *Gray-level shift invariance:*
  $T_t(0) = 0$, *and for any constant* c, $T_t(u_0 + c) = T_t(u_0) + c$.
- *Translation invariance:*
  $T_t(u_0(\mathbf{x}+h)) = T_t(u_0(\mathbf{x})) + h$
- *Reflection invariance:*
  $T_t(-u_0(\mathbf{x})) = -T_t(u_0(\mathbf{x}))$

- *Isometry invariance:*
  Let $H : \mathbb{R}^2 \to \mathbb{R}^2$ *be an orthogonal transformation where* $(Hf)(x) = f(Hx)$ *then* $T_t(Hu_0) = H(T_t u_0)$.

- *Conservation of average value:*
  $T_t(\int\limits_\Omega u_0 d\mathbf{x}) = \int\limits_\Omega T_t u_0 d\mathbf{x}$

- *Semi group property:*
  $T_{t+s}u_0 = T_t(T_s u_0)$.

- *Comparison principle:*
  If $u_0 \le v_0$ *then* $(T_t u_0)(\mathbf{x}) \le (T_t v_0)(\mathbf{x})$.

The invariance properties given above are easily observable in image processing and are quiet natural for the image analysis point of view. For example, the gray-level shift invariance means that the analysis must be independent of the range of the brightness of the initial image; translation invariance property means that the treatment of the image is independent of translation of initial image u_0.

Bibliography

[1] E. E. Adams and L. W. Gelhar, Field study of dispersion in a heterogeneous aquifer 2. spatial moments analysis, Water Resources Research 28 No. 12 (1992) 3293–3307. (Cited on page 19.)

[2] R. P. Agarwal, V. Lakshmikantham and J. J. Nieto, On the concept of solution for fractional differential equations with uncertainty, Nonlinear Analysis:TMA 72 (2010) 2859–2862. (Cited on pages 40 and 63.)

[3] S. Aja-Fernández, R. L. García and D. T. X. Li, Tensors in Image Processing and ComputerVision, Springer-Verlag,London, 2009. (Cited on pages 15, 35 and 103.)

[4] H. Amann, Time-delayed Perona-Malik type problems, in: K.Mikula, et al. (Ed.), Proceedings of the International Conference on Differential Equations, Bratislava, Czech Republic, 25-29 July2005), Comenius University Press, 2005, pp.15-38. (Cited on pages 33, 102 and 125.)

[5] M. Andrle, F. Ben Belgacem and A. El Badia, Identification of moving pointwise sources in an advection-dispersion-reaction equation, Inverse Problems 27 (2011),no. 2, 025007 22 pp. (Cited on page 63.)

[6] J. Bai and X. C. Feng, Fractional anisotropic diffusion for image denoising, IEEE Transactionson Image Processing, 16 (2007) 2492-2502. (Cited on page 105.)

[7] D. Baleanu, Z. B. Guvenç and J. A. T. Machado, New Trends in Nanotechnology and Fractional Calculus Applications, Springer Verlag (2009). (Cited on pages 17, 19, 21 and 63.)

[8] E. C. Baran and A. G. Fatullayev, Determination of an unknown source parameter in two-dimensional heat equation, Appl. Math. Comput. 159, 881-886, (2004). (Cited on page 63.)

[9] D. Barash, A fundamental relationship between bilateral filtering, adaptive smoothing and the nonlinear diffusion equation, IEEE Transactions on Pattern Analysis and Machine Intelligence, 24 (6) (2002) 844-856. (Cited on page 103.)

[10] S. Bartels and A. Prohl, Stable discretization of scalar and constrained vectorial Perona- Malik equation, Interfaces and Free Boundaries 9 (4) (2007) 431- 453. (Cited on pages 15, 35 and 103.)

[11] G. Bellettini and G. Fusco, A regularized Perona-Malik functional: some aspects of the gradient dynamics, in:F. Dumortier, H. Broer, et al.(Eds.), Proceedings of the International Conference of Differential Equations, Hasselt, Belgium, 22-26 July 2003, World Scientific, 2003, pp.639-644. (Cited on pages 33 and 102.)

[12] H. Brunner, Collocation methods for Volterra integral and related functional equations, in: Cambridge Monographs Applied and Computational Mathematics, Cambridge University Press, 2004. (Cited on page 110.)

[13] A. Buades, B. Coll and J. M. Morel, The staircasing effect in neighborhood filters and its solution, IEEE Transactionson Image Processing, 15 (2006) 1499-1505. (Cited on pages 103 and 113.)

[14] M. Calvo, E. Cuesta and C. Palencia, Runge-Kutta convolution quadrature methods for well-posed equations with memory. Numer. Math. 107,(2007), 589–614. (Cited on pages 55, 107, 108, 109, 110, 111 and 128.)

[15] M. P. Calvo, E. Cuesta and C. Palencia, Backward Euler method as a positivity preserving method for abstract integral equations of convolution type, in: A. E. Oustaloup(Ed.), Proceedings of Fractional Differentiation and its Applications 06, 2006, pp. 530-534. (Cited on page 110.)

[16] F. Catte, P. L. Lions, J. M. Morel and T. Coll, Image selective smoothing and edge detection by non linear diffusion, SIAM Journal on Numerical Analysis, 29 (1) (1992) 182-193. (Cited on pages 33, 102 and 125.)

[17] J. Cheng, J. Nakagawa, M. Yamamoto and T. Yamazaki, Uniqueness in an inverse problem for a one-dimensional fractional diffusion equation, Inverse Problems 25 (2009) doi:10.1088/0266-5611/25/11/115002. (Cited on pages 9, 26 and 80.)

[18] J. R. Cannon, S. P. Esteva and J. V. D. Hoek, A Galerkin procedure for the diffusion subject to the specification of mass, SIAM J. Numer. Anal. 24 No. 3 (1987), 499–515. (Cited on page 80.)

[19] J. R. Cannon, Y. Lin and S. Wang, Determination of a control parameter in a parabolic partial differential equation, J. Austral. Math. Soc. Ser. B, 33 (1991), 149–163. (Cited on page 80.)

[20] E. Cuesta, Some advances on image processing by means of fractional calculus, in: T. Machado, et al. (Ed.), Nonlinear Science and Complexity, Springer, 2011, pp. 265-271. (Cited on page 105.)

[21] E. Cuesta and J. Finat, Image processing by means of a linear integro-differential equation, IASTED (2003) 438-442. (Cited on pages 14, 34, 63, 104 and 126.)

[22] **E. Cuesta, M. Kirane and S. A. Malik, Image structure preserving denoising using generalized fractional time integrals, Signal Processing, 92 (2012) 553-563**. (Cited on pages 98, 125, 126, 127, 128, 129, 133 and 134.)

[23] **E. Cuesta, M. Kirane, and Salman A. Malik, On the Improvement of Volterra Equation Based Filtering for Image Denoising, In H. R. Arabnia et al, Proceedings of IPCV 2011, Las Vegas Nevada, USA, pp. 733-738**. (Cited on page 122.)

[24] E. Cuesta and C. Palencia, A numerical method for an integro-differential equation with memory in Banach spaces, SIAM Journal on Numerical Analysis, 41 (2003) 1232-1241. (Cited on pages 109 and 110.)

[25] K. Dabov, A. Foi, V. Katkovnik and K. Egiazarian, Color image denoising via sparse 3D collaborative filtering with grouping constraint in luminance-chrominance space, in: IEEE International Conference on Image Processing, ICIP, 2007. (Cited on page 111.)

[26] S. Didas, Denoising and Enhancement of Digital Images, Variational Methods, Integrodifferential Equations, and Wavelets, Ph.D. Thesis, Saarland University, 2008. (Cited on page 105.)

[27] S. Didas, B. Burgeth, A. Imiya and J. Weickert, Regularity and scale-space properties of fractional high order linear filtering, Scale Space and PDE Methods in Computer Vision, Lecture Notes in Computer Vision, vol.3459, 2005, pp. 13-25. (Cited on page 105.)

[28] S. Didas and J. Weickert, Integrodifferential equations for continuous multiscale wavelet shrinkage,Inverse Problems and Imaging 1 (1) (2007) 47-62. (Cited on page 105.)

[29] S. D. Eidelman and A. N. Kochubei, Cauchy problem for fractional diffusion equations, J. Differential Equations 199 (2004) 211-255. (Cited on page 20.)

[30] I. C. Dolcetta and R.Ferretti, Optimal stopping time formulation of adaptive image filtering, Applied Mathematics and Optimization. 43, 245-258 (2001). (Cited on pages 13 and 31.)

[31] W. Feller, The parabolic differential equations and associated semi-groups of transformations, Annal. Math., 55 No. 3 (1952) 468-519. (Cited on page 61.)

[32] W. Feller, Diffusion processes in one dimension, Trans. Amer. Math. Soc, 77 No. 1 (1952) 1-33. (Cited on page 61.)

[33] Y. Fujita, Integro-differential equation which interpolates the heat equation and the wave equation, Osaka Journal of Mathematics, 27 (1990) 319-327. (Cited on pages 14, 20, 34, 105 and 126.)

[34] Y. Fujita, Integro-differential equation which interpolates the heat equation and the wave equation (ii), Osaka Journal of Mathematics 27 (1990) 797-804. (Cited on pages 14, 20, 34 and 105.)

[35] K. M. Furati and M. Kirane, Necessary conditions for the existence of global solutions to systems of fractional differential equations, Fractional Calculus & Applied Analysis 11 (2008) 281–298. (Cited on pages 4, 21, 22, 39, 40, 41 and 42.)

[36] V. D. Gejji and H. Jafari, Analysis of a system of nonautonomous fractional differential equations involving Caputo derivatives , J. Math. Anal. Appl. 328 (2007) 1026–1033. (Cited on page 40.)

[37] V. D. Gejji, Positive solutions of a system of non-autonomous fractional differential equations , J. Math. Anal. Appl. 302 (2005) 56–64. (Cited on page 40.)

[38] R. Gorenflo and F. Mainardi, Fractional Calculus: integral and differential equations of fractional order, in: A. Carpinteri, F. Mainardi (Eds.), Fractals and Fractional Calculus in Continuum Mechanics, Springer Verlag, Wien, 1997, pp. 223–276. (Cited on pages 8, 25, 40, 51 and 71.)

[39] G. Gerig, O. Kubler, R. Kikinis and A. Jolesz, Nonlinear anisotropic filtering of mridata, IEEE Transactions on Medical Imaging, 11 (2) (1992) 221-232. (Cited on pages 33, 112 and 129.)

[40] M. Gilli, Strange attractors in delayed cellular networks, IEEE Trans. CAS I, 40 (11) (1993) 849-853. (Cited on page 19.)

[41] P. Guidotti, A new well-posed nonlinear nonlocal diffusion, Nonlinear Analysis: TMA(2010). (Cited on page 33.)

[42] P. Guidotti, A new nonlocal nonlinear diffusion of image processing, J. Differential Equations 246 (2009) 4731-4742. (Cited on page 33.)

[43] P. Guidotti and K. Longo, Two enhanced fourth order diffusion models for image denoising, J. Math. Imaging Vis. (2011) 40: 188-198. (Cited on page 34.)

[44] P. Guidotti and J. V. Lambers, Two new nonlinear nonlocal diffusions for noise reduction, J. Math. Imaging Vis., vol. 33, pp. 25-37, 2009. (Cited on pages 33, 34 and 125.)

[45] A. B. Hamza, H. Krim and G. B. Unal, Unifing probabilistic and variational estimation, IEEE Signal Processing Magazine, 2 (2002) 37-47. (Cited on page 102.)

[46] Y. Hatano and N. Hatano, Dispersive transport of ions in column experiments: An explanation of long tailed profiles, Water Resources Research 34 (5) (1998) 1027–1033. (Cited on pages 20 and 80.)

[47] R. Hilfer, Applications of Fractional Caluclus in Physics, World Scientific (2000). (Cited on page 18.)

[48] T. Iijima, Theory of pattern recognition, Electronics and Communications, 123–134 (1963). (Cited on pages 13 and 31.)

[49] V. A. Il'in, How to express basis conditions and conditions for the equiconvergence with trignometric series of expansions related to non-self-adjoint differential operators, Computers Math. Applic. 34 (5/6) 641-647, (1997). (Cited on pages 11, 29, 60, 76, 145 and 147.)

[50] N. I. Ionkin and V. A. Morozova, The two-dimensional heat equation with nonlocal boundary conditions, Differential Equations 36 (7) 982–987, (2000). (Cited on pages 12, 30, 83, 84 and 91.)

[51] R. L. Magin and M. Ovadia, Modeling the Cardiac Tissue Electrode Interface Using Fractional Calculus, Journal of Vibration and Control, 2008 vol. 14 no. 9-10, 1431-1442. (Cited on page 19.)

[52] R. Metzler and J. Klafter, The random walk's guide to anomalous diffusion: a fractional dynamics approach, Phys. Rep. 339 (1) (2000) 1-77. (Cited on pages 20, 80 and 86.)

[53] N. I. Ionkin and E. I. Moiseev, A Two-Point Boundary Value Problem for a Heat Conduction Equation, Differentsialnye Uravneniya 15 (7) 1284-1295, (1979). (Cited on pages 10, 28 and 65.)

[54] V. Isakov, Inverse parabolic problems with the final overdetermination, Comm. Pure Appl. Math. 44, 185-209, (1991). (Cited on pages 26 and 63.)

[55] G. Jumarie, Laplace's transform of fractional order via the Mittag–Leffler function and modified Riemann–Liouville derivative, Appl. Math. Lett. 22 (2009) 1659–1664. (Cited on page 42.)

[56] I. A. Kaliev and M. M. Sabitova, Problems of Determining the Temperature and Density of Heat Sources from the Initial and Final Temperatures, Journal of Applied and Industrial Mathematics, 4 (3) 332-339, (2010). (Cited on page 63.)

[57] J. Kačur and K. Mikula, Solution of nonlinear diffusion appearing in image smoothing and edge detection, Applied Numerical Mathematics, 17 (1) (1995) 47-59. (Cited on pages 102 and 125.)

[58] J. Kačur and K. Mikula, Slow and fast diffusion effects in image processing, Computing and Visualization in Science, 3 (2001) 185-195. (Cited on pages 102 and 125.)

[59] V. L. Kamynin, On the inverse problem of determining the right-hand side of a parabolic equation under an integral overdetermination condition , Mathematical Notes, 77 (2005), No. 4, 482–493. (Cited on page 74.)

[60] M. V. Keldysh, On the completeness of the eigenfunctions of some classes of non-selfadjoint linear operators, Russ. Math. Surv. 26 (4) 1971, doi:10.1070/RM1971v026n04ABEH003985. (Cited on pages 60 and 76.)

[61] S. Kichenassamy, The persona-malik paradox, SIAM J. Appl. Math, vol. 147, pp. 1328–1342, 1997. (Cited on pages 33 and 125.)

[62] A. A. Kilbas, H. M. Srivastava and J. J. Trujillo, Theory and Applications of Fractional Differential Equations, Elsevier, 2006. (Cited on pages 17, 40, 41, 42, 44, 63, 104, 126 and 127.)

[63] M. Kirane, Y. Laskri and N.-e. Tatar, Critical exponents of Fujita type for certain evolution equations and systems with spatio-temporal fractional derivatives, J. Math. Anal. Appl. 312 (2005) 488–501. (Cited on pages 17 and 40.)

[64] **M. Kirane and S. A. Malik, The profile of blowing-up solutions to a nonlinear system of fractional differential equations, Nonlinear Analysis: TMA 73 (2010) 3723-3736**. (Cited on pages 15, 34, 35, 36 and 63.)

[65] **M. Kirane and S. A. Malik, Determination of an unknown source term and the temperature distribution for the linear heat equation involving fractional derivative in time, Appl. Math. Comp. 218, Issue 1, 163–170**. (Cited on pages 60, 76, 80 and 82.)

[66] **M. Kirane and S. A. Malik, Determination of an unknown source term for a one dimensional fractional diffusion equation with an integral type overdetermination condition, submitted**. (Cited on page 74.)

[67] M. Klimek, Sequential fractional differential equations with Hadamard derivative, Commun. Nonlinear Sci. Numer. Simul. 16 (12) (2011), 4689–4697. (Cited on page 40.)

[68] N. Kosmatov, Integral equations and initial value problems for nonlinear differential equations of fractional order, Nonlinear Analysis:TMA 70 (2009) 2521–2529. (Cited on pages 40 and 63.)

[69] G. A. Kriegsmann and W. E. Olmstead, Source identification for the heat equation, Appl. Math. Lett. 1 (3), 241-245, (1988). (Cited on page 63.)

[70] V. Lakshmikantham, S. Leela and J. V. Devi, Theory of Fractional Dynamic Systems, Cambridge Scientific Publishers, 2009. (Cited on pages 40 and 63.)

[71] T. A. M. Langlands, B. I. Henry and S. L. Wearne, Fractional cable equation for anomalous electrodiffusion in nerve cells: infinite domain solutions, J. Math. Biol. 59 (2009) 761–808. (Cited on pages 21, 39 and 63.)

[72] J. S. Lee, Digital image smoothing and the sigma filter, Computer Vision, Graphics, and Image Processing, 24 (1983) 253- 269. (Cited on page 102.)

[73] M. López-Fernández and C. Lubich, Adaptive fast and oblivious convolution in evolution equations with memory, SIAM Journal on Scientific Computing, 30 (2008) 1015-1037 (Cited on page 110.)

[74] M. López-Fernández and C. Palencia, On the numerical inversion of the Laplace transform of certain holomorphic mappings, Applied Numerical Mathematics, 51 (2004) 289-303. (Cited on page 110.)

[75] C. Lubich, Convolution quadrature and discretized operational calculus I, Numerische Mathematik, 52 (1988) 129-145. (Cited on pages 107 and 109.)

[76] C. Lubich, Convolution quadrature and discretized operational calculus II, Numerische Mathematik, 52 (1988) 413-425. (Cited on page 107.)

[77] C. Lubich, Convolution quadrature revisited. BIT 44, 503–514 (2004). (Cited on pages 53, 54, 107, 108, 109, 126 and 128.)

[78] C. Lubich and A. Ostermann, Runge-Kutta methods for parabolic equations and convolution quadrature, Mathematics of Computation, 60 (1993) 105-131. (Cited on pages 107, 126 and 128.)

[79] S. Y. Lukashchuk, Estimation of parameters in fractional subdiffusion equations by the time integral characteristics method, Computers and Mathematics with Applications 62 (2011) 834-844. (Cited on pages 9, 27 and 80.)

[80] M. Lysaker, A. Lundervold and X. C. Tai, Noise removal usingfourth-order partial differential equation with applications to medical magnetic resonance images in space and time, IEEE Transactions on Image Processing, 12 (12) (2003) 1579-1590. (Cited on page 102.)

[81] J. T. Machado, V. Kiryakova and F. Mainardi, Recent history of fractional calculus, Commun Nonlinear Sci. Numer. Simulat. 16 (2011) 1140-1153. (Cited on page 17.)

[82] F. Mainardi, M. Raberto, R. Gorenflo and E. Scalas, Fractional calculus and continuous-time finance II: the waiting-time distribution, Physica A, 287, 468-481, (2000). (Cited on page 21.)

[83] F. Mainardi, Fractional calculus and waves in linear viscoelaticity, Imperial College Press 2010. (Cited on pages 17, 19 and 21.)

[84] B. Mathieu, P. Melchior, A. Oustaloup and C. Ceyral, Fractional differentiation for edge detection, Signal Processing, 83 (2003) 2421-2432. (Cited on page 105.)

[85] M. W. Michalski, Derivatives of noninteger order and their applications. Dissertations Mathematicae, CCCXXVIII (1993). (Cited on page 40.)

[86] E. I. Moiseev, The Solution of a Nonlocal Boundary Value Problem by the Spectral Method, Differential Equations 35 (8), 1105-1112, (1999). (Cited on pages 10, 28 and 66.)

[87] P. Mrázek and M. Navara, Selection of Optimal Stopping Time for Nonlinear Diffusion Filtering. Int. journal of Computer Vision. 52, 189–203 (2003). (Cited on pages 13, 31 and 134.)

[88] T. Odzijewicz, A. B. Malinowska and D. F. M. Torres, Fractional variational calculus with classical and combined Caputo derivatives, Nonlinear Analysis: TMA 75 (2012), 1507–1515. (Cited on page 40.)

[89] W. E. Olmstead and C. M. Kirk, Private communication. (Cited on page 140.)

[90] W. E. Olmstead, C. A. Roberts and K. Deng, Coupled Volterra equations with blow-up solutions, Journal of Integral Equations & Applications 7 (1995) 499–516. (Cited on pages 7, 24, 25, 50, 51, 140, 142 and 143.)

[91] P. Perona and J. Malik, Scale-space and edge detection using anisotropic diffusion, IEEE Transactions on Pattern Analysis and Machine Intelligence, 12 (7) (1990) 629-639. (Cited on pages 32, 101, 103 and 125.)

[92] I. Petras, Fractional-Order Nonlinear Systems Modelling, Analysis and Simulations, Springer-Verlag (2011). (Cited on page 18.)

[93] P. Pongsumpun and I. M. Tang, Transmission of dengue hemorrhagicfever in an age structured population, Mathematical and Computer Modelling 37 (2003) 949-961. (Not cited.)

[94] S. Pooseh, H. S. Rodrigues and D. F. M. Torres, Fractional derivatives in Dengue epidemics, AIP Conf. Proc. 1389, pp. 739-742; doi:10.1063/1.3636838. (Cited on page 19.)

[95] N. Pottier, Relaxation time distribution for an anomalously diffusing particle, Physica A 390 (2011), 2863–2879. (Cited on page 86.)

[96] T. R. Prabhakar, A singular intgeral equation with a generalized Mittag-Leffler function in the kernel, Yokohama Math. J 19 , 7-15, (1971). (Cited on pages 71 and 82.)

[97] J. Pruss, Evolutionary Integral Equations and Applications, Birkhäuser Verlag, Basel, 1993. (Cited on pages 107, 126 and 128.)

[98] S. G. Pyatkov, Certain inverse problems for parabolic equations, Journal of Mathematical Sciences, 150 (5), 2422-2433, (2008). (Cited on page 63.)

[99] C. Quintano and E. Cuesta, Improving satellite image classification by using fractional type convolution filtering, International Journal of Applied Earth Observation, 12 (2010) 298-301. (Cited on page 105.)

[100] L. Rudin, S. Osher and E. Fatemi, Nonlinear total variation based noise removal algorithm, PhysicaD, 60 (1992) 259-268. (Cited on page 102.)

[101] J. Sabatier, O. P. Agarwal and J. A. T. Machado, Advances in Fractional Calculus: Theoretical Developments and Applications in Physics and Engineering, Springer Verlag (2007). (Cited on pages 21 and 63.)

[102] S. G. Samko, A. A. Kilbas and D. I. Marichev, Fractional Integrals and Derivatives: Theory and Applications, Gordon and Breach Science Publishers, 1993. (Cited on pages 17, 40, 63, 81 and 87.)

[103] E. Scalas, R. Gorenflo and F. Mainardi, Fractional calculus and continuous-time finance, Physica A, 284, 376-384, (2000). (Cited on page 21.)

[104] A. Sever, A stability estimate of an inverse problem in financial prospection, Appl. Math. Comput. 150, 803-810, (2004). (Cited on page 63.)

[105] A. L. Skubachevskii, Nonclassical boundary-value problems. I, Journal of Mathmeatical Sciences. 155, No. 2, (2008) 199-327. (Cited on page 61.)

[106] B. Stankovich and T. M. Atanackovic, On an inequality arising in fractional oscillator theory, Fractional Calculus & Applied Analysis 7 (2004) 11–20. (Cited on page 52.)

[107] V. E. Tarasov, Fractional Dynamics Applications of Fractional Calculus to Dynamics of Particles, Fields and Media, Springer-Verlag (2010). (Cited on page 18.)

[108] N. Tatar, A blow up result for a fractionally damped wave equation NoDEA. 12,(2005), 215–226. (Cited on page 17.)

[109] C. Tomasi and R. Manduchi, Bilateral filtering for grey and color images, in: Proceedings of the 6th International Conference on Computer Vision, NewDelhi, India, 1998, pp. 839-846. (Cited on page 102.)

[110] A. D. Venttsel, On boundary conditions for multidimensional diffusion processes, Theory of probability and its applications, 04 No. 2, 164-177, (1959). (Cited on page 61.)

[111] F. Voci, S. Eiho, N. Sugimoto and H. Sekiguchi, Estimating the gradient threshold in the Perona-Malik equation, IEEE Signal Processing Magazine, 39-46, (2004). (Cited on page 33.)

[112] J. Weickert and B. Benhamouda, A semidicrete nonlinear scale-space theory and its relation to the Perona-Malik paradox, in: F. Solina, W. G. Kropatsch, R. Klette, R. Bajcsy (Eds.), Advances in Computer Vision, Springer, Wien, 1997, pp. 1-10. (Cited on page 102.)

[113] J. Weickert, A Review of Nonlinear Diffusion Filtering, vol. 1252, Springer, Berlin, 1997. (Cited on pages 15, 35 and 103.)

[114] J. Weickert, Anisotropic Diffusion in Image Processing, B. G. Teubner, Stuttgart, 1998. (Cited on pages 101, 125 and 127.)

[115] X. T. Xiong, Q. Zhou and Y. C. Hon, An inverse problem for fractional diffusion equation in 2-dimensional case: Stability analysis and regularization, J. Math. Anal. Appl. (2012), doi:10.1016/j.jmaa.2012.03.013 (Cited on page 80.)

[116] L. P. Yaroslavsky, Digital Picture Processing. An Introduction, Springer-Verlag, NewYork, 1985. (Cited on page 102.)

[117] G. H. Zhang and T. Wei, A new regulization method for solving a time-fractional inverse diffusion problem, J. Math. Anal. Appl. 378 (2011) 418-431. (Cited on pages 9, 27 and 80.)

[118] Y. Zhang and X. Xu, Inverse source problem for a fractional diffusion equation, Inverse Problems 27 (2011), doi:10.1088/0266-5611/27/3/035010. (Cited on pages 9, 27 and 80.)